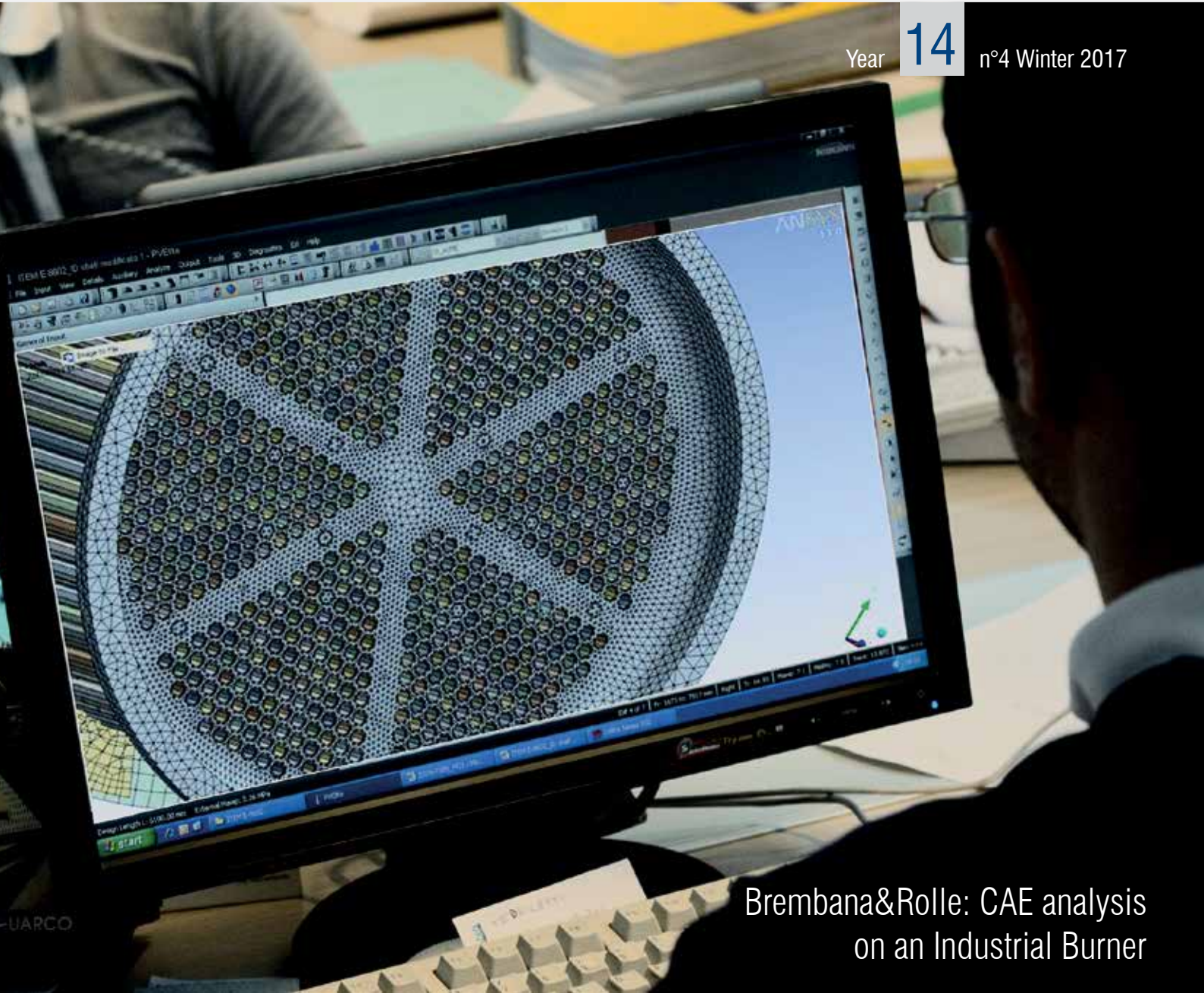




# Newsletter

Simulation Based Engineering & Sciences

Year **14** n°4 Winter 2017



Brembana&Rolle: CAE analysis on an Industrial Burner

Thermo-fluid dynamics simulation of the **combustion phenomenon** at SIT Group

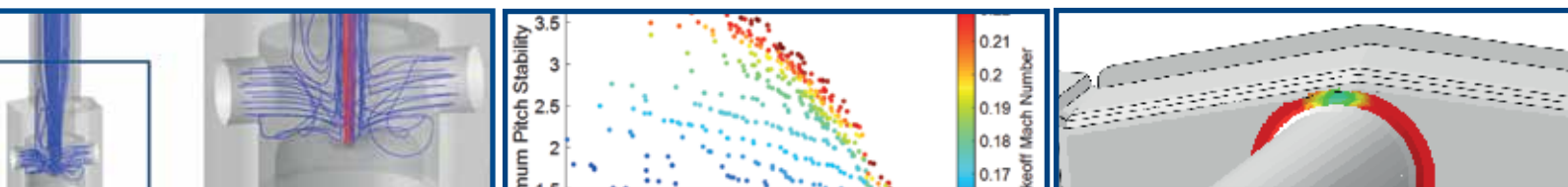
Electronica: Ultra-Wide Band Radome CAE Optimization

Front-End Loader Linkage **Durability Analysis** Using Load Input from True-Load

CFD analysis on an **industrial burner** at Brembana & Rolle

Filming the Bloodhound **Super Sonic Car** Land Speed Record

Topology Optimization for **Additive Manufacturing**



# Contents

## INTERVIEWS

- 4 Interview with Marco Croin Mechanics R&D Manager at SIT Group

## CASE HISTORIES

- 6 CFD analysis of an industrial burner for a regeneration gas heater application
- 10 Ultra-Wide Band Radome CAE Optimization
- 12 Filming the Bloodhound Super Sonic Car Land Speed Record
- 15 Azimut Benetti propels cruise speed with modeFRONTIER
- 17 Front-End Loader Linkage Durability Analysis Using Load Input from True-Load
- 21 Topology Optimization with Enforced Patterns and Applications for Additive Manufacturing
- 24 Evaluation of dam performance under seismic loads with DCR time history procedure
- 27 Composite Materials for the Sustainable Refurbishment of Bridges
- 30 Latest Accomplishments offer new Opportunities in the Field of high Strength Injection and Motor Components
- 33 Development of New Metallic Rear Crash Boxes to Replace a Plastic one for a Passenger Car
- 36 CAE software to optimize feeding system of butt-welded valve
- 39 NOZZLE-FEM: piping and pressure vessel nozzle analysis tool for every engineer
- 42 Multiscale FEM analysis system embedded in ANSYS Workbench using ACT technique

## SOFTWARE UPDATES

- 46 Short preview of ANSYS Mechanical R19 new functionalities
- 47 Multi-Body-Simulation Unlimited
- 48 Sigmetrix Launches EZtol – A New 1D analysis tool
- 49 MapleSim Explorer advances MBSE democratization through organization-wide sharing of MapleSim models

## INTERNATIONAL CAE CONFERENCE 2017

- 50 Simulation: The Soul of Industry 4.0
- 52 On the importance of Anisotropy in Biological Materials: Application to Aortic Tissues
- 54 Mechanical Analysis of the Toroidal and Poloidal Field Coils for DEMO<sup>strating</sup> Nuclear Fusion Reactor
- 56 A Multiscale Simulation Framework of the Accumulative Roll Bonding Process Accounting for Texture Evolution
- 58 Structural optimization and geometric modeling of lattice structures for Additive Manufacturing
- 60 Electro-thermal Finite Element Analysis for biomedical application. Reconstruction of a phantom: from EM safety up to treatment planning
- 62 A summary from the metal forming & steelmaking session @ 33<sup>rd</sup> CAE Conference

## Newsletter EnginSoft

### Year 14 n°4 - Winter 2017

To receive a free copy of the next EnginSoft Newsletters, please contact our Marketing office at: [l.cunico@enginsoft.com](mailto:l.cunico@enginsoft.com)

All pictures are protected by copyright. Any reproduction of these pictures in any media and by any means is forbidden unless written authorization by EnginSoft has been obtained beforehand. ©Copyright EnginSoft Newsletter.

### EnginSoft S.p.A.

24126 BERGAMO c/o Parco Scientifico Tecnologico  
Kilometro Rosso - Edificio A1, Via Stezzano 87  
Tel. +39 035 368711 • Fax +39 0461 979215  
50127 FIRENZE Via Panciatichi, 40  
Tel. +39 055 4376113 • Fax +39 0461 979216  
35129 PADOVA Via Giambellino, 7  
Tel. +39 049 7705311 • Fax +39 0461 979217  
72023 MESAGNE (BRINDISI) Via A. Murri, 2 - Z.I.  
Tel. +39 0831 730194 • Fax +39 0461 979224  
38123 TRENTO fraz. Mattarello - Via della Stazione, 27  
Tel. +39 0461 915391 • Fax +39 0461 979201  
10133 TORINO Corso Marconi, 10  
Tel. +39 011 6525211 • Fax +39 0461 979218

[www.enginsoft.it](http://www.enginsoft.it) - [www.enginsoft.com](http://www.enginsoft.com)  
e-mail: [info@enginsoft.it](mailto:info@enginsoft.it)

The EnginSoft Newsletter is a quarterly magazine published by EnginSoft SpA

### COMPANY INTERESTS

EnginSoft GmbH - Germany  
EnginSoft UK - United Kingdom  
EnginSoft France - France  
EnginSoft Nordic - Sweden  
EnginSoft Turkey - Turkey  
VSA-TTC3 - Germany  
[www.enginsoft.com](http://www.enginsoft.com)

CONSORZIO TCN [www.consorziotcn.it](http://www.consorziotcn.it) • [www.improve.it](http://www.improve.it)  
Cascade Technologies [www.cascadetechnologies.com](http://www.cascadetechnologies.com)  
Reactive Search [www.reactive-search.com](http://www.reactive-search.com)  
SimNumerica [www.simnumerica.it](http://www.simnumerica.it)  
M3E Mathematical Methods and Models for Engineering [www.m3eweb.it](http://www.m3eweb.it)

### ASSOCIATION INTERESTS

NAFEMS International [www.nafems.it](http://www.nafems.it) • [www.nafems.org](http://www.nafems.org)  
TechNet Alliance [www.technet-alliance.com](http://www.technet-alliance.com)

### ADVERTISEMENT

For advertising opportunities, please contact our Marketing office at: [l.cunico@enginsoft.com](mailto:l.cunico@enginsoft.com)

### RESPONSIBLE DIRECTOR

Stefano Odorizzi

### ART DIRECTOR

Luisa Cunico - [l.cunico@enginsoft.com](mailto:l.cunico@enginsoft.com)

PRINTING Grafiche Dalpiaz - Trento

The EnginSoft Newsletter editions contain references to the following products which are trademarks or registered trademarks of their respective owners: ANSYS, ANSYS Workbench, AUTODYN, CFX, FLUENT, FORTE, SpaceClaim and any and all ANSYS, Inc. brand, product, service and feature names, logos and slogans are registered trademarks or trademarks of ANSYS, Inc. or its subsidiaries in the United States or other countries. [JCEM CFD is a trademark used by ANSYS, Inc. under license]. (www.ANSYS.com) - modeFRONTIER is a trademark of ESTECO Spa (www.esteco.com) - Flownex is a registered trademark of M-Tech Industrial - South Africa (www.flownex.com) - MAGMASOFT is a trademark of MAGMA GmbH (www.magma-soft.de) - FORGE, COLDFORM and FORGE Nxt are trademarks of Transvalor S.A. (www.transvalor.com) - LS-DYNA is a trademark of LSTC (www.lstc.com) - Cetol 6σ is a trademark of Sigmetrix L.L.C. (www.sigmetrix.com) - RecurDyn™ and MBD for ANSYS is a registered trademark of FunctionBay, Inc. (www.functionbay.org) - Maplesoft are trademarks of Maplesoft™, a subsidiary of Cybernet Systems Co. Ltd. in Japan (www.maplesoft.com)

# FLASH



The International CAE Conference marks the end of another remarkable year. The rapid rise of new intelligent technology in every sector is astounding. It poses a number of issues, vital for our engineering community to discuss and collaborate in, as we move towards the future of Industry 4.0.

It was a privilege to learn the depth in which simulation is embedded into organizations today. While being far from a mere traditional engineering practice, simulation is still developing new smarter technologies and finding new areas of application. The future of which is ever more promising given the quality of new engineers coming through, as demonstrated by the quality of the Poster's submitted for the conference's Poster Award. Discover the highlights of the 33rd edition of the conference and the winning posters at the end of this Newsletter.

As we approach 2018, I am delighted to announce our joint venture with FunctionBay GmbH to form RecurDyn Europe. We look forward to bringing together a new European network for Multi-body Simulation Solution, RecurDyn – more information can be found on p. 47.

Another exciting development, in time for the New Year, follows on p. 48. The 1D tolerance analysis tool, EZtol, encourages product reliability which can often be compromised by the use of traditional hand calculations or spreadsheets to conduct tolerance stack up analyses.

On behalf of everyone at EnginSoft, we thank you all for your contribution and look forward to continuing this in the year ahead with more opportunities to collaborate with many of you. EnginSoft wishes you, your colleagues and families a Merry Christmas and prosperous New Year.

Stefano Odorizzi, Editor in chief

# Interview with Marco Croin

## Mechanics R&D Manager at SIT Group



SIT group develops and manufactures measuring devices and systems for the safety, comfort, and performance of domestic gas equipment. The two Divisions are Heating and Smart Metering. The company offers mechanical controls, electronic controls, fans (for heating appliances and range hoods), integrated systems, sensors, flue kits, accessories, and gas meters. SIT was founded in 1953, it is headquartered in Padua and it serves customers worldwide through a network of representative and sales offices in Europe, the United States, Asia, and Oceania.

### What is the perceived value of your products according to your customers?

The market of gas valves is very conservative and rather opposed to change. The most recognized values for our customers are safety and reliability indeed, intended as the life span of the products and as a percentage of components that guarantee their operation. In order to ensure the reliability of our products, the focus of SIT Group is mainly on to prevent the risk of gas leakage through a controlled approach to failure.

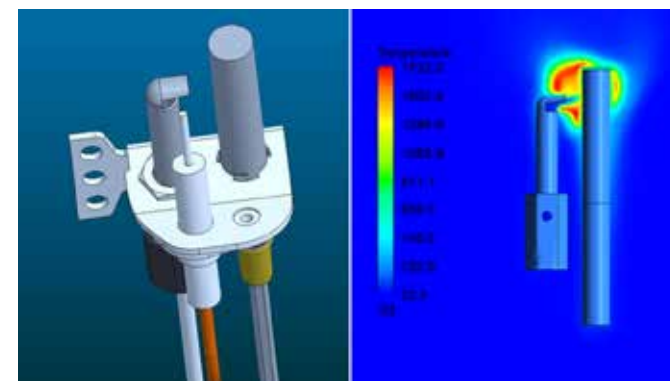


Figure 1 - Left: CAD model of the pilot burner. Right: Temperature distribution from CFD analyses on a longitudinal cut-plane at the beginning of the combustion in the pilot burner

### When did you first introduce simulation in your company and what were the key reasons for introducing engineering simulation?

SIT has started using ANSYS products since the early '90s. At first it started with structural and electromagnetic analyses then, in 2014 CFD analysis was introduced, followed by multi-disciplinary design optimization tools for process integration and parametric optimization.

The reasons for introducing engineering simulation were, on one hand, to reduce the time between product ideation and go-to-market, on the other hand, to significantly minimize the risk of errors and failures. Our key business objectives related to the introduction of engineering simulation were in fact safety, comfort and performance of gas equipment. Another decisive factor was the desire to align with the requests of an increasingly demanding market segment, in terms of cutting edge products, which is why we have been thinking of extending the use of engineering simulation also to the line of ventilation products. Our goal is to switch our role from component supplier to full solution provider, and we strongly believe that technology improvements such as extensive engineering simulation will help us achieve this target.

### What goals are reached thanks to engineering simulation?

From a technical point of view, the added value of engineering simulation compared to experimental

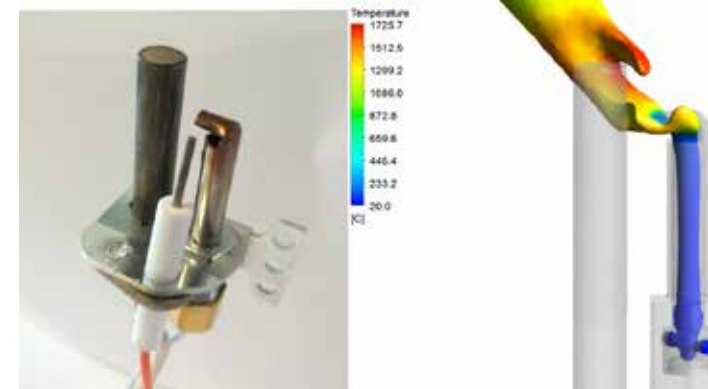


Figure 2 - Real and virtual representation of the pilot burner. Mixed gas-air flow exiting the pilot burner colored by temperature

analysis stands in the possibility to explore what is happening inside the products, for example inside the burner, even reaching those areas that would be inaccessible through regular thermal probes, and obtaining a comprehensive map of the temperature distribution inside the combustion chamber. This has allowed us to have a realistic a priori evaluation of the combustion phenomenon and of the impacts it has on user safety during operation and to achieve a better feasibility assessment of our products. The main impacts on business are due to the considerable reduction in product development times, from weeks to days, due to the reduction in the number of laboratory experiments thanks to preventive screening. Moreover, we achieved an increased product safety assurance which has facilitated us during the quality certification process. Finally, we noticed that introducing engineering simulation in our product development process encouraged the designers to be more conscious of the technological impacts of product innovation and consequently to be more involved into the company goals.

### How do you apply engineering simulation to everyday product development?

Engineering simulation is nowadays used in almost all phases of the production chain, from design to validation, although the main focus nowadays is given to the verification of the functional requirements of our products, in order to facilitate the process of quality certification. The entire production chain is conceived around the concept of reliability, from the product itself to the process of foundry production that we have internalized. In the first case, product simulations are carried out internally by a dedicated team of 3 users, through multi-physics analysis ranging from structural simulations of large deformations to thermo-fluid dynamics, to parametric analysis. The simulations of the foundry process, from the thermo-fluid dynamic analysis of the casting process to the thermal stabilization of molds, on the other side are outsourced.

### What are your future plans for expanding the use of simulation in your Company?

Parametric product optimization is currently underway, though only at the beginning, this will certainly be an area that we will continue to leverage. Secondly, we are going to be extensively involved in electromagnetic analysis. Finally, more and more attention will be given to modeling dynamic phenomena and multi-physical modeling, downstream of case study studies. To date, the relationship between numerical and experimental activities is still biased towards the latter, both for historical reasons and for a sort of dichotomy between designers and analysts in the

product concept phase. However, we are gearing up to give greater emphasis to business impacts linked to engineering simulation, so that these benefits are understood and shared by everyone, for example by associating the simulation with each new project and intensifying its use and number of people involved, especially during the design phase.

### What added value can EnginSoft bring to you?

EnginSoft has been a valid development partner where internal skills were lacking, driving the company towards the development of more innovative products such as the new compact burner system. Through training and technology transfer EnginSoft has guaranteed the transfer of specific skills, like those needed to model complex phenomena such as combustion. EnginSoft's attention also through good post-sale technical support has prompted SIT to choose ANSYS solutions in the field of multi-physics analysis.

### Can you provide a short summary of the case study analyzed during the technology transfer in collaboration with EnginSoft?

The scope of the technology transfer activity was the thermo-fluid dynamics simulation of the combustion phenomenon within the pilot burner, i.e. the driving element that ignites the main burner at the user's request. Technically speaking, this is a Bunsen beak that heats a thermocouple so the temperature increment in the metal junction induces a voltage difference.

The boundary conditions for the analysis were the pressure and the relative position of the burner brackets with respect to the flame front.

The ultimate goal of the study was to ensure a final burner design in compliance with regulations, based on the performance index calculated as the time required to reach a stable voltage difference the voltage to decrease, in order to guarantee safe operating conditions.

The product performance indicators analyzed at the end of the job were the spatial temperature distribution and the time to reach the operating temperature, which during the exercise can result in greater or lesser safety for the user, thus determining the compliance with applicable laws. Parallel to the case study, an experimental activity was carried out to validate the computational model and to ensure its replicability. Further developments will consist of a sensitivity analysis on model parameters with the aim of increasing the fields of application and the versatility of computational models.

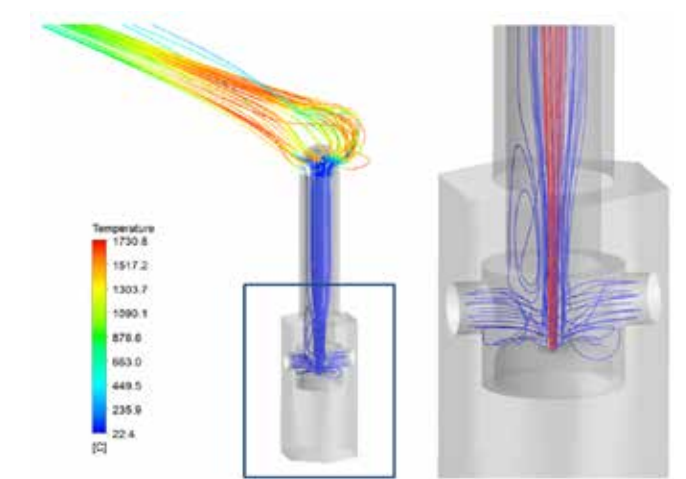


Figure 3 - Streamlines showing the starting phase of mixing between air and gas near the air inlets



# CFD analysis of an industrial burner for a regeneration gas heater application

Burners are widely used to satisfy the request of thermal energy in many industries. The design of a burner and the related heat transfer equipment must fulfill severe safety requirements, in order to avoid issues during the operation stage. One of the risk is that the flame can impinge onto tubes or other part of the equipment, with consequent safety issues. In the oil and gas industry, some fired equipment design practices dictate the maximum flame height with respect to the size of the radiant chamber. Flame length is usually determined by performing a dedicated firing test, but CFD can be conveniently used for this purpose. The present work describes a numerical analysis of a gas-fired burner in a vertical cylindrical fired heater. Starting from the 2D drawing, a 3D model of the burner and the radiant section of the heater was created and meshed with ICEM CFD. The solver ANSYS CFX was used to run the simulation. The analysis was developed in cooperation with EnginSoft, especially in the development of the 3D model and meshing stage. Different load conditions of the burner have been tested, in order to check the flame height at different conditions.

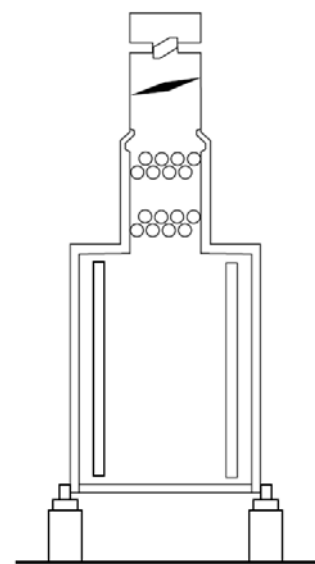


Figure 1 - Typical fired heater: cylindrical heater with vertical coil



## Introduction

Burners are used to convert the chemical energy of a fuel into thermal energy through a combustion process. The aim of these devices is to mix the fuel and air in the right proportion, initiate and maintain ignition and ensure the stability of the flame. A burner shall also be operated safely: this means that the flame shall be stable and the flame pattern shall not damage the equipment, like refractory or heat transfer surfaces. It shall also meet the required turndown capacity and fulfill the local requirements in term of pollutants emissions. Burners are widely used in the Oil&Gas industry and are key components within API 560 direct fired heaters. In direct fired heaters, the heat released by the burners is transferred to a process stream that can be used for many different purposes (e.g. feed for a reactor or a distillation column, regeneration gas for an absorption unit, hot oil heating, etc.). A typical

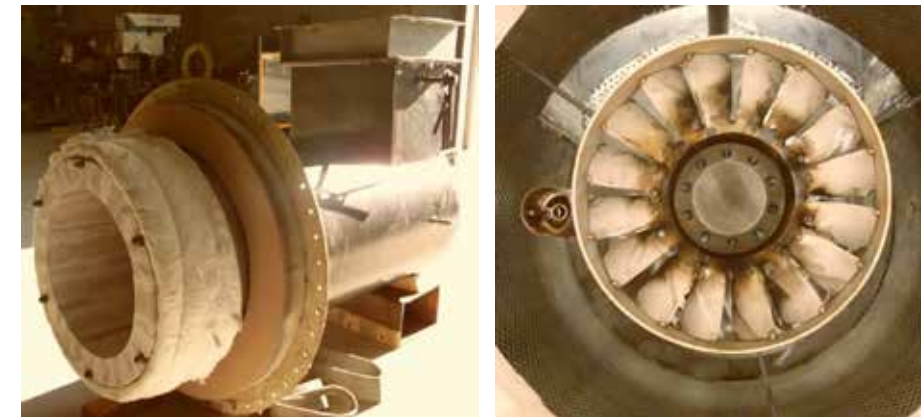


Figure 2 - Burner, (a) General arrangement, (b) swirler and burner tip

API 560 direct fired heater is divided into two sections: a radiant section, where the combustion process takes place, in which the heat is mainly transferred by radiation, and a convection section, where the flue gas cools down by convection heating the fluid inside the tubes (Figure 1). In API 560 design, the first three tube rows encountered in the convection section are made by plain tubes and are called shock tube rows: they shield the remaining part of the convective section, typically made by finned tubes, from the direct radiation of the flame. Part of the heat in the shock tube rows is transferred by direct radiation of the flame.

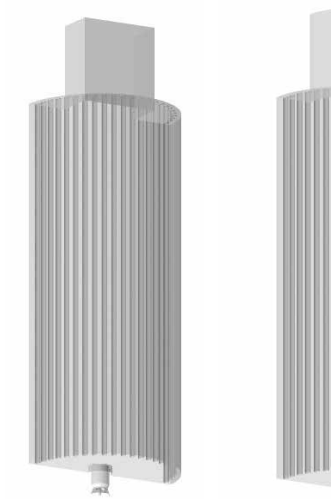


Figure 3 - 3D models, (a) 180° model, (b) 60° model

During fired heater design stage, a number of requirements regarding burner selection and arrangement has to be fulfilled to ensure a safe operation of the heater. Some fired equipment design practices dictate the maximum flame height with respect to the size of the radiant chamber. The height of the flame is usually assessed with a firing test, except when the burner capacity exceeds the maximum allowable load of the test facility. In this case CFD can be conveniently used for the purpose of a preliminary assessment, since the only opportunity to perform a physical test would be given with the burner already installed at field. The development of an accurate CFD model could represent an economical and time saving alternative to both firing tests and field tests.

	Case 1	Case 2	Case 3
Burner heat release (MW)	15.52	12.37	8.7
Radiation duty absorbed by radiant tubes (MW)	8.57	7.38	5.81
Radiation duty absorbed by shock tubes (MW)	0.45	0.37	0.27
Air mass flow (kg/s)	5.873	4.689	3.406
Fuel mass flow (kg/s)	0.352	0.283	0.191

Table 1 - Analysis cases

## Case Study

The case study is a regeneration gas fired heater designed and supplied for a project in Oman. Design is of the vertical cylindrical type according to API 560. The heater is equipped with a single burner and forced draft fan. The fuel is a gas constituted by a mixture of various hydrocarbon. The main components are methane, ethane and propane: those components accounts for the 90% of the total mixture. The radiant section is cylindrical, and the process tubes are vertical. The fluid is distributed in four parallel passes, with 12 tubes per pass (Total 48 tubes in the radiant section). The burner is placed on the floor of the chamber. It's a staged fuel burner: a portion of the fuel and all the combustion air are mixed in a primary combustion zone, while the remaining part of the fuel is supplied through a series of nozzles around the perimeter of the burner. Before entering the combustion chamber, the air flows through a swirler, to ensure proper mixing in the primary combustion region. A picture of the burner is reported in Figure 2.

Aim of the analysis is to determine the flame length in three different operating conditions: Table 1 reports the burner heat release, duty absorbed and flow rates

for both air and fuel for the three cases considered. Many definitions for the flame surface are possible: for the purpose of this work the flame has been defined as the iso-surface at a temperature of 1400K.

## CFD model

The model has been implemented by Enginsoft. Starting from the burner manufacturer drawings, a 3D model has been created directly using ICEM CFD, which was also used to mesh it. Since the focus of the analysis is the flame structure, only the radiant chamber has been modeled. There is the possibility to analyze just a portion of the domain, given the symmetries that are present. Unfortunately those symmetries doesn't quite match between each other: there are 6 nozzle for the staged fuel, 10 for the primary fuel, 4 tube passes and 48 tubes. The only effective symmetry is a 180° portion of the domain, also because the outlet of the domain is rectangular, not circular. Simulating half of the radiant chamber would be the better solution from an accuracy point of view. Anyway it would require a significant computational time. In order to understand the effect of the periodicity, two models have been created: one model has a periodicity of 180°, one of 60° (the periodicity of the staged fuel nozzles). The nozzle diameter of the burner for the second model has been opportunely scaled in order to obtain the correct exit velocity. Also the temperature of the process fluid has been

adapted to remove the correct process duty out of the domain. The aim is to understand the impact of the assumptions of the simplified model on the flame height. For this purpose, the two models have been solved for Case 1, and the results have been compared. The two models are depicted in figure 3. The case has been solved with ANSYS CFX. The following boundary conditions have been set:

- Inlets: Mass flow rate, composition and temperature have been specified for both air and fuel. For the 60° an inlet velocity profile has been set; it has been determined with an independent model of the swirler.
- Outlet: gas flow exit the fluid domain. A pressure has been set. An energy sink has been defined in order to consider the radiant heat transfer to the shock tubes. A pressure drop has been set to simulate the presence of the tubes of the convective section and set the correct air pressure at the inlet.
- Process tube walls: Heat transfer coefficient and bulk temperature have been set; temperature values are indicate in datasheet, wall heat transfer coefficient and tube emissivity have been set in order to extract by tubes the heat duty defined in table 1.
- External walls: the heat loss is simulated with a heat transfer coefficient and an outside temperature

The chemical reactions which take place in the system have been explicitly simulated in order to accurately predict the temperature field in the entire system. The following reaction mechanism has been included in the model:

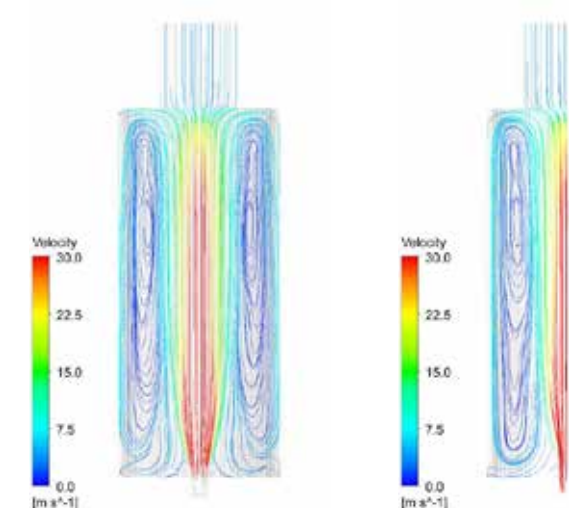
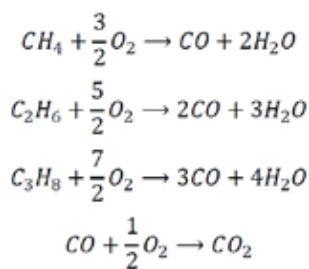


Figure 4 - Velocity streamlines, Case 1, (a) 180° model, (b) 60° model,

SST (Shear Stress Transport) turbulence model has been applied. Buoyancy effect has been considered. Monte Carlo Radiation Model has been applied for the radiation heat transfer.

### Results

The Velocity streamlines are reported in Figure 4 for the 180° model and the 60° model. It can be seen the typical flow pattern of a heater: fuel and air enters at the bottom, flue gas flows through the center of the chamber. Part of the cold flue gas flows downward along the tubes, at the periphery of the chamber. The streamlines patterns are quite similar for the two models.

Figure 5 reports the temperature profile at the symmetry plane for the two models: the points with highest temperature are located in the combustion region over the burner, where the chemical reactions take place. The coldest region is located in the lower part

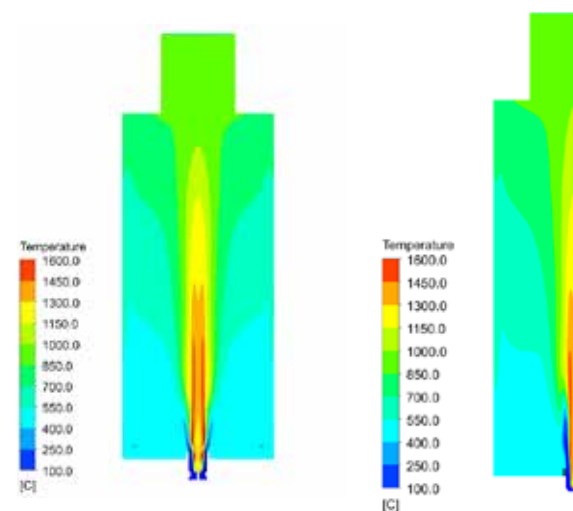


Figure 5 - Temperature profile, Case 1, (a) 180° model, (b) 60° model

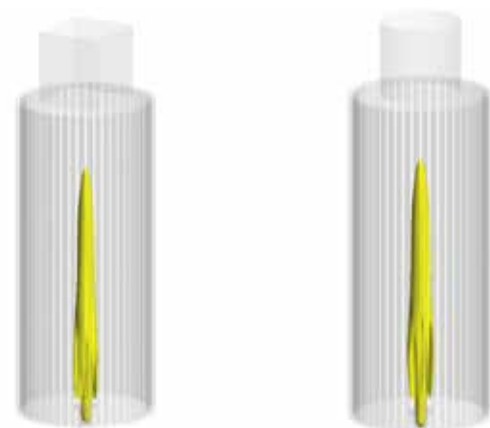


Figure 6 - Iso-surface at 1400K, Case 1, (a) 180° model, (b) 60° model

of the chamber far from the burner: the recirculating flue gas flows downward and it's cooled by the process tubes. The difference in the temperature profiles between the two models are concentrated in the lowest part of the chamber.

The iso-surface at 1400K are depicted in Figure 6. There are some differences in the shape of the surfaces, especially in the bottom part. Figure 7 reports the maximum height of a iso-surface for many temperatures: at 1400K the difference between the values

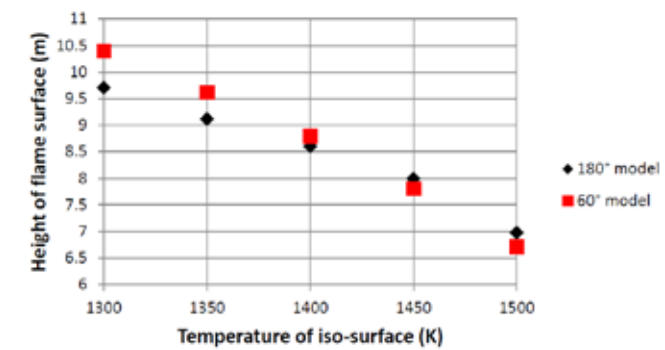


Figure 7 - Maximum height for iso-surfaces at given temperatures

predicted by the two models is limited. Both the values are lower than the maximum flame height for this specific heater (9 m). The other cases have been run with the 60° model. The streamlines for those cases are reported in Figure 8, while the iso-surfaces are depicted in Figure 9. The flame height are respectively 7.37m and 4.83m for case 2 and 3.

### Conclusions

A CFD analysis of an industrial burner has been performed. Two models have been created and compared: in the first one half of the radiant chamber has been simulated, in the other one sixth. The two models have been tested with the same conditions: velocity streamlines, temperature profile and flame surface have been compared. Although the smallest model doesn't fulfill all the symmetry requirements of the real geometry, its results are in good agreement with the biggest model calculation. Other two cases have been analyzed, and the flame height has been determined. The results proof that the flame height can be determined with reasonable accuracy with the 60° model, with a consequent save in terms of computational efforts. The heater is planned to be started-up in 2018. Accurate observation of the flame will provide significant feedbacks to the outcomes from the CFD study. Positive feedbacks will provide strong support in confirming CFD models as a reliable alternative to firing tests.

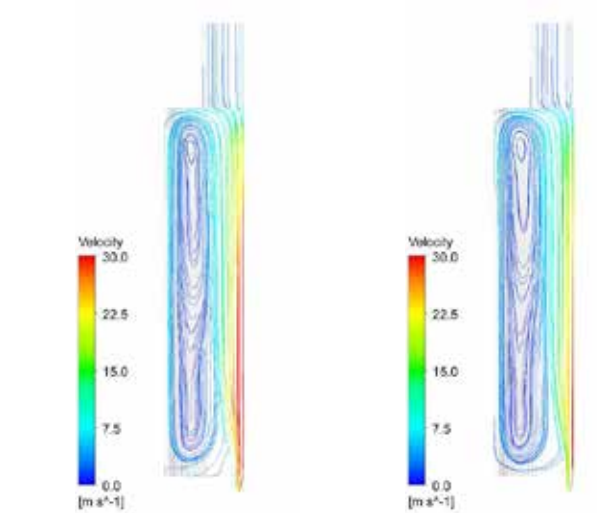


Figure 8 - Velocity streamlines, 60° model, (a) Case 2, (b) Case 3



Figure 9 - Iso-surface at 1400K, 60° model, (a) Case 2, (b) Case 3

D. Agazzi, T. Odry, M. Rottoli - Brembana & Rolle  
A. Troia - EnginSoft

## Thermal Analysis with ANSYS

The effects of heat and thermal management of structures is more and more critical as performance limits are pushed further by the need to have lighter, smaller and more efficient designs. Convection, radiation and conduction loads are obvious, but the need to include the effect of power losses and thermal energy from external sources such as pipe flows means that analysts need to have more tools at their disposal to simulate thermal models accurately.

For more information: Anna Rosa Troia, EnginSoft  
a.troia@enginsoft.com

# Ultra-Wide Band Radome CAE Optimization



Fig. 1 - Radome in Elettronica SpA anechoic chamber

We show here the design of a radome for electronic warfare covering an entire signal intelligence system. The radome design was very challenging from both an electromagnetic (EM) and a mechanical point of view because of its size and bandwidth. In particular, we want to show how the choice of the correct simulation environment can prevent simulation artifacts, leading to a successful design.

## Introduction

A radome is a cover placed above an antenna to protect it from the external environment. An ideal radome would protect the antenna from any physical damage and be electromagnetically transparent in its operational frequency band. Nowadays, radomes are widely used on ground, airborne and maritime application.

The growth in the use of the electromagnetic spectrum lead to an improvement in the radome performance. In particular, during the last decades composite materials became the preferred choice for antenna radome due to their low thickness and high mechanical strength.

A radome can be designed in a monolithic or sandwich fashion. The monolithic radome is made of a single solid layer, while the sandwich radome alternates high-density (aramid fiber, fiberglass) and low-density materials (honeycomb, foam). In this work, we focus on sandwich radomes.

A sandwich stratification can be electromagnetically modeled using an equivalent transmission line: each layer is represented by a shunt impedance, defined through the thickness of the layer and its characteristic impedance. Eventually, one can predict the transparency of the whole stratification knowing the electric behavior of each layer. It is worth noting that a larger number of layer does not necessarily mean higher reflectivity. In fact, the sandwich stratification can be viewed as a shunt-inductance-coupled filter, where the goal is to insert a pole in the operational band.

## Radome scenario

In Elettronica SpA we design and produce system for electronic warfare (EW). Each system has to meet different requirements, depending on the platform and the purpose (jamming, support measurement).

In this case, we consider a terrestrial system for signal intelligence, using more than 40 ultra-wide band (UWB) antennas to detect the

threats. The peculiarity of this system is that a single radome has to protect all the antennas. In this scenario, the radome design represents a great challenge from both a mechanical and an electromagnetic (EM) point of view. In fact, the shape of the radome is, approximately, a cylinder with a diameter of 1 m and a height of 0.8 m, as shown in Fig. 1. It has to be strong to withstand difficult environmental conditions. At the same time, it has to be electromagnetically transparent from DC to 40 GHz.

## Radome design

The first step for the EM design consists in the maximization of the transmission coefficient of the sandwich stratification, given the mechanical constraints. In our case, the constraints are related to the total thickness of the radome and the thickness of the inner and outer layers of prepreg.

## First Prototype

A numerical optimization of the stratification has been performed. The chosen stratification alternates aramid fiber and honeycomb. The total thickness, after the optimization is 8 mm.

EM full wave simulations have been performed on the antennas behind the radome to evaluate the perturbations introduced on the radiation pattern. The radome dramatically increases the simulation spatial domain and, for some of the antennas, the problem was too complex with the available computational resources. On these antennas, approximations in the simulation setup have been introduced. In particular, a sinuous antenna working in a band 1-18 GHz has been substituted by a field source radiating behind the radome. The simulation results show that the level of perturbation on the radiation patterns was considered acceptable and a first prototype has been manufactured.

The radome has been measured, but the result was unexpected: the radiation pattern of the sinuous antenna was deeply deformed, exhibiting a minimum at the boresight for some frequencies.

## Solution identification

The perturbation of the radiation pattern is particularly strong in the higher part of the band, where the radiating surface of the antenna is small compared to its physical size. This destructive

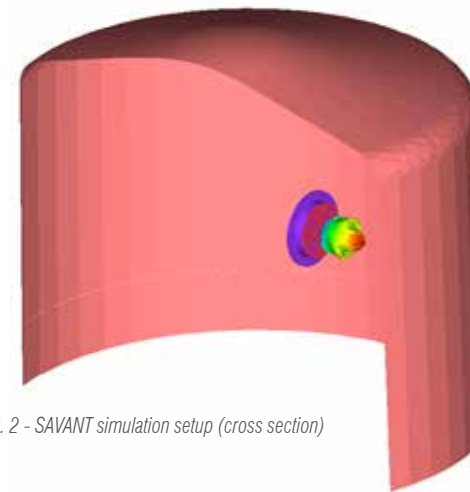


Fig. 2 - SAVANT simulation setup (cross section)

phenomenon is related to the reflected field contributions bouncing on the inactive part of antenna itself, radiating with opposite phase.

A smart simulation environment had to be tailored to reproduce the pattern perturbation, giving confidence for a successful redesign. The solution has been found in cooperation with EnginSoft, making use of ANSYS Savant. The software is based on a ray-tracing method. The setup is shown in Fig. 2: the equivalent field source is placed inside the radome. In order to reproduce the perturbation effect, the structure of the antenna has been placed in its position (without being fed). This expedient allows the antenna structure to reflect without overcomplicate the simulation.

The simulated radiation pattern at 17 GHz is shown in Fig. 3. This frequency has been chosen to clearly show the described phenomenon. The simulation is in line with the measurement results.

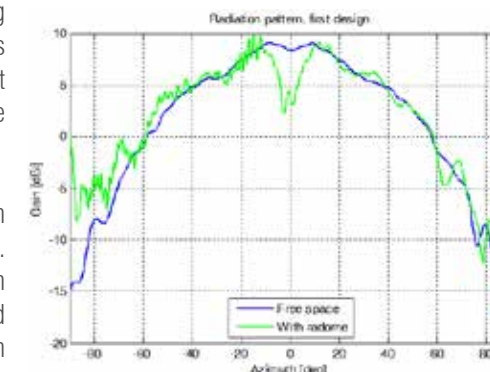


Fig. 3 - First design, simulated radiation pattern @ 17 GHz

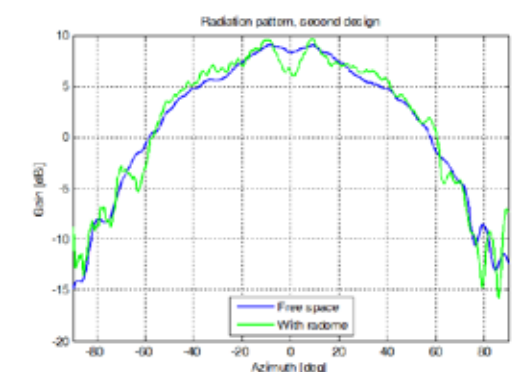


Fig. 4 - Second design, simulated radiation pattern @ 17 GHz

## Second Prototype

With a greater confidence on the simulation results, a second stratification has been designed. The design of the stratification favors the transparency in the higher portion of the band of the sinuous antenna. The simulation results are shown in Fig. 4. The prototype of this new stratification has been manufactured and measured. The measurement results are in line with the simulations.

## Conclusions

In this paper, we showed the design of a challenging radome. The operational band is from DC to 40 GHz and it covers an entire system for signal intelligence. The approximations introduced during the design lead to a strong perturbation in the radiation pattern of an UWB sinuous antenna, discovered in the measurement stage. Identifying a more effective simulation setup, a second version of the radome has been successfully designed and manufactured, with an agreement between simulations and measurements.

Francesco Scattone, Antonio Manna - Elettronica  
Andrea Serra - EnginSoft

# ANSYS HFSS SBR+ Solver Option

The ANSYS HFSS SBR+ Solver Option - formerly Delcross Savant can be added to the ANSYS Electronics Desktop or any of the ANSYS products that utilize the ANSYS Electronics Desktop. This solver-only option does not include a GUI. With this option, you can add the HFSS SBR+ solver to your existing ANSYS Electronics Desktop cost-effectively and maximize your investment in ANSYS technology.

HFSS SBR+ is an advanced antenna performance simulation software that provides fast and accurate prediction of installed antenna patterns, near-fields and antenna-to-antenna coupling on electrically large platforms. HFSS SBR+ analyzes installed antenna performance on platforms that are tens to thousands of wavelengths in size. It leverages the asymptotic Shooting and Bouncing Ray Plus (SBR+) technique to efficiently compute accurate solutions with incredible speed and scalability.

The state-of-the-art technology in HFSS SBR+ includes advanced physics models such as creeping waves, UTD diffraction rays and surface curvature extraction not available in other commercial electromagnetic solvers.

For more information: Andrea Serra, EnginSoft - a.serra@enginsoft.com



# Filming the Bloodhound Super Sonic Car Land Speed Record

The Bloodhound project was inceptioned in 2008 by Richard Noble and Andy Green, past and present holders of the land speed record. The project aims to set the new land speed record of 1000mph, with the Bloodhound Super Sonic Car (SSC), Figure 1. The record attempt is set to take place on an 18km long stretch of the Hakskeen salt pan in the Northern Cape, South Africa. An inspiration to the next generation of scientists and engineers, the project aims to promote interest in Science, Technology, Engineering and Maths (STEM) subjects among school learners and to stimulate cutting edge research. The Hakskeen track, chosen for its length, uniformity and favourable weather conditions, is an exciting chapter for South Africa, promoting tourism and even creating many jobs in the preparation of the track.

The Bloodhound is powered by a Eurojet EJ200 jet engine and a Nammo rocket cluster, producing a maximum combined thrust of 210kN, and is projected to accelerate from 0 to just over 1000mph in under a minute, Figure 1.

## The Filming System

The topic of a final year Mechanical Engineering project was to design a system to film the Bloodhound land speed record attempt. The system was required to film the Bloodhound at a distance of 50m. The system could not interfere with the vehicle in any way.



Figure 2 - S-18 Supersonic Filming Drone

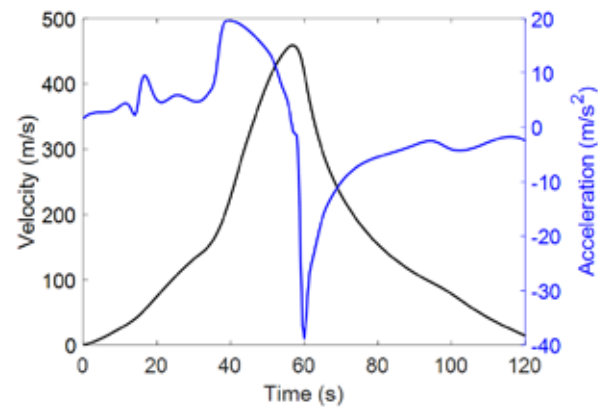


Figure 1 - Bloodhound SSC - Projected Performance

## The S-18 Supersonic Filming Drone

A supersonic aircraft drone prototype, Figure 2, was designed based on accepted aircraft design estimates for drag, stability and stall, ahead of CFD and wind tunnel testing.

## The Design Process

Aircraft design commonly relies on analytical and empirical estimates to produce prototype designs. Given the complex dynamics of aircraft performance, these prototypes must always be tested and developed numerically (CFD) and physically (wind tunnel data). It is crucial that prototype solutions be optimal, according to all design estimates, to reduce iteration at the testing stage, which is often costly and time consuming. Thus, the design process was focused on optimizing available design estimates to produce an effective prototype.

## Parametrization

Considering existing drones designed for supersonic flight, such as military target drones, the aircraft geometry was parameterized to include a wide range of reasonable solutions. A set of independent input parameters were selected, usually dimensionless ratios, and corresponding ranges were defined for optimization. This parameterization is illustrated in Figure 3.

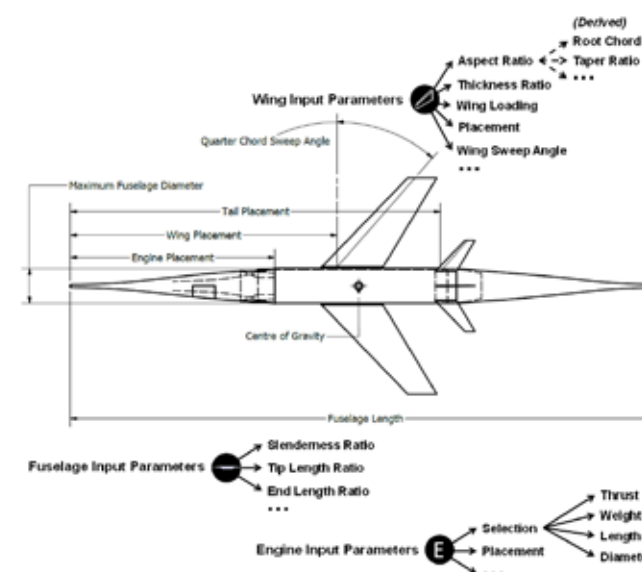


Figure 3 - Parameterization

## Aerodynamic Drag Performance

Drag estimates for the wing, fuselage and tail were combined to estimate the total drag over the operating range ( $M < 1.29 \approx 1000\text{mph}$ ). The required thrust was estimated as the sum of the aerodynamic drag and the inertial constraint – matching the Bloodhound acceleration, Figure 4. For any engine selection, the minimum margin between the available and required thrust was determined. This margin is the drag performance outcome. The margin must be positive, and should be maximized to ensure that the aircraft is always capable of matching the Bloodhound's acceleration.

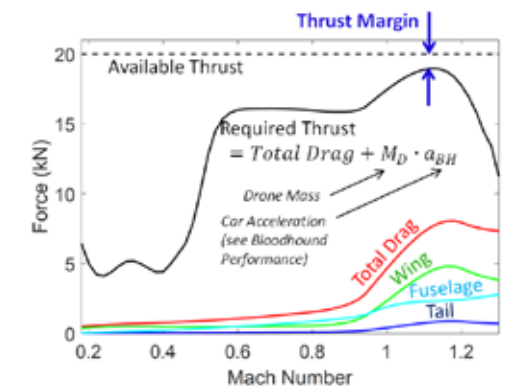


Figure 4 - Drag Performance

## Longitudinal Stability

Maintaining level flight requires a balance of forces, between the total lift and weight of the aircraft, and a balance of moments, producing zero pitching moment. The basic force diagram of this configuration is given in Figure 5.

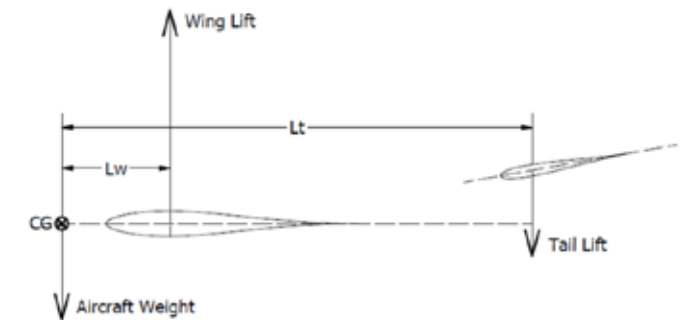


Figure 5 - Longitudinal Stability

A further requirement of steady flight is positive pitch stiffness. Fluctuations in pitching moment should produce negative feedback to restore balance. This pitch stability may be characterized by the pitch stiffness – the derivative of pitching moment coefficient with respect to angle of attack:  $\text{Pitch Stiffness} = -(\partial C_m) / \partial \alpha$

The pitch stability was estimated over the operating range of the aircraft under level flight conditions, Figure 6. The stability is seen to increase drastically near Mach 1, caused an aft shift of the centre

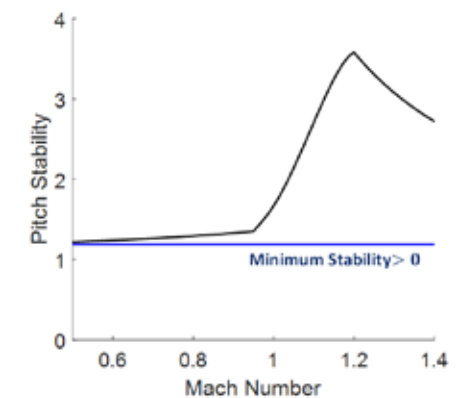


Figure 6 - Pitch Stability

of lift. The minimum stability is the longitudinal stability design outcome. It must be positive, and should be maximized to ensure stability at all operating conditions.

### Stall

By solving the longitudinal balance, the effective wing and tail angles for level flight were determined over the operating range, Figure 7. Assuming a moderate constant stall angle of 15°, the minimum take-off velocity was approximated, which is the stall design outcome. Minimizing the take-off velocity allows rapid take-off, with improved repeatability.

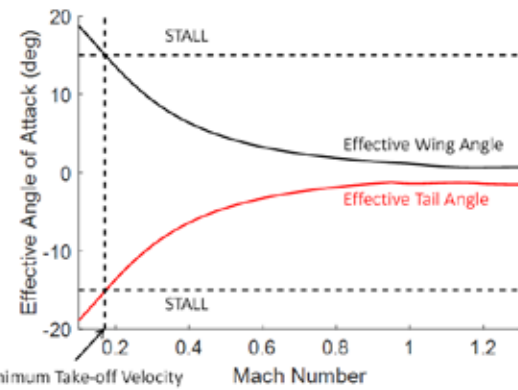


Figure 7 - Stall

### Performance Model

Analytical and empirical performance estimates for drag, stability and stall were encoded digitally in MATLAB codes. Given a set of independent input parameters, the entire parameterization could be automatically constructed, and performance estimates could be rapidly generated for optimization.

### Optimisation

The MATLAB performance model was optimized in modeFRONTIER, using a multi objective genetic optimization algorithm, MOGA II. The modeFRONTIER workflow is illustrated in Figure 8. A

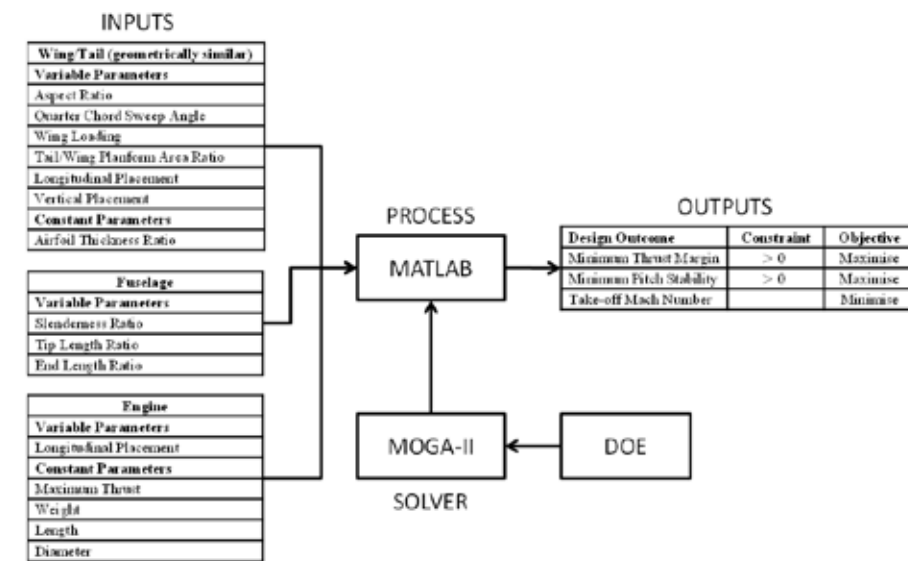


Figure 8 - modeFRONTIER Workflow

design of experiments (DOE) was constructed from 100 random parameterizations. The MOGA II genetic algorithm tested the DOE via the MATLAB model, and evolved parameter sets based on the performance outputs until over 8000 valid solutions were generated and a 3-dimensional Pareto Frontier was resolved, Figure 9. This frontier characterizes optimal trade-offs between the design objectives.

A moderate selection from the frontier was made and reduced based on further area ruling considerations. The 18th item from the frontier was selected as the primary prototype for further development. This is the S-18 design.

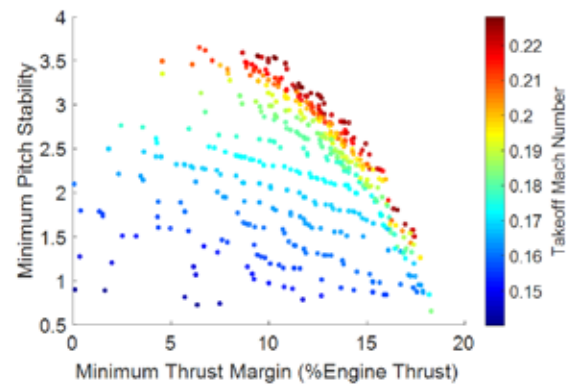


Figure 9 - Pareto Frontier

### Conclusion

A prototype supersonic aircraft was developed to film the Bloodhound land speed record. By optimizing a generalized aircraft configuration within a large design space, the potential of available design estimates could be maximized, avoiding guess work in the preliminary design phase. A successful prototype design should reduce the time and cost of numerical (CFD) and wind tunnel testing.

Timothy Missing, Michael Boer  
University of the Witwatersrand,  
Johannesburg, South Africa

For more information:  
Francesco Franchini, EnginSoft  
f.franchini@enginsoft.com



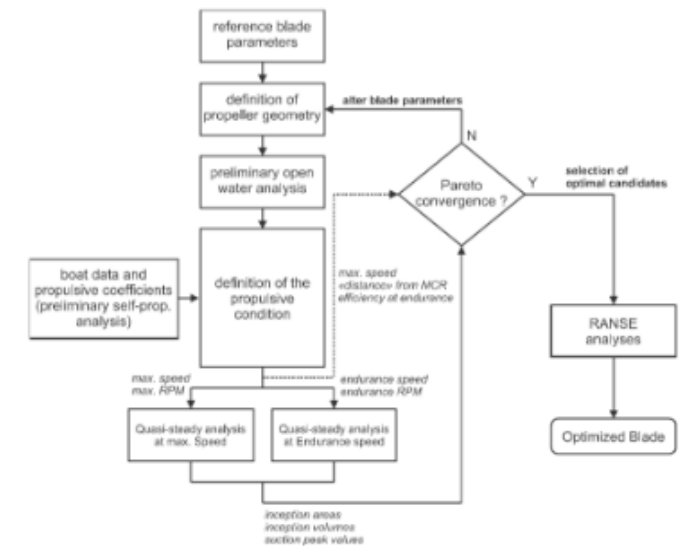
## Azimut Benetti propels cruise speed with modeFRONTIER

Azimut Benetti Group is the world's largest network producing megayachts and leading private group in the luxury yacht industry. Azimut-Benetti's R&D Centre develops unique technologies, for an effortless and safe navigating experience. The Naval Architecture and Marine Engineering Unit (DITEN Department) of Genoa University work jointly with DETRA Custom Propellers and Azimut Benetti's R&D Centre, using modeFRONTIER to optimize the design of a custom propeller for a high-speed Azimut Benetti 95 RPH yacht.

modeFRONTIER helped increase cruise speed and reduce cavitation in marine propellers

### CHALLENGE

The design of a propeller is always a trade-off between competing objectives and constraints: maximizing the propulsion efficiency and ship speed while avoiding cavitation and maintaining a sufficient blade strength. The traditional lifting line / surface methodologies define the propeller shape by including simplified geometric assumptions that make them not suitable for modern fast propellers design. The application of more accurate flow solvers and the automatic investigation, possible through the parametric description of the geometry (unconventional combinations of pitch, camber, or, for instance, local hydrofoil shapes), proves to be a successful design alternative for a high-speed propeller.



The modeFRONTIER optimization environment has been selected to build the optimization flow

### SOLUTION

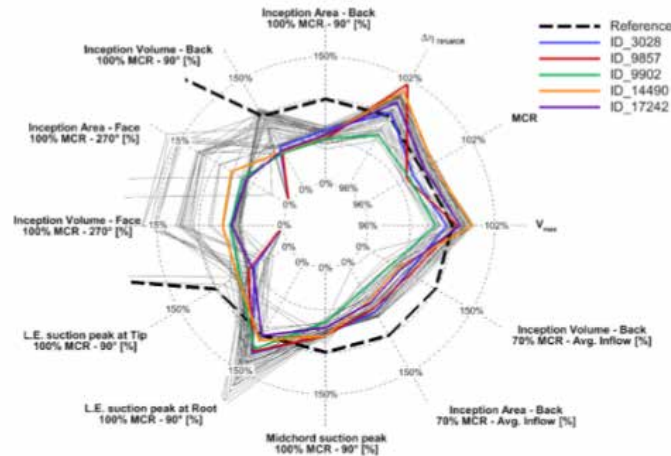
Following this new approach, the optimization of a reference propeller with modified rake distribution was driven by the MOGA-II, the genetic algorithm included in the automation workflow in modeFRONTIER. The experimental data collected at the cavitation tunnel confirmed the reliability of both the Boundary Elements Method and RANSE numerical approaches. A dedicated full-

scale sea trials, performed with propellers manufactured by Detra, showed that the cruise speed achieved with the optimized propeller is 1 kn higher than the baseline propeller speed,

geometry by while the cavitating behavior was also significantly enhanced. "The result is remarkable, especially keeping in mind that the increase of cruise speed, together with the enhancement of comfort onboard, is crucial to the perception of luxury yacht customers", said Francesco Serra, R&D Office, Azimut Benetti Group.

#### modeFRONTIER ADVANTAGES

modeFRONTIER helped build an optimization framework to interact with the parametric description of the geometry to define each new blade shape and employ flow solvers to quantify how each propeller fulfills the constraints and the objectives of the design. "Starting from a set of 48 blade parameters to alter the reference propeller geometry, the use of MOGA-II algorithm allowed to compute and test 50,000 different geometries in about 5 days to achieve a satisfactory Pareto convergence and choose optimal candidates (one for any rake distribution) for RANSE analyses" said Michele Viviani, Associated Professor at DITEN Department, Genoa University.



Pareto diagram. Optimization with the modified rake distribution

## NEW INTEGRATION COUPLING modeFRONTIER WITH ROCKY DEM ANNOUNCED

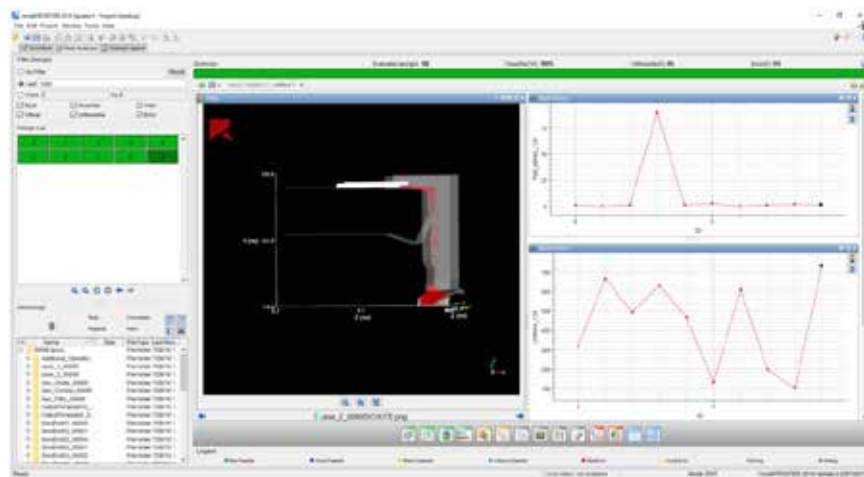
ESTECO is proud to announce that users of process integration and optimization software modeFRONTIER and Rocky Discrete Element Modeling (DEM) will now be able to couple the two software with a new integration node

The ESTECO platform provides a multiobjective optimization environment for users of the Rocky DEM particle simulator. Rocky uses Discrete Element Modeling (DEM) to predict the behavior of bulk solids and aids in the efficient design and optimization of material handling equipment and processes. Rocky DEM is capable of simulating realistic and concave particle shapes, particle breakage, boundary surface reduction due to wear, sticky and dry material contact laws, multiphysics, and more. Its explicit DEM solver uses either multi-core CPU or GPU processing that drastically reduces computational run times.

With the new integration node, linking input and output parameters related to material properties is now effortless. Users just need to drag and drop Rocky parameters into the modeFRONTIER workflow. After creating an initial DOE, the user can select and exploit the most suitable optimization algorithm, that will automatically drive the simulation

process to optimize a given geometry. modeFRONTIER advanced optimization and process automation capabilities lead to optimal design solutions in shorter time.

For more information: Francesco Franchini, EnginSoft  
f.franchini@enginsoft.com



## Front-End Loader Linkage Durability Analysis Using Load Input from True-Load



Figure 1 - CAD model of vertical lift loader assembly on chassis

This document describes the use of Abaqus/CAE, Abaqus/Standard, True-Load, and Verity weld analysis in fe-safe software to evaluate the durability of a front-end loader linkage. Dynamic field loading for FEA of construction equipment is not always easily replicated by traditional linear static loading methods. Wolf Star Technologies True-Load software along with unit load FEA in Abaqus was used to determine time history loads for a field operation with dynamic loading that resulted in fatigue failures of the linkage. The time history loading was then used in fe-safe to compare the durability of design alternatives and determine a design that met the simulation criteria. The methodology greatly improved the confidence of the design developed through simulation because the field loading was accurately reproduced.

### 1. Introduction

Finite element analysis is a useful tool for the evaluation of the structural components of construction equipment. A common approach is to apply static loads to the finite element models to represent loading under normal field operations. The static loads applied often represent "worst-case" forces under those operations. The structure under investigation is then determined to be acceptable or not based on meeting target values for stress, strain, deflection, and/or some other criteria. One concern with this approach is that it may miss potential fatigue issues. Estimated fatigue life for a given load can be determined using stress-life or strain-life calculations. However, the dynamic nature of the loading is difficult to reproduce. A single field operation may require numerous static load cases to simulate the complete range of forces applied, and cycle counts are difficult to estimate. Another

problem with representing dynamic loading with worst-case static loads is that it neglects the relatively low strain, but high cycle loads that can result in fatigue problems. Machines such as skid steer loaders (SSLs) and compact track loaders (CTLs) perform a wide variety of tasks that often involve highly dynamic loading. Accurately reproducing these dynamic loads in the finite element simulations greatly improves the confidence in the results of the evaluation and allows the analyst to compare design alternatives effectively.

The finite element modeling capabilities available in Abaqus/CAE allow the analyst to create simulation models that provide accurate response to the applied boundary conditions and loading. The key to using this technology for the fatigue analysis of construction equipment is applying loading that reflects the dynamics of the field operations. True-Load software accurately duplicates time-history field loads and has a user interface that is directly integrated with Abaqus/CAE. A unit load model, in which any possible load path into the structure is represented by a unit load, is first solved in Abaqus to determine strain response to the unit loads. True-Load/Pre-Test then uses the strain response to determine optimal strain gauge locations that effectively turn the structure into its own load transducer. Strains are then recorded at the True-Load strain gauges during field test. The test strain data is then read into True-Load/Post-Test to determine the time history load functions by calculating the scaled unit loads that recreate the strains produced during the test. Once the time-history loading is determined, the full field response of the structure is determined by applying the scaled loading in True-QSE, which superimposes the time-history

loading on the unit load model. The time-varying stress, strains, and deflections are determined at each node and element of the structure. True-Load/Post-Test also has built-in functionality to automatically output the time series loading in fe-safe format so that fatigue analysis of the structure can be completed. In the case study presented in this paper, design alternatives for a front-end loader linkage were evaluated by the linear static FEA approach as described above and by an approach utilizing True-Load software to recreate field loading on the Abaqus FE model. Once accurate field data were applied to the model, Verity weld fatigue analysis was used to validate a design that met the simulation durability target.

## 2. Background

Skid steer loaders and compact track loaders are used in the construction, landscaping, and agricultural industries and perform a wide variety of tasks. The current product line for Case Construction and New Holland Construction SSLs and CTLs include machines with either radial lift or vertical lift loader assemblies. The radial lift machines employ a loader arm that pivots about a single axis of rotation on the chassis and lift cylinders to raise and lower the arm along a radial path. The vertical lift loader arm includes linkages that attach at different points on the chassis and loader arm so that the arm raises and lowers along a path with a greater vertical reach, which is more advantageous for certain operations. An assortment of front-end loader attachments are available that allow an operator to perform a wide range of jobs. These various field operations create a challenge for the analyst to validate designs through simulation.

The purpose of this project was to validate a design solution to resolve fatigue failures on the H-link in the vertical lift loader arm assembly. The H-link is a welded assembly that is connected to the chassis at two pins and to the loader arm boom at two pins. Figure 1 illustrates the CAD geometry for the vertical lift loader arm at the maximum height orientation and assembled to the chassis. The H-link is shown in the dark grey color.

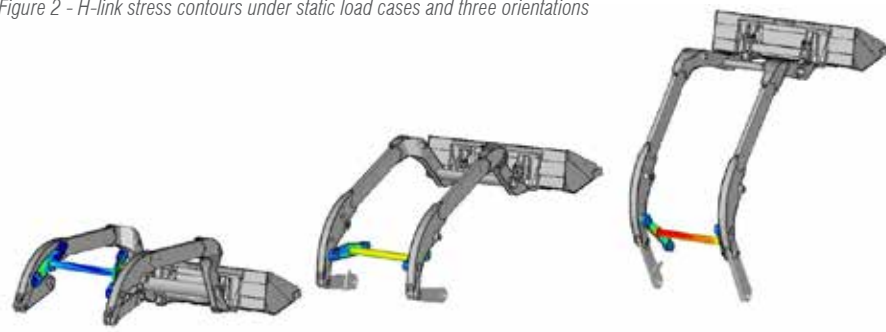
## 3. Methodology

It was determined that the failures were occurring on machines used primarily for one particular field operation, which involved the use of a specialized attachment at the front of the loader. Once the primary operation causing the fatigue problems and the failure location on the H-link were identified, design alternatives were developed through simulation prior to a final field test of the recommended design.

### 3.1 Linear Static Loading Approach

The first step in evaluating the alternative designs was to update existing FE models of the current loader assembly design and run linear static loads calculated to be the expected maximum for the operation of concern. In order to approximate the operation, the models were run with the loader arm at three different orientations and various load scenarios were applied at these orientations. Stress values were compared for the current design and for the

Figure 2 - H-link stress contours under static load cases and three orientations



alternative H-link designs. Stress-life calculations were then used to estimate the expected life improvement of the design alternatives. The target life improvement was determined by comparing the number of hours to failure against the desired number of hours for the operation. Figure 2 illustrates the stress contours of H-link with the loader assembly at the three orientations with one of the static load cases applied. The design developed through this approach was later evaluated with field loading, but it did not meet the goal for the number of hours for the operation.

### 3.2 True-Load Approach

To increase confidence in the simulation results a better understanding of the loading for this operation was required. An Abaqus/CAE unit load finite element model of the current H-link was created. The mesh consisted of shell, hexahedron, and beam elements. Because the only load paths into the H-link are through the four pin locations, the model was set-up with unit loads at each of the four pin joints. Each joint is free to rotate in the direction of the pin axis (in the model Z direction), freeing up one degree of freedom. Unit loads were applied for each of the five remaining degrees of freedom, three force unit loads in the X, Y, and Z directions and the two moment unit loads orthogonal to the pin

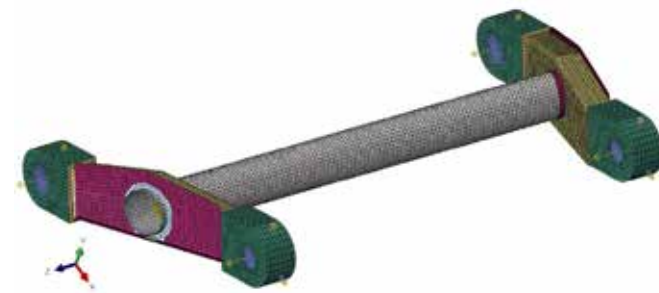


Figure 3 - H-link unit load model with pin forces and moments

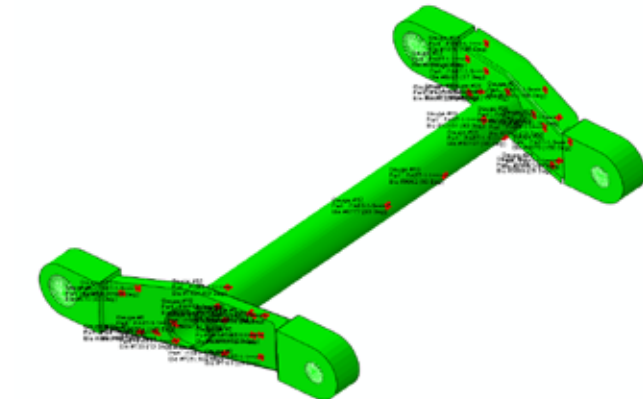


Figure 4 - H-link unit load model with strain gauges placed by True-Load



Figure 5 - True-Load gauge dimensioned in Abaqus/CAE and located on test part

axis in the X and Y directions. Inertia relief was included to prevent rigid body motion. This resulted in twenty unit load cases. Figure 3 shows the unit load model with the forces and moments applied at each pin in Abaqus/CAE.

A linear perturbation analysis was solved in Abaqus/Standard and the result file loaded into True-Load/Pre-Test, which determined the optimal placement of the 33 strain gauges it determined were needed to accurately reproduce the loading based on the strain field for all unit loads. Figure 4 shows the Abaqus/CAE H-link unit load model with the strain gauge locations as identified by True-Load.

Through the True-Load user interface, the analyst can easily relocate gauges and place dimensions to the gauges directly on the Abaqus/CAE model. This ensures the gauges will be placed on the physical part in the correct locations determined by True-Load and that the gauges are placed in accessible areas where they will not be damaged during test. A STEP file of the H-link geometry was read into Abaqus/CAE so that dimensions could be placed relative to actual part surfaces as opposed to the mid-surfaces where the shell mesh was placed. Figure 5 shows one of the True-Load strain gauges dimensioned on the Abaqus/CAE model and the location marked on the test part.

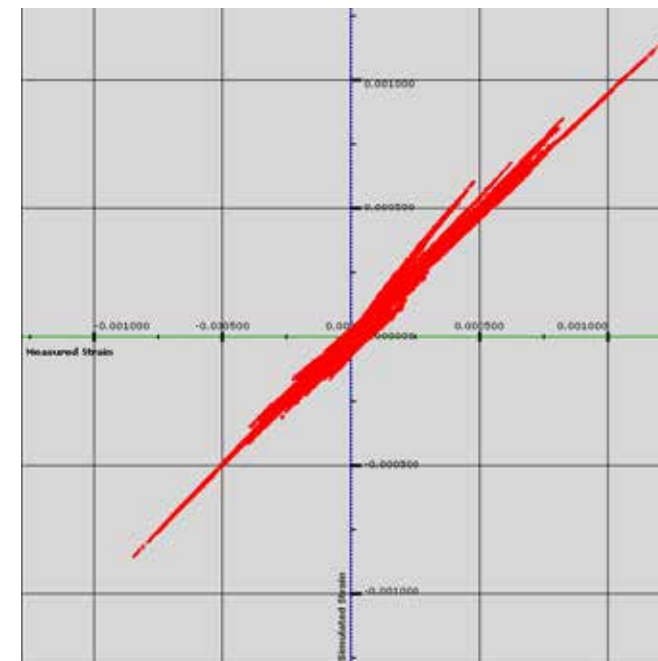


Figure 6 - Strain correlation plot between simulated strain and measured strain for all True-Load strain gauges

After the True-Load gauges were placed, a field test that duplicated the operation of concern was completed and the strain results were loaded into True-Load/Post-Test. The load functions were then calculated and output in fe-safe format for subsequent fatigue analysis. The load scale factors were then used in True-QSE to use superposition of the load functions on the unit load model to simulate the field loading on the entire H-link FE model. To confirm that the simulated strains are correlating well with

the strains measured during test, True-Load/Post-Test produces a detailed summary of the analysis that includes True-Load gauge correlation results. For the H-link, the report indicated excellent correlation with the worst True-Load gauge producing 10.3% Root-Mean-Square (RMS) error and the best producing 0.14% RMS error. To further illustrate the excellent correlation results, Figure 6 shows the cross plot comparing the simulated strain to the measured strain for all 33 of the H-link True-Load gauges.

In addition to the True-Load gauges, strain gauges were also placed in the expected low life locations. The ability to load the entire model with the time series loading in True-QSE means that the time-varying stress, strains, or deflections at any point in the model can be determined for the field operation. Figure 7 shows a segment of the time trace comparing the simulated strain from the Abaqus model to that same time segment at one of the gauges in the expected low-life location. The nearly identical strain traces greatly improved the confidence that the simulation model was accurately duplicating the strains produced on the entire H-link.

The next step in the current production H-link analysis was to complete the fatigue analysis. The loading histories as determined by True-Load/Post-Test and the Abaqus odb results file were loaded into fe-safe. The fe-safe results were created in a new odb file that could be opened and post-processed in Abaqus/CAE. The initial fatigue model for the current production design indicated the lowest life was expected near a weld that connects the cross-tube to the side arm of the H-link. This matched the failure location on the field machines. The Abaqus/CAE model was then updated to include shell elements to represent the weld at the interface between the cross-tube and the side arm. Verity weld fatigue was then run in the fe-safe analysis and the predicted number of hours was similar to the number of hours to failure.

After creating the current production model that correlated well with the failure location and number of hours, the next step was to analyze new designs to determine the solution that will meet the simulation goal. An Abaqus/CAE unit load model was created for the new design with the same unit loads applied as the production H-link model. After solving the unit loads in Abaqus/Standard, the results file and the same time series loading produced for the current production H-link were loaded into fe-safe. The initial results again showed the lowest life location near the weld that joined the cross-tube to the side arm of the new H-link. Verity weld fatigue analysis was again used to determine the predicted fatigue life at the weld for the new H-link design. The result was that the new design met the simulation goal with an estimated fatigue life improvement of 7.8 times over the

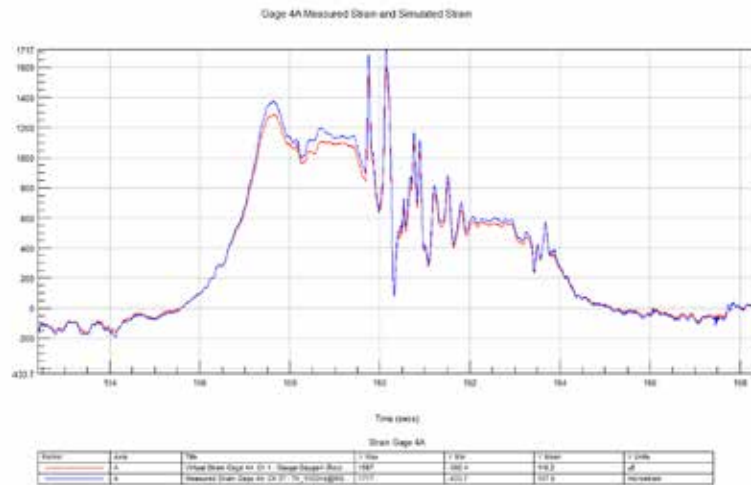


Figure 7 - Time trace comparing simulated strain to measured strain at low life location

current production design. Figure 8 illustrates the Verity fatigue life contours comparing the current production design to the final design.

#### 4. Conclusions

The integration of Abaqus/CAE, True-Load, and fe-safe allowed for an efficient and thorough investigation of the H-link design. Abaqus accurately reproduced the behavior of the H-link under the field loading conditions. True-Load created very accurate duplication of the field loads that could then be used to correlate the current design to actual results and to validate alternative designs. The excellent correlation between simulated and measured strain significantly increased the confidence in the results of the simulations. Finally, the ability to use actual time-history loading in fe-safe provided accurate fatigue life estimates of the entire H-link assembly. Correlation of the Verity fatigue analysis to the failure location and number of hours provided an additional

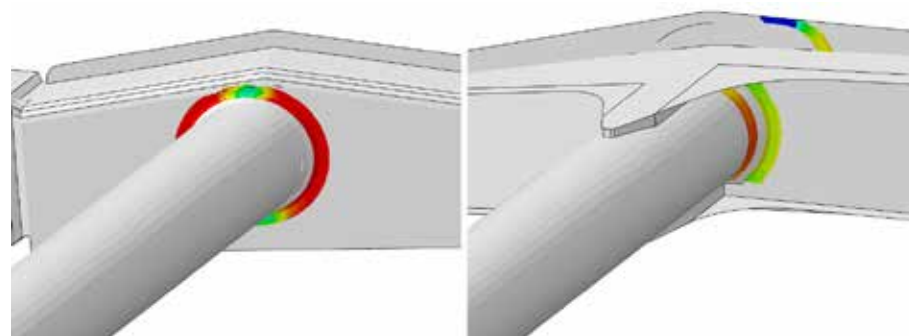


Figure 8 - Life contours of the current production (left) and the final design (right) from Verity weld analysis in fe-safe

field loading, as opposed to isolating the focus of the simulation to a single location. The process reduces the number of design and test iterations. The overall impact is a reduction of development time and cost.

David N. Slowinski - CNH Industrial

## TRUE LOAD



True-Load is a first to market to solution that leverages FEA models to place strain gauges on unmodified physical parts and then back calculate loading. Output directly feeds into True-QSE events, a powerful post processing tool that supports rapid virtual iteration.

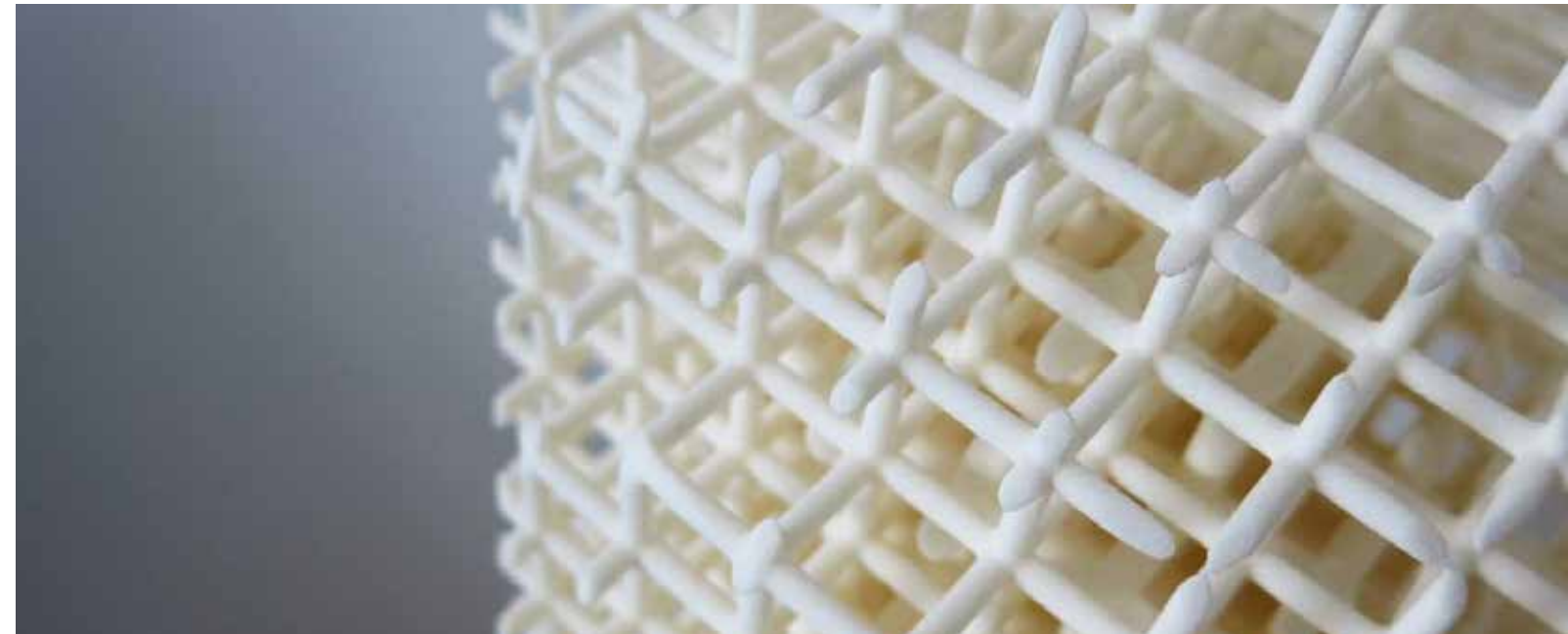
True-Load directly interfaces to FEA fatigue software to make FEA based fatigue with correlated loading events a natural part of the design cycle.

- Create multi-channel load cells leveraging your parts and FEA models
- Determine optimal strain gauge placement from FEA model
- Calculate Load Proportionality Matrices
- Use Measured Strains to back calculate Operating loads
- Create Quasi-Static Events to be used with True-QSE

One of the most challenging tasks for an analyst is to develop load cases for their FEA model that match measured strain values. Typically, it will take weeks to develop the right load cases that match just one or two strain gauges at a single point in time. True-Load makes that situation a thing of the past. True-Load will determine optimal gauge placement based on the FEA model. Once strains are collected at these optimal gauge locations, the strain data is read into True-Load to calculate load time histories that will typically match the measured strain to within 2% at every point in time. When combined with True-QSE, interrogating any point in the model for strain, stress or displacement is easy and interactive. Typically, it takes a few minutes to determine the strain gauge placement and a few minutes to back calculate the loading profiles.

For more information: Fabio Bernasconi, EnginSoft  
f.bernasconi@enginsoft.com

## Topology Optimization with Enforced Patterns and Applications for Additive Manufacturing



Topology optimization is often used by designers and engineers to generate novel and sometimes organic shaped designs. In addition, additive manufacturing processes are becoming more and more capable to print organic shaped structures and lattice structures. While, lattice structures may sometimes occur naturally in topology optimization, usually some design constraint must be imposed in the optimization process to produce a lattice-like result. In this article, we discuss how to enforce topology patterns to get final topology result to match certain desirable shapes that can be both easier to manufacture and/or to enforce a design requirement. The methods presented are implemented in the GENESIS structural optimization software and its preprocessor Design Studio. These two computer programs can be accessed in ANSYS using the GTAM and GSAM ACT extensions.

We will present two examples. In the first example, we will generate lattice structures directly using only topology optimization with some basic fabrication constraints. In the second example, we will generate the lattice structures using a Design Studio plugin that uses the topology density levels obtained by standard topology runs. Before discussing the problems we will briefly discuss what the topology optimization problem looks like and some basic concepts associated with it.

#### The Topology Optimization Problem

The topology optimization problem can be stated as in Fig. 1. In the above equations  $m$  is the number of constraint functions,  $n$  is the number of design variables,  $F$  is the objective function,  $g_j$  are the constraints,  $\rho_i$  are the design variables.

$$\begin{aligned} & \text{Min } F(\rho_1, \rho_2, \dots, \rho_n) \\ & \text{such that :} \\ & g_j(\rho_1, \rho_2, \dots, \rho_n) \leq 0, \quad j = 1, m \\ & 0.0 \leq \rho_i \leq 1.0, \quad i = 1, n \end{aligned}$$

Figure 1 - Optimization Problem Statement

#### Objective Function

Strain energy, mass, displacements, and natural frequencies are typically used as objective functions. In our implementation, practically any of the finite element responses or combination of them can be used as the objective function for minimization or maximization.

#### Constraints

As with the objective function, practically any of the finite element responses can be used as a constraint. In most problems, mass, displacements, velocities, accelerations, and natural frequencies are used as constraints. In addition, buckling load factors, stresses, strains, and/or temperatures can be also used as constraints.

#### Design Variables

In topology optimization, the design variables are parameters that can change the Young's modulus and the density of each element. The variables are usually defined to take a value between 0.0 and 1.0. A value close to 0.0 corresponds to an element that should be discarded, while a value close to 1.0 corresponds to an element that should be kept.

## Solving the optimization problem

To solve the optimization problem we used the GENESIS software that uses approximation concepts to efficiently solve the optimization problem.

## Directly Generated Lattices

When a low mass fraction is used, topology optimization, may produce a truss or lattice structure. When the results of the topology produce long members, it becomes harder to print due to the need of creating support structures. To reduce the need to support structures, we can force topology to create repeated short distance patterns to reduce the need of support structures. Our first example, will show this case.

## Indirectly Generated Lattices

When topology optimization is used with solid elements and when higher mass fractions are used, it is possible to convert part or all topology results into a lattice pattern. Our second example, will show this case.

## Examples

Two examples that show how to generate lattice structures will be presented next. The first example will show directly generated lattice structures. The second example will show how to convert a topology result into a lattice structure design.

# Topology Optimization to Directly Generate Lattice Structures

## Description of the Example

The purpose of this example is to demonstrate that optimization can be used to get lattice structures using simple fabrication constraints.

## Designable Region

The dimensions of the design domain are 200 length unities by 50 length unities. A vertical load is applied in the middle of the bottom edge of the structure. The structure is simply supported by constraining the two corners of the bottom edge.

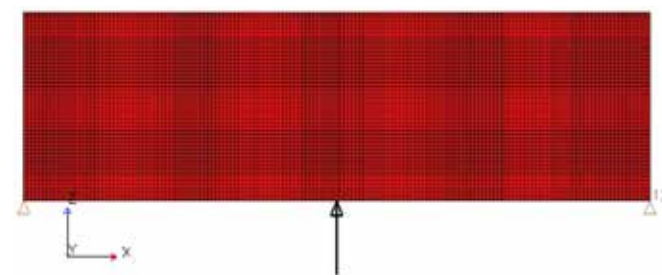


Figure 2 - Initial Design, Loads and Boundary Conditions

The designable domain was discretized with 7,680 QUAD4 elements.

## Problem Statement

The following optimization problem will be created, solved, and post-processed:

Minimize Strain energy  
Subject to:  
Mass fraction < 0.45

## Case Studies

Several cases studies are run to show the impact of using different periodic constraints. Comparing the results, will show that some of the results are more suitable to be printed than other.

### Case 1

A simple topology optimization is performed without any fabrication constraints being used.

#### Result 1

Figure 3, below, shows a reference answer. This structure has long members that would require a support structure to be built.

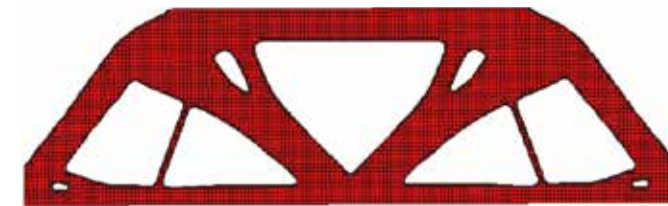


Figure 3 - Final Design, Case 1

### Case 2

A periodic fabrication constraint with a pitch of 50 is used to get a pattern repeated 2 times on each side of a symmetry plane located in the middle of the structure.

#### Result 2

Figure 4 shows the results of imposing symmetry and a periodic pitch of 50 units. This result is better than the one in case 1, but still produces long members, so this might not be as good as case 3 or 4 as candidate for printing.



Figure 4 - Final Design, Case 2

### Case 3

A periodic fabrication constraint with a pitch of 25 is used to get a pattern repeated 4 times on each side of a symmetry plane located in the middle of the structure.

#### Result 3

Figure 5 shows the results of imposing symmetry and a periodic pitch of 25 units. This case, as case 4, is a more suitable candidate for printing. This case however, is not as good as case 4 in term of member lengths.



Figure 5 - Final Design, Case 3

### Case 4

A periodic fabrication constraint with a pitch of 25 is used to get a pattern repeated 4 times on each side of a vertical symmetry plane located in the middle of the structure. In addition, a second periodic fabrication constraint with a pitch of 12.5 is used to get a pattern repeated 2 times on each side of a horizontal symmetry plane located in the middle of the structure.

#### Result 4

Figure 6 shows the results of imposing double symmetry and periodic constraints that produced a lattice structure with multiple short members. This case is the most suitable candidate for printing when compared with the other 3 cases.

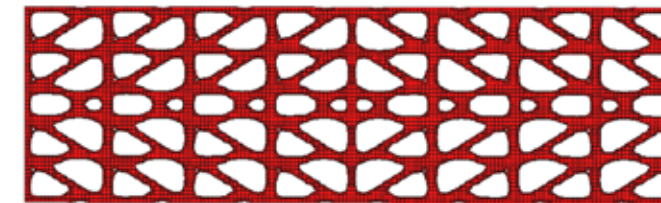


Figure 6 - Final Design, Case 4

## Lattice Structure Design

### Description of Problem

The purpose of this example is to show how to create a lattice structure using results of a standard topology optimization run.

### Problem Statement

The following optimization problem is solved:

Minimize Mass, Subject to:  
Displacement (load case 1) < target 1  
Displacement (load case 2) < target 2

### Designable region

The topology design region is shown in red in Figure 7. There are two loadcases in this problem which are also shown in the Figure.

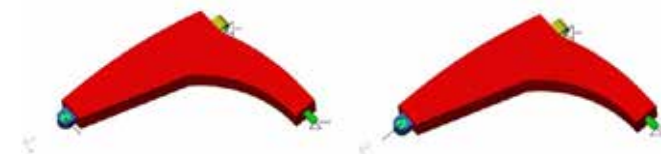


Figure 7 - Initial Design, Two Load cases, and Boundary Conditions

The topology optimization results are shown in Fig. 8.

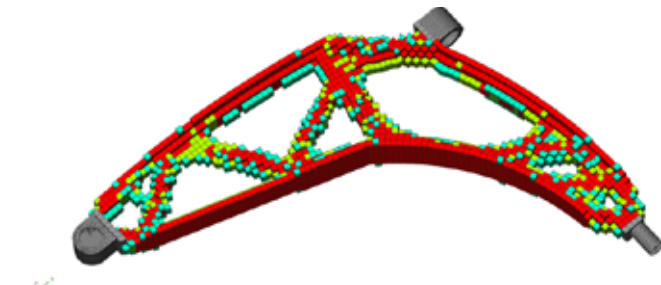


Figure 8 - Topology Optimization Results

The elements with high density are shown in red. Elements with intermediate density are shown in green and light blue.

## Lattice Pattern

To create a lattice structure, elements with intermediate densities will be converted using a lattice pattern available in Design Studio software. Figure 9 shows 3 available patterns.

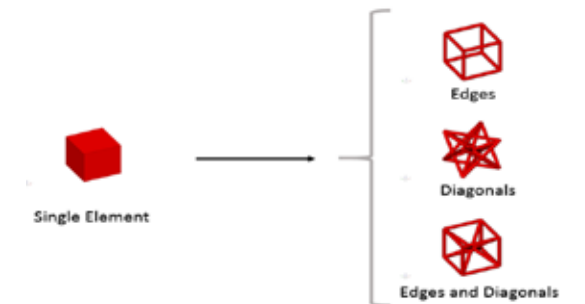


Figure 9 - Lattice Patterns

## Lattice Structure

Figure 10 shows the final results using the Edges and Diagonals pattern.

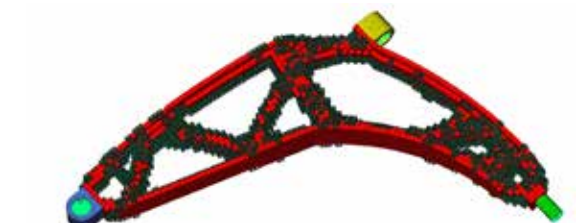


Figure 10 - Lattice Structure

## Alternative Lattice Structure Patterns

Figure 11 shows details of alternative lattice patterns.

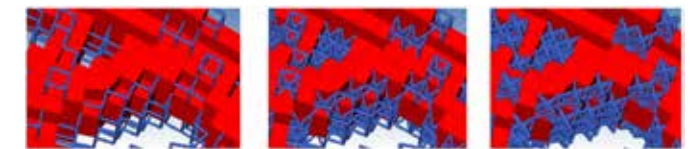


Figure 11 - Details of Alternative Lattice Patterns

## Discussion on Example 2

Lattice elements were successfully created with Design Studio. A lattice structure could also be created over the whole structure or in all elements above a density cutoff. The generated lattice could be further optimized using sizing, topometry or topology optimization.

## Conclusions

Topology optimization can be used directly or indirectly to generate lattice structures. Lattice structures offer the opportunity of creating light, strong and innovative designs.

## Acknowledgements

The authors would like to thank Mr. Om Joshi of VR&D for his help on solving the second example used in this article.

Juan Pablo Leiva, Brian C. Watson  
Vanderplaats Research and Development, Inc.



GERDP hydroelectric project, Main Dam general layout

## Evaluation of dam performance under seismic loads with DCR time history procedure: Case study of GERD main dam design

This article presents systematic and rational application of the DCR/CID methodology to estimate the behavior of concrete structures under seismic loads, using time-history analysis. This rational approach, proposed by USACE EM 1110-2-6051, can be used to evaluate the safety of new or existing structures and moreover to optimize the construction costs during the design phase. Such method has been systematically implemented, through the development of a dedicated calculation code, in order to analyze the behavior under seismic loads of the Grand Ethiopian Renaissance Dam (GERD), along the Nile River. The dam, currently under construction, has a maximum height of 175 m, it's 1780 m long and it has a global RCC volume of 10.2 Mm<sup>3</sup>. It is designed to store 74 Bm<sup>3</sup> of reservoir serving a 6140 MW Power Plant.



Fig.1 - GERDP Dam under construction

### GERD Project

The Grand Ethiopian Renaissance Dam (GERD) Project is located 500 km north west of the Ethiopian capital Addis Abeba, in the Benishangul – Gumaz region, along the Blue Nile River. The Ethiopian Electric Power company (EEP) is the employer, Salini-Impregilo SpA is the EPC Contractor and Studio Pietrangeli Srl is the designer. The plant, with its 6'140 MW of installed power and 15.7 TWh of annual energy production, is one the most important projects committed by the Ethiopian Government so to meet the country

present and future power requirements. The hydropower plant is currently under construction. Once completed, GERD will be the largest plant in Africa.

### Post processor

The rational method, described in the introduction, has been practically applied, thanks to a dedicated computation code that has been developed, tested, validated and systematically adopted by Studio Masciotta engineers. The computation code consists of a series of Excel Macros and

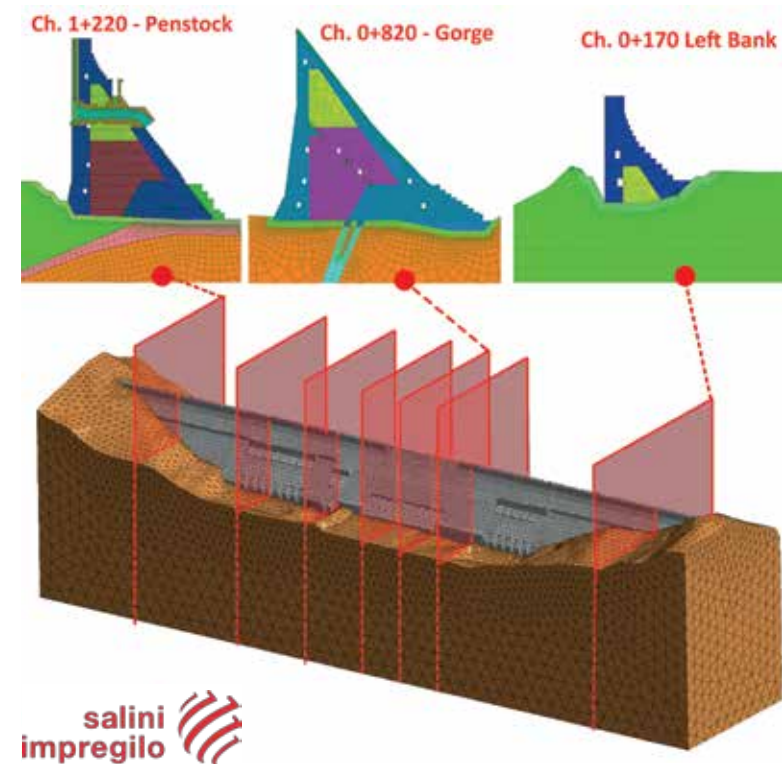


Fig. 2 – Main Dam 3d Model and representative sections

Straus 7 API (Application Programming Interface), aiming at extracting the results out of the FEM model and computing the Demand-Capacity Ratio and the Cumulative Inelastic Duration of selected control points within the dam body. The dam behavior analysis, considering its relevant length (about 2 kilometers) and with a great variety of geometries and foundation characteristics, required a series of fifteen transversal sections to be analyzed (about a section every 130 meters of length), using a dedicated 2-D FEM models.

Every section has been analyzed considering at least two possible and alternative geometries, in order to identify the optimum one. Within every transversal section of the dam, an average number of about fifteen control points has been fixed in order to assess the dynamic behavior of the dam under seismic events. Every transversal section has been analyzed considering six different earthquakes and four possible combinations of horizontal and vertical component signs for every seism. Each hypnotized earthquake lasts 35 seconds and, assuming that an integration step is set every 0.005 seconds in the linear time history analysis, seven thousand steps of integration characterize each earthquake combination.

The inquired points have been analyzed both in terms of vertical stresses (to be compared with lift joint tensile strength) and maximum principal stresses (to be compared with parent tensile strength), so to have two relevant quantities to be examined at each control point.

It is therefore easy to infer that the quantity of the data to be processed to obtain the graphs of DCR and CID for the inquired sections is the result of:  $15 \times 2 \times 15 \times 6 \times 4 \times 7000 \times 2 \approx 151$  millions of data. Assuming that an engineer can process a datum every two seconds, working 8 hours a day, it would take him/her 10500 days, which is more than 28 years, to get the required result, with a clear possibility of introducing widespread human errors in the processed data, whose reliability would be strongly affected. The idea of developing a dedicated software was therefore deemed, not just a reasonable optimization of the work of the engineers, but rather an absolute necessity to comply with the times agreed between the Designer Studio Pietrangeli Srl and the EPC Contractor Salini Impregilo. The post processing software is articulated in five sub-routines: Init, Eval DCR-CID, Graphs, Synth, Print and it assumes to have correctly performed a linear time history analysis of the dam sections, thus all result files are supposed to be available for this specific purposes.

Init is the interface with the FEM software Straus 7. It contains the calls to Straus 7 API. The user can choose whether the API shall get either the vertical stresses or the maximum principal ones and select which plates to investigate. The engineering assessment is fundamental at this stage in order to limit contain the size of data to be processed by the software. The routine cycles on the FEM model elements and extracts the time history of vertical/maximum principal stresses of the selected ones at saved times.

Eval DCR-CID is the core of the calculation process performed by the software. It considers the time history of stresses extracted during the Initialize (Demand) phase and compares them, step by step, with the Capacity value introduced by the user. It evaluates the Cumulative Inelastic Duration (CID) for DCR values, ranging from 1 to 2 (a DCR higher than 2 is not allowed).

Graphs uses the data computed by the sub-routine Eval DCR-CID to produce the DCR and CID graphs, in order to compare them with the limit line prescribed by USACE code, and to establish whether stability can be assessed by the simplified Linear Analysis (Low to moderate damage) or it's necessary to perform a further Non Linear Analysis (Significant damage).

Synth is a routine responsible only for the chart sorting and formatting. It generates an Excel sheet for every selected element of the FEM model and matching the graphs with the related element in the sheet. The charts are formatted do to make them easy to be read, printed and presented in a calculation Report.

Print gets the graphs produced by the routine Synth and generates a pdf file for every graph, ready to be assembled in the Annex of a Calculation Report of the Dam.

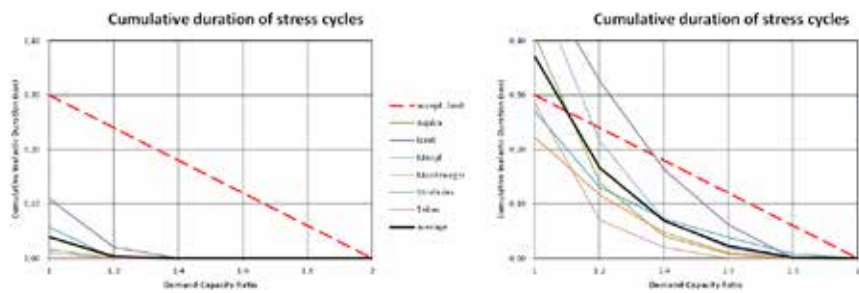


Fig. 3 – Examples of an element fully verified according to DCR method (left) and of an element not verified (right)

**Results of DCR/CID analysis**

The typical results of an DCR analysis performed by the software are reported in Fig. 3, presenting an element fully verified and another not verified, this exceeding the acceptance limit.

The dam optimization process through the linear time history procedure was carried out essentially during level 2 Design.

The dam was well dimensioned during basic and level 1 Design, using simplified pseudo static methods (Seismic Coefficient Method, Equivalent Lateral Force Method) and modal analyses with Response Spectrum.

The analyzed geometries and sections were generally verified and the linear time history procedure with DCR-CID method was used essentially to optimize the sections. The systematic procedure allowed to achieve the required values, typically 20% lower than the predicted ones during level 1 Design by means of Modal Analysis with Response Spectra

Fifteen sections were systematically analyzed during Level 2 Design, adopting the simplified DCR approach and the relative calculation reports were produced. An approximate number of 9.000 DCR-CID synthesis graphs was generated by the software as described above.

Summarizing, fourteen sections were fully verified and their stability under earthquake SEE was assessed through the linear time history analyses.

Only the stability of the highest section of the dam, in correspondence to the Gorge, proved to have some

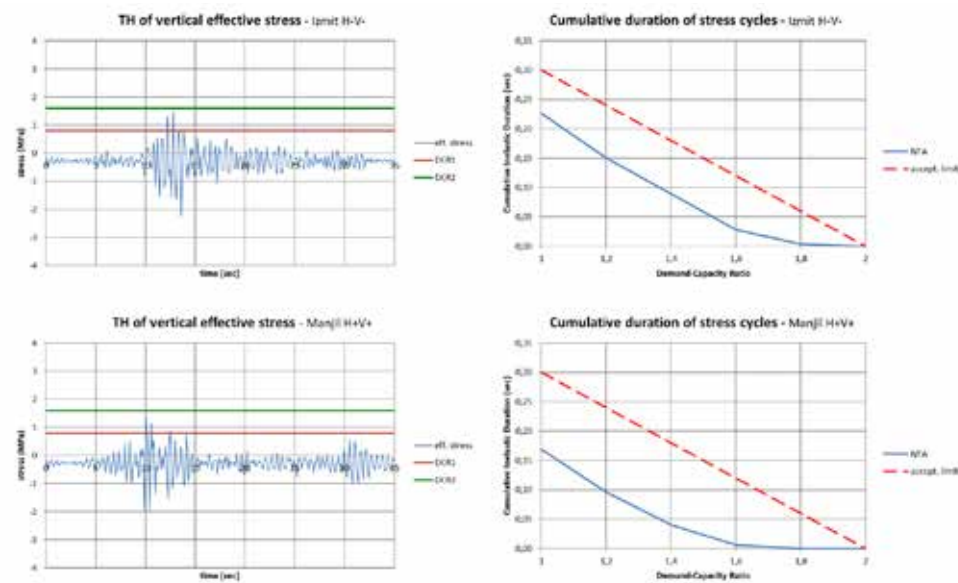


Fig. 4 – Examples of section elements fully verified through DCR method – Time history of stress (left) and DCR-CID graph (right) for two different earthquakes

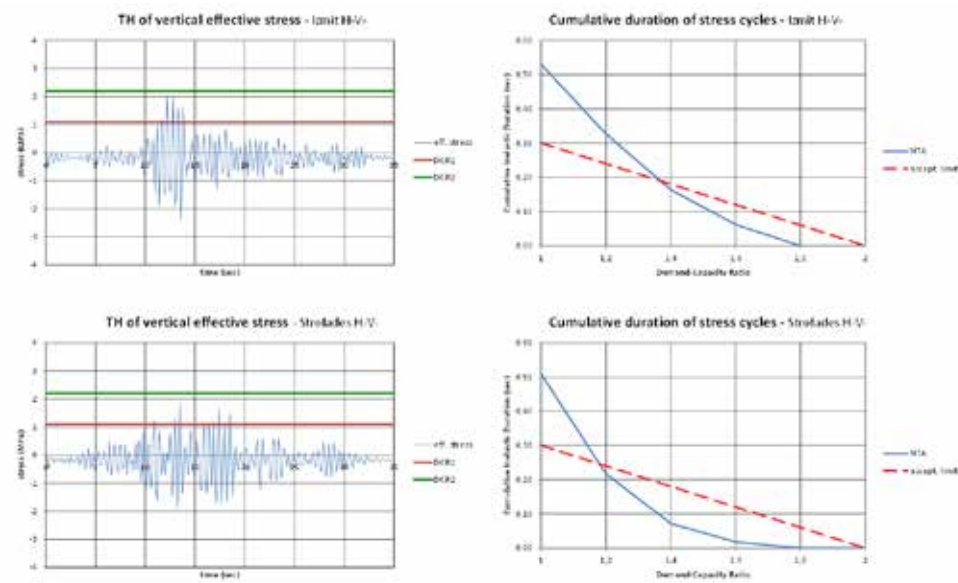


Fig. 5 – Examples of section elements not verified through DCR method – Time history of stress (left) and DCR-CID graph (right) for two different earthquakes

critical points, since the DCR values were exceeded, adopting the tensile strength values fixed during Level One Design. Further Non Linear Analyses were performed, assuming the potential crack surfaces identified by means of the linear time history analyses. Such activity confirmed the stability of the section and no permanent sliding displacements did occur.

Alessandro Masciotta, Carlo Fontana,  
Angelo Fiorani - Studio Masciotta  
Alberto Bezzi - Studio Pietrangeli



# Composite Materials for the Sustainable Refurbishment of Bridges

The European project SUREBridge is developing a new technique for the structural strengthening of road bridges. Its effectiveness has been demonstrated through finite element analyses and full-scale laboratory tests



The SUREBridge Project Consortium is composed by:



Chalmers University of Technology, Goteborg, Sweden (Coordinator)



FiberCore Europe, Rotterdam, The Netherlands



A.I.C.E. Consulting S.r.l., San Giuliano Terme, Pisa, Italy



Department of Civil and Industrial Engineering, University of Pisa, Italy

**Introduction**

Providing an innovative and sustainable solution for the refurbishment of road bridges and users safety: this is the aim of the European research project SUREBridge (Sustainable Refurbishment of Existing Bridges), co-financed by the European Commission through the ERA-NET Infravation 2014 Call.

Due to the expected increase in the traffic volume, existing bridges will be subjected to more severe actions in the near

future. Consequently, the need to refurbish these infrastructures, often structurally deficient and obsolete, will increase dramatically. At present, construction and maintenance activities relating to bridges imply costly and time-consuming procedures, with a negative impact on traffic flow and welfare in wider terms. In addition to disturbance, disruption, and pollution, other main challenges are the inefficient use of resources, i.e. materials, energy, waste management, and recycling. Thus, the target of the SUREBridge project is to increase the load-carrying capacity of concrete and steel-concrete

bridges to the desired level, exploiting the remaining capacity of the superstructure and preserving the structural elements of the deck. This is achieved by using tailor-made glass fibre-reinforced polymer (GFRP) panels, installed on top of the existing concrete slab, and carbon fibre-reinforced polymer (CFRP) laminates, applied to the bottom side of the girders. Such laminates are pre-stressed by using an innovative technique, which avoids stress peaks in the CFRP-concrete interface, thus preventing early

delamination. Furthermore, the GFRP panels can be manufactured of the same width or wider than the existing deck, enabling to widen the road section if needed.

### A case study bridge

To prove the effectiveness and feasibility of the proposed technique for real-life applications, a bridge located in the municipality of San Miniato (Tuscany, Italy) was selected as a case study (Figure 1). Dynamic modal and linear static analyses were carried out with the commercial software Straus7 to assess the load-carrying capacity before and after the widening and strengthening intervention provided for the bridge (Figure 2). The increment in the load-carrying capacity obtained with the SUREBridge solution was evaluated with a simplified calculation datasheet. It was demonstrated that the combined use of GFRP panels and CFRP laminates enables to bring the bridge load-carrying capacity from 51% (current conditions) up to the 100% of the traffic loads prescribed by the current Italian regulations.



Figure 1 - The San Miniato bridge - Current conditions

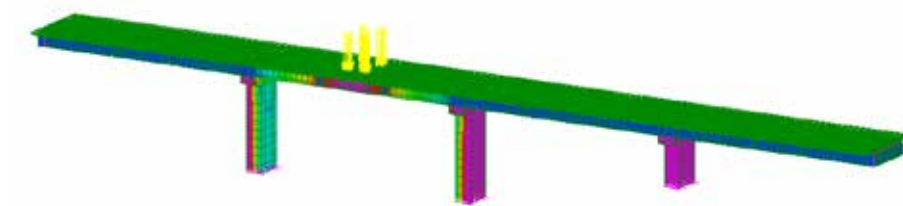


Figure 2 - The San Miniato bridge - Finite element model

### Laboratory tests on prototype beams

A clear demonstration of the high strengthening capacity of the proposed technique was given through full-scale tests on T-shaped cross-section prototype beams. These tests are representative of the conditions often occurring in real concrete bridges – as the San Miniato bridge – since the T-shaped cross section acts as a simplified version of a longitudinal girder with an upper collaborating slab. In August 2017, four 6-m long prototype beams (Figure 3) were tested under four-point bending in the laboratory of the Structural Engineering Division of the Department of Civil and Environmental Engineering at Chalmers University of Technology (CTH). Earlier in July 2017, theoretical predictions of the structural behaviour of such specimens were carried out by means of finite element non-linear analyses at the University of

Pisa. In particular, a fibre-modelling approach was used, whereas the tested beam is represented as the assemblage of small BEAM elements representing ideal longitudinal fibres.

Two of the four prototype beams – the reference reinforced concrete beam (specimen 1) and prototype beam strengthened with longitudinal GFRP panels and pre-stressed CFRP laminate (specimen 3) – were modelled with the software Straus7 using the above-mentioned approach (Figure 4). Such models were accurately calibrated referring to the experimental results obtained during some preliminary laboratory tests on rectangular cross-section beams, conducted at CTH in October 2016.

Going into details of the finite element models, the cross section of the beams was subdivided into three different parts – unconfined concrete, confined concrete, and steel reinforcements – each corresponding to a different material with specific mechanical properties and stress-strain curves.



Figure 3 - Prototype beam strengthened with the SUREBridge technique and tested in the laboratory

The modified model by Kent and Park (1971) was used to define the stress-strain curves for confined and unconfined concrete in compression. Besides, the stress-strain curves both for confined and unconfined concrete in tension were extrapolated from the values of the elastic modulus and mean tensile strength.

An elastic-plastic stress-strain curve was chosen for the steel reinforcements, while an elastic-brittle stress-strain curve was considered for the CFRP laminates of the strengthened prototype beam. Such elements were connected to the bottom of the concrete beam using an epoxy adhesive layer, schematised as a continuous distribution of springs and introduced into the finite element model by using CONNECTION elements. The equivalent shear and axial stiffness of such elements were computed based on the thickness of the adhesive layer and the values of its elastic moduli given by the producer. Furthermore, the pre-stress distribution on the CFRP laminates was obtained considering the maximum pre-stressing value and the typical length needed to introduce such pre-stressing force with the set-up developed at CTH. The GFRP panels, installed on the top of the strengthened beam with the webs oriented in the longitudinal direction, were modelled with LAMINATE elements. In particular, the different layers of the panel have been defined as

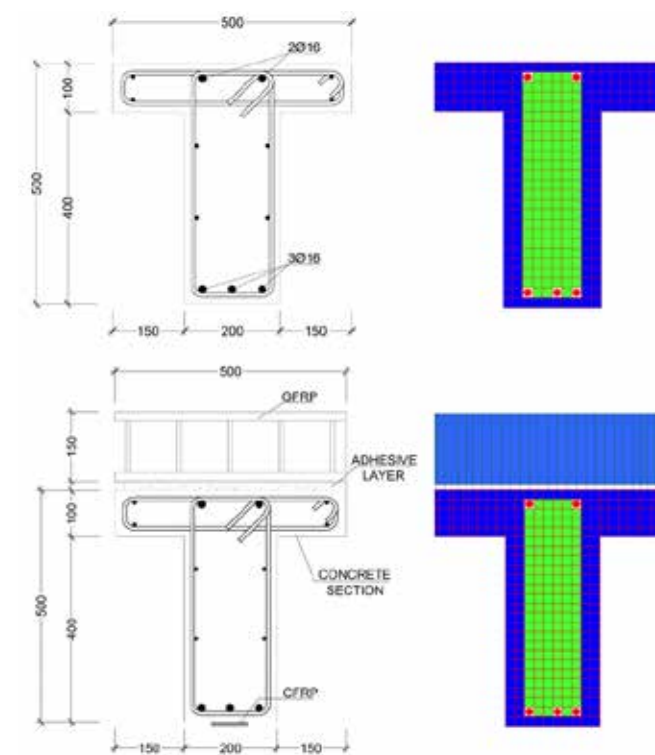


Figure 4 - Cross sections and finite element models of the prototype beams (specimens 1 and 3)

individual PLY elements, then combined into a LAMINATE element representing the panel. An equivalent internal core replaces the actual spatial distribution of the webs in order to simplify the model and reduce computational time. Such modelling approach was validated first by separate finite element analyses on single GFRP panels, showing a good agreement between the accurate and simplified core models. In addition, the same assumption made for the CFRP-concrete bonding were also made for the GFRP-concrete bonding.

The non-linear analysis of the models was developed with progressive and appropriate load increments to obtain the theoretical load-deflection curves, which were compared to the experimental curves once the laboratory tests were performed (Figure 5). A very good matching between the theoretical predictions and experimental results was obtained and, in this respect, it should be stressed that the finite element models were not calibrated against the experimental results – conducted one month later than the delivery of the models – for the simulated tests.

### Conclusions

“We are confident to obtain even better agreement with experimental results, once the output of mechanical tests on material samples will be available” states Prof. Paolo S. Valvo, Scientific Responsible person of the University of Pisa working group. Such tests are currently (October – November 2017) being carried out at the Chalmers University of Technology and the finite element models will be updated accordingly. “Bridges are critical transport infrastructures, fundamental for the performance of the

road transport network. The refurbishment of the existing obsolete structures is crucial for the users’ safety” concludes Prof. Valvo. The technique developed within the SUREBridge project can represent a sustainable and effective solution for the refurbishment of concrete and steel-concrete bridge. The key role for the effectiveness of the proposed technique is played by the combined use of GFRP panels, installed on the top of the existing deck, and CFRP pre-stressed laminates applied to the bottom side of the longitudinal girders. This was demonstrated through the structural analysis of the case study bridge, where the separate use of CFRP laminates and GFRP panels enabled to reach the desired load-carrying capacity, but with major problems such as high thickness of the panels or high number of laminates.

The excellent strengthening capacity of the CFRP-GFRP combined use was further demonstrated through laboratory tests on full-scale prototype beams, where the observed structural response was successfully predicted based on finite element non-linear analysis.

E. Davini, P.S. Valvo - University of Pisa  
For further information: [www.surebridge.eu](http://www.surebridge.eu)

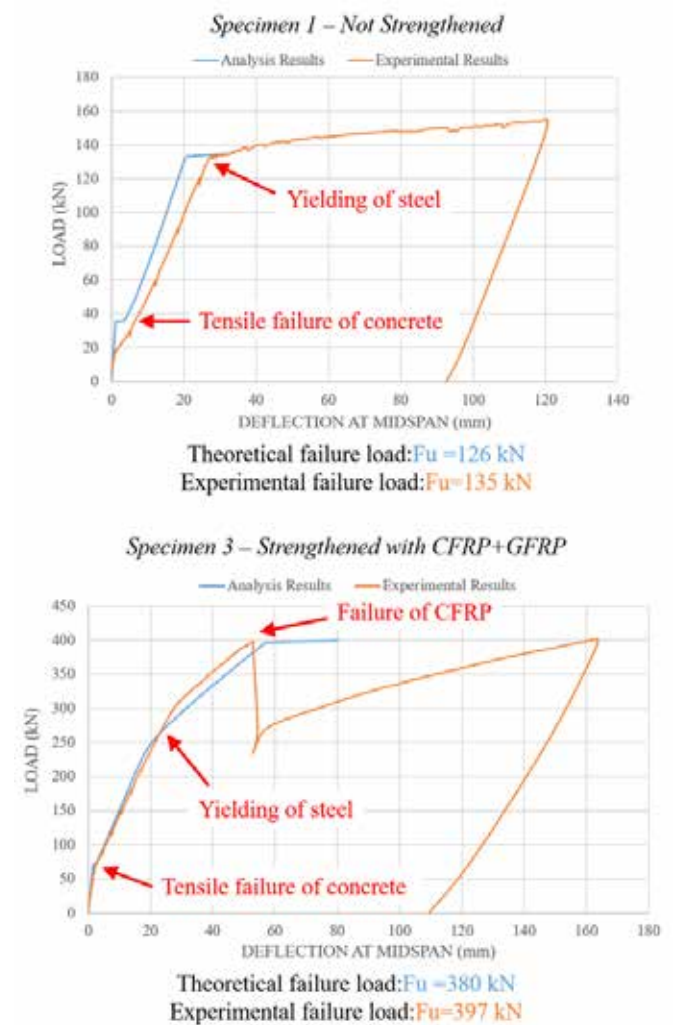
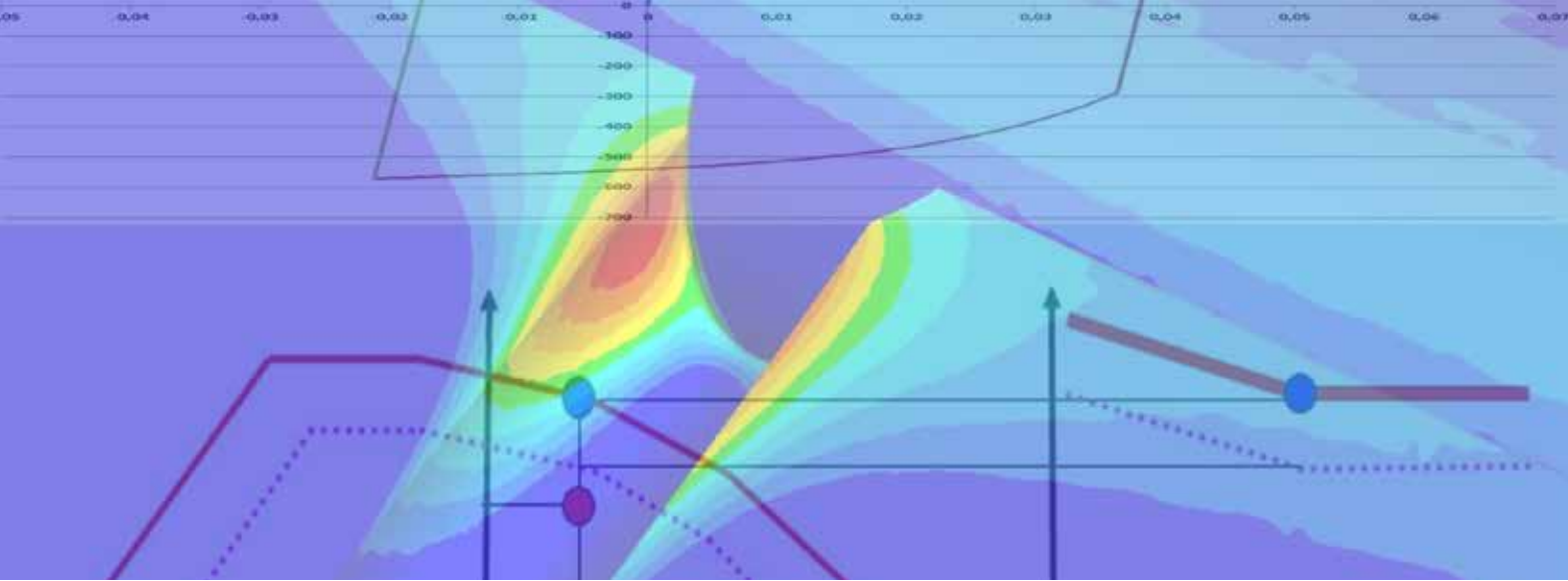


Figure 5 - Comparison between the theoretical and experimental load-deflection curves



## Latest Accomplishments offer new Opportunities in the Field of high Strength Injection and Motor Components



Mr. Jochen Heizmann

The Hirschvogel Automotive Group, headquartered in Denklingen, is among the world's largest automotive suppliers in the area of steel and aluminum forging and machining. Their customers include all renowned automotive manufacturers and suppliers worldwide. [www.hirschvogel.com](http://www.hirschvogel.com)



bearing capacity as well as fatigue-life. In the course of hydraulic autofrettage thick-walled metallic cylinders are subjected on the inner diameter to a high internal pressure. At present, the level has been recorded at three to four times the nominal working pressure. Thereby material at the inner diameter is expanded under tensile

loading above its elastic limit (illustration 1), whereas deformation in outer sections still remains in the elastic area of the material. After release of the autofrettage-pressure the outer zone of the cylinder will relieve elastically. Material in the area of the inner diameter, particularly at the bore-intersection will undergo plastic deformation again, this time under compressive loading. After achieving the state of equilibrium, plastically deformed sections will end up in a condition of compressive residual stresses. Later, under impact of internal working pressure this will have a positive effect, as compressive residual stresses resulting from autofrettage compensate tensile stresses: During operation reduced equivalent stresses as well as shifted local mean-stresses can lead to higher admissible amplitude stresses.

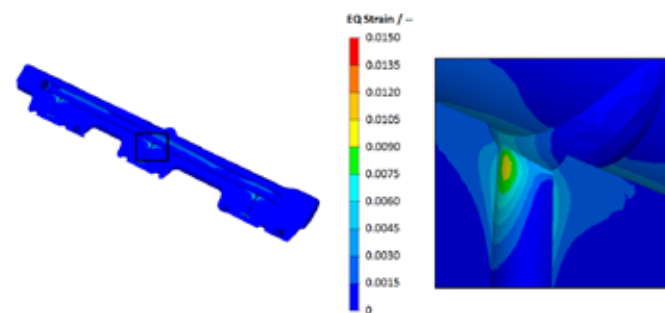


Fig.1 - Plastic Strain due to Autofrettage, general View (left) and Detail View (right)

### Title Strip

Hydraulic autofrettage as a means of increasing fatigue life of components charged with internal high-pressure (e.g. common-rails for Diesel-injection systems) is establishing itself progressively in the field of off-highway-engines. During computational layout of this process-step, consideration of anisotropic material behaviour is of primary importance. Advanced development-tools for assessment of fatigue life already enable the integration of resulting compressive residual stresses on basis of kinematic material models. So far, local quite possibly directional component-strength (e.g. due to prior autofrettage) has not been taken into account among standards to evaluation of durability for forged components. In the context of a joint development project this gap has been closed by Hirschvogel Automotive Group, Engineering Center Steyr GmbH & Co. KG and Transvalor SA.

### Principle of hydraulic Autofrettage

Injection pressures beyond 2.000bar contribute significantly to a more efficient exploitation of fuel in prospective engines. The so-called autofrettage method ensures, that hydraulic tubes and pipes are able to withstand ever-increasing alternating loads. Autofrettage is a means of generating residual stresses in pipes, in order to improve its load-

### Optimisation of forged high Strength Components

Technical systems of modern times – both for automotive and off-highway applications – contain forged high-strength components, many times. Its key role particularly can be explained by the massive load-bearing capacity, which is the crucial point whenever it comes to transmission of exalted forces, torques or pressures. Increasing requirements regarding power density necessitate more intense component optimisation, which takes painstaking tuning of material, component-geometry as well as numerous parameters along the entire development- and process-chain for granted.

In the course of full utilisation of mechanical-geometrical potentials at ideally lowest costs, vigorous application as well as continuous development of advanced design tools gains great importance. Thanks to long-standing know-how and software-tools as CAD, topology- and shape-optimisation as soon as linear-elastic FEM simulation the Hirschvogel Automotive Group is in a position to reliably design components on the basis of requirements and design-rules of customers. Furthermore, Hirschvogel recently has acquired numerous further competences and refined these together with industrial and academic partners (e.g. regarding understanding of micromechanical material-mechanisms). Such as in-house application of elasto-plastic forming-simulation in combination with advanced material-models creates the possibility, to not only compute least plastic deformations precisely adjusted during autofrettage, but also to postprocess resulting residual stresses. Generally, whenever it comes to classical forming simulation in combination with metallic materials, isotropic hardening is assumed. In the case of minor plastic deformation and particularly in combination with cyclic material loading, as a rule kinematic hardening dominates. These will now by means of suitable models in combination with material-specific parameters be taken into consideration during FEM simulation of the autofrettage-process followed by a fatigue analysis.

### Previous Approaches adopted to assess Fatigue Life of Common-Rails

In cases where autofrettage does not come to fruition or whenever one chooses conservative approaches during layout of common-rails, engineers are tempted to regard empirical values related to diameter ratios. If FEM-software good for linear-elastic analysis of operating states (without prior autofrettage) is available, various geometry-proposals can be assessed via empirical formula which take material strength (e.g. YS or UTS) and von Mises equivalent stress into account at the same time. In the event of deploying formulations of material science and fatigue, the Goodman-diagram (illustration 2) may be applied, in order to quantify the relation of mean stress and alternating strength with respect to durability of the material. The area underneath the graph indicates, that at given stresses the material should not fail. The area above the curve represents potential failure of the material. Thereby  $\sigma_A$  stands for stress amplitude,  $\sigma_M$  for mean stress,  $\sigma_{FAT}$  represents fatigue limit for exclusively alternating load and  $\sigma_{TS}$  stands for ultimate tensile strength

respectively  $\sigma_{CS}$  for ultimate compressive strength of the material. The general trend, shown by the Goodman-diagram e.g. provides decreasing sustainable stress amplitudes with increasing tensile mean stress.

In the course of fatigue-life assessment (e.g. common rails) taking autofrettage into consideration, while following advanced approaches, as a rule elasto-plastic FEM-software (e.g. FORGE) is applicable. Simultaneously the so-called "Bauschinger-Effect" in terms of kinematic hardening models is included in the computations, so that a realistic distribution of residual stresses can be transferred from a prior autofrettage simulation to the subsequent fatigue-life analysis (e.g. FEMFAT). Thanks to the description of the material-characteristic by Haigh-diagrams, compared to the Goodman-diagram mean stress sensitivity of the material can be considered at a higher level of detail (Fig 2).

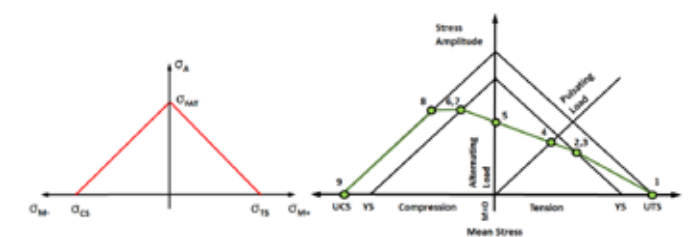


Fig. 2 - Goodman-Diagram (left) and Haigh-Diagram (right)

### New Accomplishments qualified for Fatigue Life Assessment of Common-Rails

Due to joint further development of models suitable for fatigue life assessment, in the future local strain hardening as well as softening effects related to plastic deformation can be integrated in terms of yield stress as well as ultimate tensile strength – as a result of a preceded elasto-plastic forming simulation – into the subsequent fatigue-analysis (Fig. 3).

This is ensured by making a distinction between isotropic and kinematic material behaviour during transfer of local parameters to durability analysis. As a rule, for the latter behaviour directional dependency of ultimate tensile strength and yield stress due to deformation during autofrettage plays a crucial role (Fig. 4).

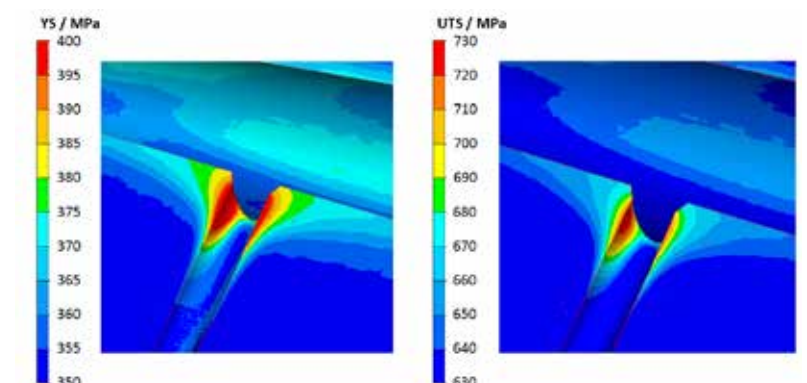


Fig. 3 - Local Increase of Yield Stress (left) and Ultimate Tensile Strength (right) due to Autofrettage

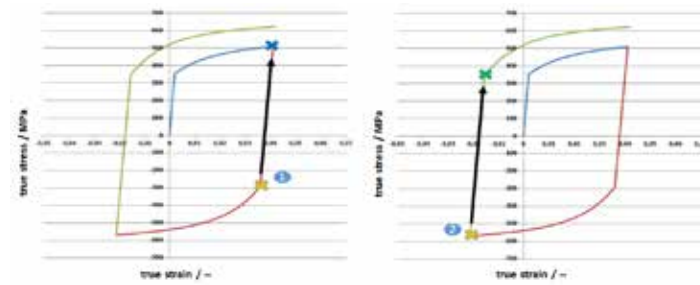


Fig. 4 - Consideration of isotropic (left) and kinematic (right) Material Behaviour

This in turn means that fatigue-life analyses do not only operate on the basis of local Haigh-diagrams, beyond that these are adapted due to present variations of strength. Whenever impacts on the material properties (such as fatigue strength) are being calculated in the FEMFAT software, the associated Haigh-Diagram changes. Positive impacts lead to an expansion of the diagram, whereas negative ones would entail a reduction of material properties, simultaneously the loading capacity would decrease. Any individual adaptation shall be made proportionally in accordance with existing local specifications for ultimate tensile strength. As a consequence, any node of the finite-element-mesh can carry a customised Haigh-Diagram and therefore also can evince a varying local s-n curve – due to dissimilar material properties and boundary conditions (e.g. temperature, notch, surface roughness etc.). Furthermore, one has not to assume homogeneous material properties anymore, because the accuracy of the material description via individual data on material strength at any finite-element-node can be transferred from forming-simulation to fatigue-life analysis (Fig. 5).

As a general rule, engine components are designed to have fatigue

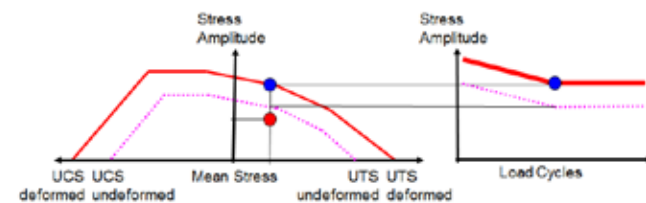


Fig. 5 - Modified Haigh-Diagram

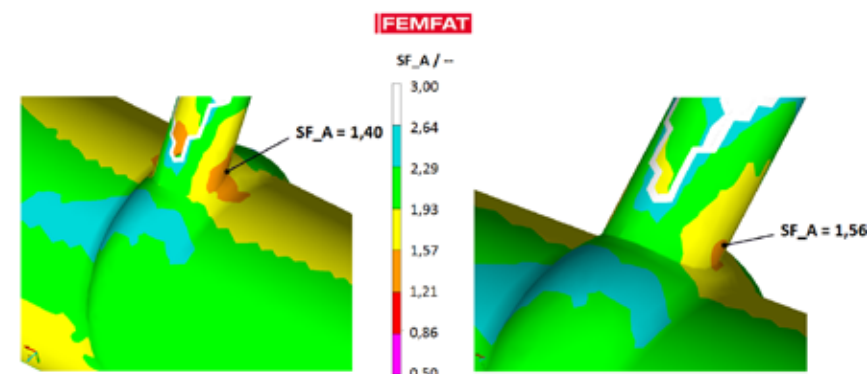


Fig. 6 - Safety Factor without (left) and in (right) Consideration of local Parameters

strength. As a consequence, during fatigue life analysis of common-rails focus is solely placed on the two critical load-cases. Considering that, the locally present safety-factor will be determined - in accordance with scatter-range, survival probability of the material to be investigated and the targeted survival probability. The calculated safety-factor enables the development engineer to assess, whether durability can be expected for the analysed component or not. Figure 6 illustrates, that the increase in ultimate tensile strength and yield stress in the critical area of the bore intersection have a significant positive impact on the respective safety-factor (increase from  $SF_A=1,40$  to  $SF_A=1,56$ ) - hence in the present example durability can be anticipated.

### Summary

Consideration of kinematic material behavior can increase precision of the layout of components charged with internal high-pressure (e.g. common-rails for Diesel-injection systems) markedly. In case one wants to particularly assess the anticipated fatigue life of the component as well, it seems appropriate, that residual stresses computed in the course of autofrettage-simulation as well as respective local strain hardening of the material should be taken into account during a subsequent fatigue-life calculation. Furthermore, new accomplishments facilitate a significant increase in the predictive quality of durability analysis. These are premised on generation and transfer of further parameters applicable for characterization of local material strength (for the time being limited to the successful implementation of local ultimate tensile strength and local yield stress of the strain hardened component).

### Thanks

The authors would like to thank Dipl.-Ing. Axel Werkhausen, FEMFAT-Sales- & -Support-Manager, and Dr.-Ing. Christian Gaier, Team-Manager of the FEMFAT-Development department, both at Engineering Center Steyr GmbH & Co. KG in St. Valentin (Austria), as well as Dipl.-Ing. Olivier Krafft, Sales-Engineer Northern Europe at Transvalor S.A. in Mougins Cedex (France) and Dipl.-Ing. Angela Kotte, Development Engineer for material & technology in the Advanced Engineering department at Hirschvogel Automotive Group in Denklingen (Germany), for their contribution during the implementation of the development project.

*“First publication as „Layout of Highly Stressed Injection and Motor Components“ in ATZoffhighway Worldwide No. August 2016, pp. 38-42, DOI <https://doi.org/10.1007/s41321-016-0521-y>“.*

Jochen Heizmann, Hans-Willi Raedt - Hirschvogel  
Patrice Lasne - Transvalor  
Helmut Dannbauer - Engineering Center Steyr

# Development of New Metallic Rear Crash Boxes to Replace a Plastic one for a Passenger Car



This study includes a development of metallic rear crash box in order to replace plastic one for a passenger car. This passenger car with the new developed crash box-traverse subsystem must pass low speed and high speed crash tests in order to meet the required performance for its market.



During the development phase of this study the greatest difficulty that we had is to have the required performance in RCAR structural test which is also known as AZT test. RCAR structural test is a low speed insurance test in which the main purpose is to have deformation only on the most rear parts like bumper beam and crash boxes. Other components joined with welding are not allowed to be deformed since their repair costs are much higher compared to the bolted components. From this point of view at the final stage of RCAR structural test there should be almost no deformation on the parts behind the crash boxes and bumper beam where this subsystem is bolted. To this end efficient energy absorption by the crash boxes is the most critical point that must be concentrated on.

In this study the development stages can be seen in detail in order to pass the RCAR structural test with new metallic rear crash boxes. Since force-displacement behavior of current honeycomb shaped plastics grow up gradually and absorb the energy uniformly without exceeding the maximum force limit not to have plastic deformations on body in white, having the same performance for RCAR structural test with metallic components is quite hard. Conventional metallic crash boxes have a reaction force very steep in the beginning which tends to decrease afterwards due to the hinge effect of metals. In order to get rid of this disadvantage of metals, another smaller and shorter

metallic crash box is used inside to get energy absorption gradually and uniformly without having hinge effect. In this way, during the crash, rigid barrier has a contact with outer crash box and before having the hinge effect it reaches another crash box inside. This results in a uniform reaction force curve without reaching high values.

### Introduction

In the era of competition two challenging issues in automotive industry are weight and cost. The enhancement of both weight and cost of the car requires an optimization between those issues. For this reason those issues are handled by this study to have a compromise in-between. Main objective of this study is to meet the low speed crash test requirements with new developed metallic crash boxes without making weight up. In ideal case, during the energy absorption crash boxes have to provide a smooth force-intrusion curve like a horizontal line after reaching a specified force value. In order to approach this case as much as possible, the main goal is to minimize the difference between the maximum and minimum force values of the force-intrusion curve during the deformation.

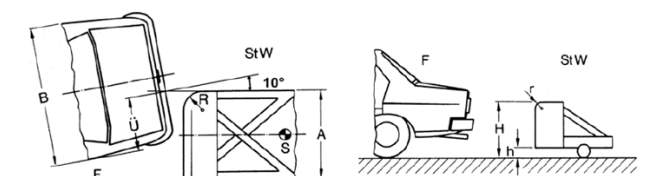


Figure 1 - RCAR Structural Test

## RCAR Structural Test (AZT insurance test)

The Research Council for Automotive Repairs (RCAR) is an international organization that works towards reducing insurance costs by improving automotive damageability, repairability, safety and security. RCAR structural test is one of the insurance tests that was established by RCAR. In this test the rigid barrier, positioned at an angle  $10^\circ$  with respect to the vehicle, has 16 km/h velocity towards the stationary vehicle from the rear with 40% overlap as shown in Figure 1.

In this test the components that are allowed to collapse are the bumper-beam and the crash-box as shown in Figure 2. Crash box is inserted between bumper beam and the side rail to absorb the total impact energy without transmitting residual energy to the parts like side rail which might increase the repair costs. After the impact, the only component that can be replaced should be bumper beam and crash-box since the main purpose of RCAR tests is to reduce the repair costs. From this point of view, crash box plays a very critical role to prevent damage to the welded parts and have the required performance in the RCAR structural tests.

In this sense the development of metallic crash box concentrates on the efficiency of energy absorption and the stability of reaction force values during the deformation in order to provide the requirements of the low speed tests.

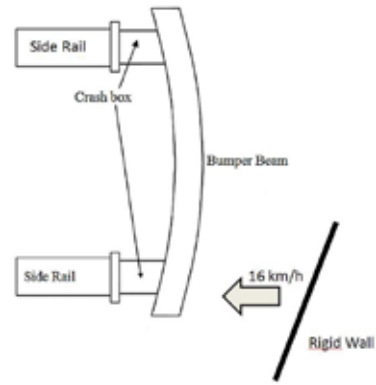


Figure 2 - RCAR Structural Test Schematic View

## Plastic Hinge

Rigid-plastic behaviour assumes that neither lateral nor axial deformation takes place at low values of the axial load,  $N$ . Each cross-section experiences the same uniformly distributed compressive stress  $\sigma = N/A$  and axial deformation is only possible when  $\sigma$  reaches the yield stress  $f_y$ ; the corresponding axial load is termed the 'squash load' and is given as:  $N_{pl} = A f_y$ . At this stage, any slight disturbance results in a lateral displacement giving rise to an additional bending moment. The member collapses with the deformation confined to a plastic hinge at some point along its length (Figure 3a); the stress distribution is bi-rectangular (Figure 3b), plastic deformation occurring in tension as well as compression. The buckled member remains in

equilibrium provided  $N$  becomes lower than the squash load; in this case the compressive yield stress is no longer attained over the entire

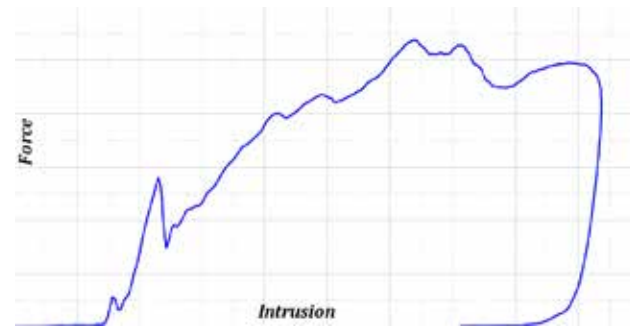


Figure 4 - Force-Intrusion Curve of Plastic Crash-Box

cross-section. The larger the lateral displacement, the larger the bending moment at the plastic hinge and thus the smaller the coincident axial load (Figure 3c).



## The Idea of New Metallic Crash-Box

Before the new metallic crash-box, force-intrusion behaviour of current plastic crash-box is given below in Figure 4. As shown in Figure 4, reaction force value of plastic crash-box increases gradually and when the force reaches a specific value, it remains there uniformly along the deformation without showing unstable behaviour. This provides an efficient energy absorption which retains the intrusion and force values in moderate levels and accordingly avoids to have damage on the components that causes high repair costs like rear door and body in white.

Based on all those features of plastic crash-box, first version of new metallic crash-box have been designed as shown in Figure 5. Basically this is composed of one single crash-box with 3 forms at both sides to orient and enable the folding process.

As shown in Figure 6, the results of first version metallic crash-box compared to the plastic one gives that the force value does not show a stable behaviour in which the difference between maximum



Figure 5 - First version of metallic Crash-Box

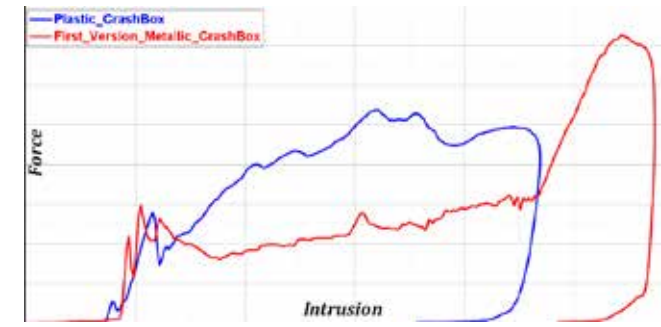


Figure 6 - Results of first version metallic crash-box compared to the plastic one

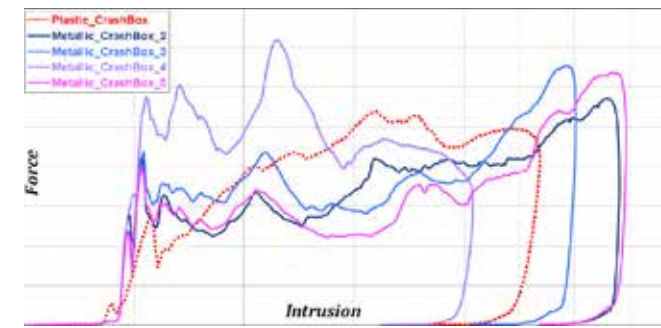


Figure 7 - Results comparison between different material and thickness combinations of metallic crash-box and the plastic crash-box

and minimum force values are so high. Such an inefficient energy absorption leads the intrusion value to be higher than acceptable values which causes the rigid barrier to damage the rear door during the RCAR structural test.

In order to increase the efficiency of energy absorption, different material and thickness combinations have been tried with the same geometry shown in Figure 5 and the results of all those combinations have been post-processed. However, in the end as shown in Figure 7 force-intrusion values still remain outside of the acceptable values compared to the plastic crash-box.

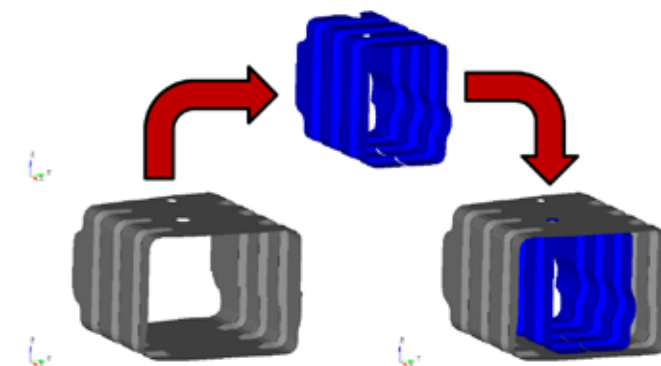


Figure 8 - Smaller and Shorter Crash-Box is inserted inside the existing new developed Crash-Box

Common behaviours of the results for metallic crash-box shown in Figure 7 are based on the phenomenon of plastic hinge effect, which leads the force and intrusion values to go beyond the limits.

At this point a smaller and shorter metallic crash-box is inserted inside the existing new developed crash-box as shown in Figure 8 so as to

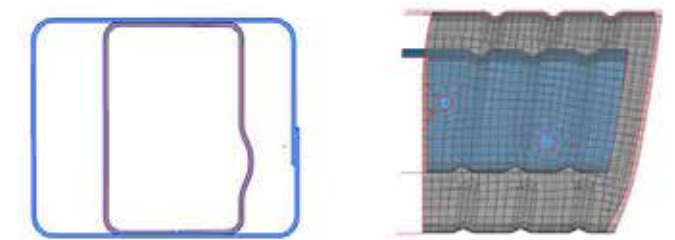


Figure 9 - Cross-Section View and Top View of the Crash-Boxes

overcome that phenomenon. The purpose is to increase the cross-section area against the barrier impact and accordingly have a more stable force-intrusion curve.

The inserted smaller crash-box is joined from its upper and lower surface to the outer box. In Figure 9 the top view and cross-section view of crash-boxes are shown.

The motivation behind having a difference between lengths of the boxes are hidden inside the force-intrusion curve. There are two important reasons that can explain this difference. Firstly, the force peak value should be moderate at the first contact between barrier and crash-boxes

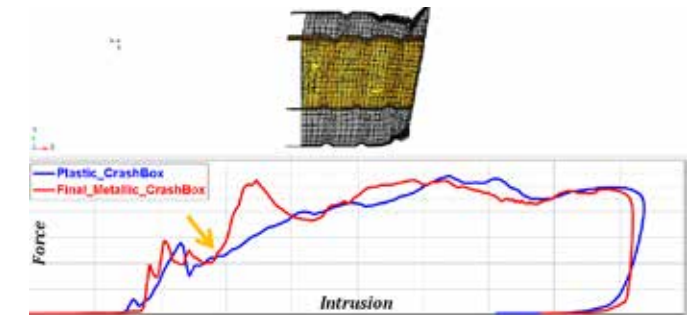


Figure 10 - Comparison of final metallic crash-box and plastic crash-box

not to damage body-in-white components behind the boxes. Having a first contact with only the outer box can lead the force values to remain inside the limits. Secondly, when the crash-boxes come into the play one after another during the impact, effect of plastic hinge can be reduced, since as this effect shows up for outer crash-box and decreases the reaction force, the inner crash-box starts to contact and become effective. So that the decrease of the force value can be reduced to some extent and the stability can be provided.

In Figure 10, yellow arrow indicates a point on force-intrusion curve which corresponds to the first contact between inner box and impact barrier. At that point, the deformation status of crash-boxes can also be observed on the upper side of the Figure 10 directly.

## Conclusions

In the end, as shown in Figure 10, the final design of metallic crash-box succeeds in providing a force-intrusion curve which complies with the limits of force and intrusions along the deformation. Plastic strain values of body-in-white components remain at moderate level which meets the requirements of RCAR structural test.

Ahmet Mert Soyer, Levent Aksel, İbrahim Özbay  
TOFAŞ TÜRK OTOMOBİL FABRİKASI

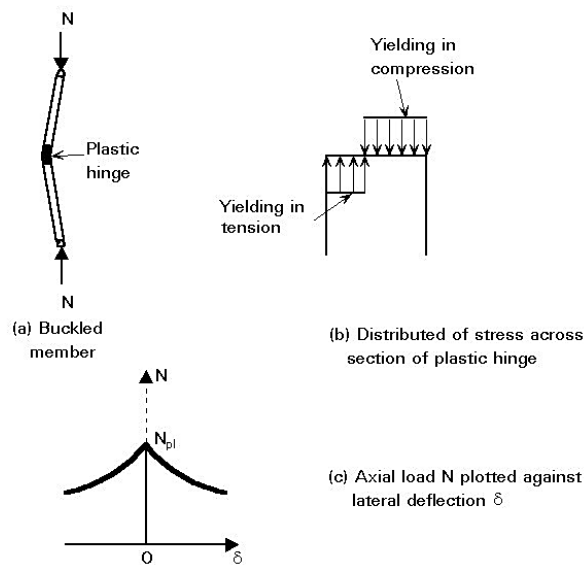


Figure 3 - Buckling of initially straight, pin-ended strut of ideal rigid-plastic material



## CAE software to optimize feeding system of butt-welded valve

In sand mold casting, one of the critical elements to have good results is the design of the feeding system, which must be optimized to increase the casting's yield and the foundry's process efficiency. The article describes activities and results within a traineeship at Politecnico di Milano in collaboration with Fonderia Augusta, Fluicon Valves and EnginSoft.

The case study consists in the design of a feeding system for butt-welding ends top entry butterfly valves for cryogenic service. Thanks to MAGMA 5, a CAE software provided by EnginSoft, the evaluation of different feeding systems and different casting's positions in the mold has been possible.

At the same time the possibility to reduce valves thickness of non-standard parts has been evaluated. The simulation of three different casting configurations has allowed to define the best solution characterized by 20% casting material reduction and a significant surface defects reduction.

### Introduction

As part of a traineeship activity at Fonderia Augusta, a steel and special alloy foundry close to Bergamo, the design of the feeding system of a top-entry butt-welded 8" valves has to be studied in order to fulfil the Fluicon Valves request of 4 units of valves.

These valves are used for low temperature applications, typically in LNG transport, and are made of CF8M UNS J92900, according to ASTM A351 / A351M – 16 (ASTM, 2016), an austenitic steel with chrome nickel and molybdenum and high corrosion resistance even in acid conditions.

The traineeship activity aim was to design the feeding system of sand casting comparing two different projects of similar valves with different thickness in some zones. It was decided to evaluate the production of the unites according to 3 different casting configurations (fig.1).

Type A uses the conventional casting system (horizontal plane molds division) to produce two components selecting the project with larger thickness.

Type B uses vertical molds orientation to produce one component: the thickness, the wood model and the molding method are the same of the type A.

To produce the third component it was used type C configuration (horizontal plane molds divisions) and a polystyrene foam model. In this configuration the thickness of some areas was reduced.

### MAGMA 5 Simulation

In order to design an efficient feeding system, it was necessary to do an early simulation (not considering fluid dynamic parameters)

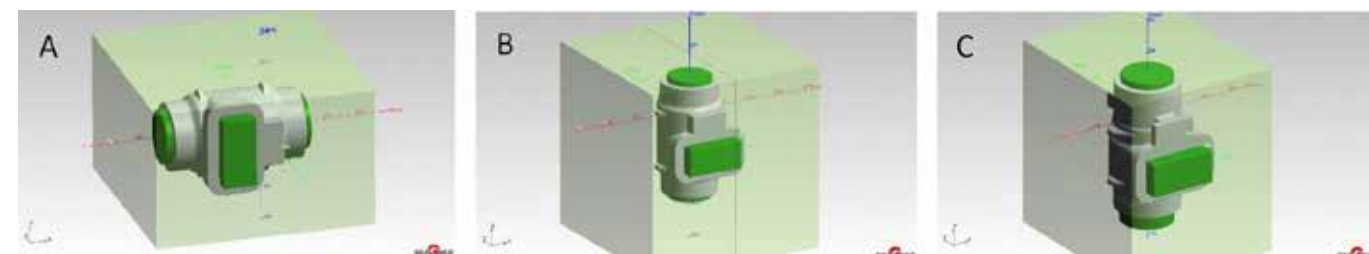


Fig. 1- 3D images of Q689/Type A (A), Q702/Type B (B), Q701/Type C (C)

to calculate the freezing module (feedmod), which will make it possible to choose the feeders' dimensions and their positions according to the Caine method (Kalpakijan & Schmid, 2012).

The simulation was performed using MAGMA 5 software; the casting process parameters were defined on the base of suggestion of Fonderia Augusta's and EnginSoft's experts.

The figure 2, 3 and 4 show the simulation results, respectively of type A, type B and type C components; different areas are highlighted in different colours according to the value of the freezing module: the areas are coloured from yellow to light blue, from the maximum to the minimum value of the freezing module. Referring to figures 2 and 3, it is possible to see that the results are the same; that's because the same geometry in this early simulation gives the same result. Differences can be seen only considering and analyzing fluid dynamic data.

It is possible to see some differences between type C and type A/B results: in fact, in figures 3 and 4, there are differences in position and value of freezing module, highlighted in figure 5 too. Nevertheless, most of the components areas have similar value especially the point with the highest value of freezing module and the areas with the lower values.

After this early simulation, it was possible to design the feeding system by placing the correct risers in the correct position. To achieve good results, different simulations with different configurations of the feeding systems were tested with fluid dynamic software module which considers primary the different temperature distribution in the casting at instant  $t=0$ .

As said before there was no difference in type A and type B results because the fluid dynamic software module was not activated, but the activation leads to different result for these two types as the orientation affect the filling time, the thermal gradient and the solidification time, too.

### Results

After some more and more detailed simulations, in which different configurations were tested, and after analyzing the results, with and without the fluid dynamic module, it was possible to reach a good feeding systems optimization.

Feeding systems of the different production configurations and related results are shown as follows.

In all the configurations the volumes of the risers are represented in red, while the coolers in blue and the pouring system in grey; the coolers actually used in the production had bigger dimensions, but

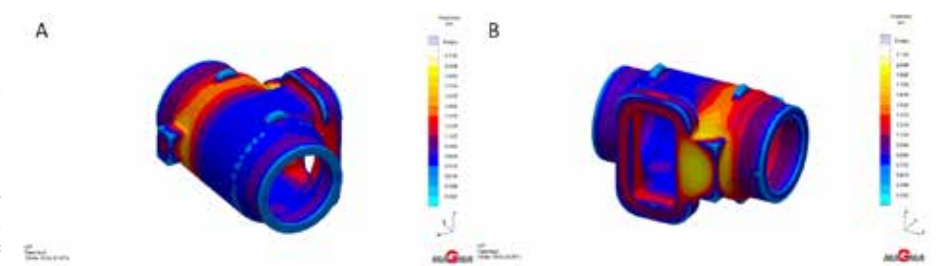


Fig. 2-Feed mod Q689/type A, back (A) and front (B) vision

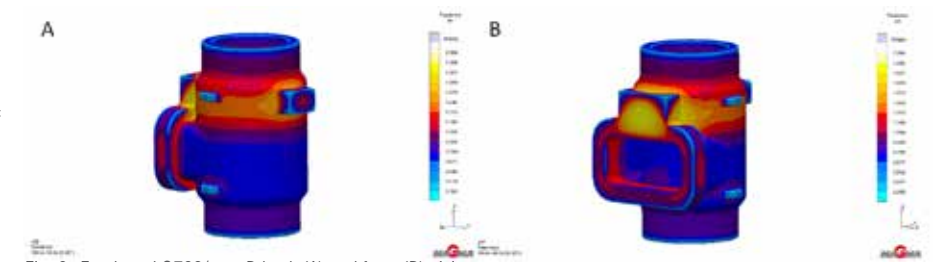


Fig. 3- Feed mod Q702/type B back (A) and front (B) vision

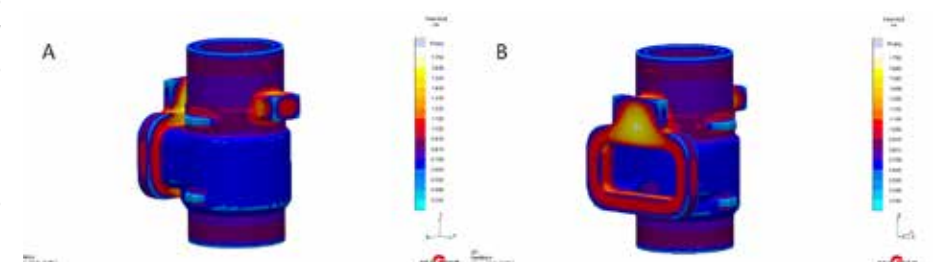


Fig. 4- Feed mod Q701/type C back (A) and front (B) vision

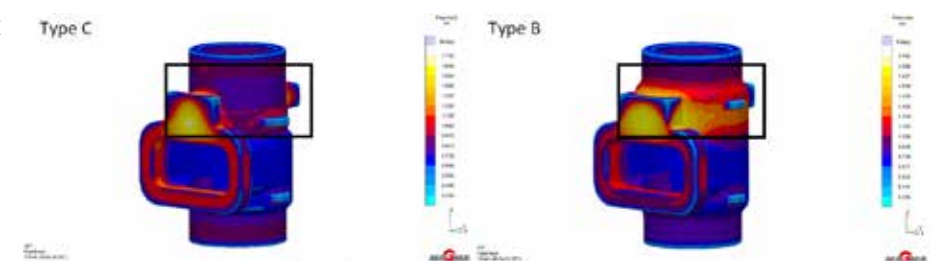


Fig. 5- Comparison between type C and type B feed mod

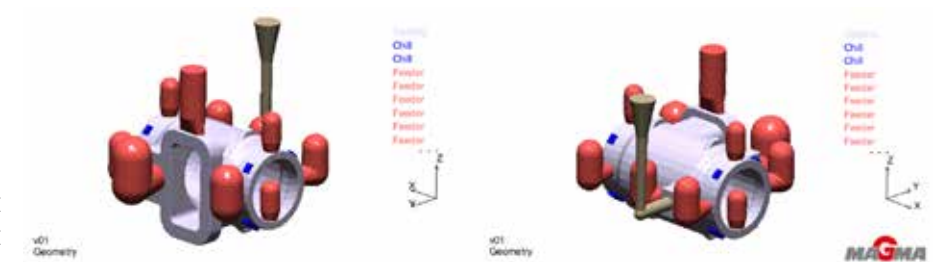


Fig. 6- Q689/type A feeding system

the differences on simulation results were minimal.

Regarding type A, figure 6 shows the chosen feeding system, while the simulation results can be seen in figure 7.

In figure 7, the main critical aspects are in the blue/yellow zones (Hot Spot FSTime results, boxes B); those zones are the most critical about Porosity results (boxes A), too.

The solution should be the design of new further risers in the critical zones, but the defects observed on the cast were considered acceptable by the production manager, considering the very low values (below 8 %). Regarding type B, figure 8 shows the chosen feeding system, while the simulation results can be seen in figure 9.

# NOZZLE-FEM: piping and pressure vessel nozzle analysis tool for every engineer

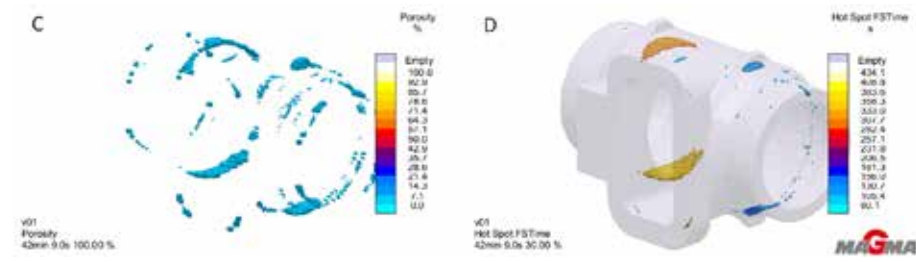


Fig. 7- Result of Soundness (A), Hot Spot (B), Porosity (C) and Hot Spot FSTime (D) for Q689/type A



Fig. 8- Q702/type B feeding system

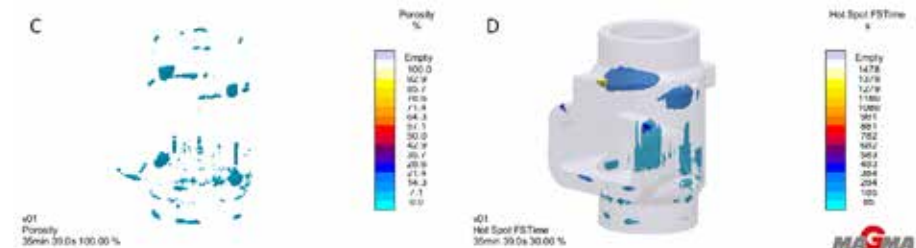


Fig. 9- Result of Porosity (A), and Hot Spot FSTime (B) for Q689/type B

Similarly to type A results, in figure 9 the main critical aspects are confirmed due to non-optimized feeding system in those zones. Moreover, other small defects are visible but they are less critical than the previous ones: boxes B show some Hot Spot FSTime, but they generate very low porosity values inside the cast, as the shrinkage cavities are fully located in the risers.

Regarding type C, figure 10 shows the chosen feeding system, while the simulation results can be seen in figures 11 and 12.

In figure 10 a red ring on the top of the model which it is an added head metal in which the impurities are located. The reason, as figure 11 shows, is due to observation that in the type B configuration (using wood model) there is a relevant presence of inclusions, suggesting the oversizing of polystyrene model (type C). The results of type C simulation highlight comparable defects, as type A and type B ones (fig. 12) but in this case, the thickness of some cast zones was significantly reduced, bringing cast weight at 22% less.

## Conclusion

MAGMA5 software, provided by EnginSoft, gave results very close to the real ones, observed on the casts produced in foundry,

except for type A where the simulation didn't highlight important defects.

The simulation of three different casting configurations (one for two type A casts, one for one type B cast and one for one type C cast) has allowed to define the best solution characterized by 20% casting material reduction and a significant surface defects reduction.

Although the customer accepted all four pieces, after the requested repairs, it is possible to foresee successive commissions following type B configuration for small batches and type C for large batches.

Giacomo Villa, Politecnico di Milano

Flavio Bettoni, Fonderia Augusta

Ernesto Imperio, CNR-Istituto di Tecnologie

Industriali e Automazione

Giampietro Scarpa, EnginSoft

For more information: Giampietro Scarpa,  
EnginSoft - g.scarpa@enginsoft.com

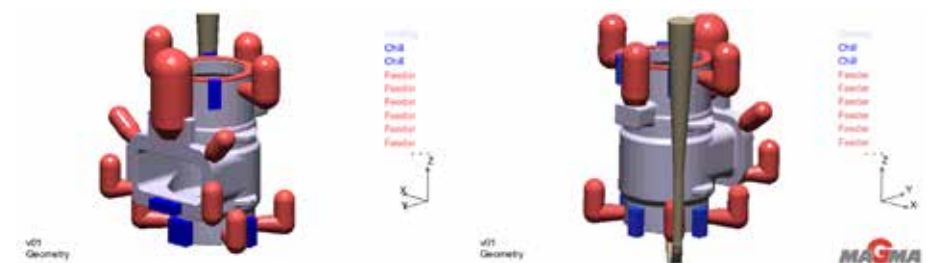


Fig. 10- Q701/type C feeding system

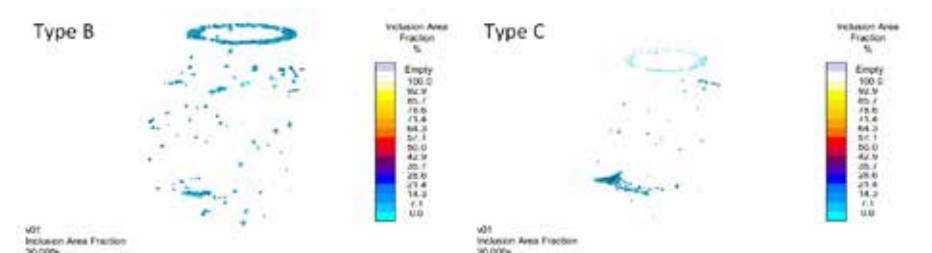


Fig. 11- Comparison to inclusion area between type B and type C

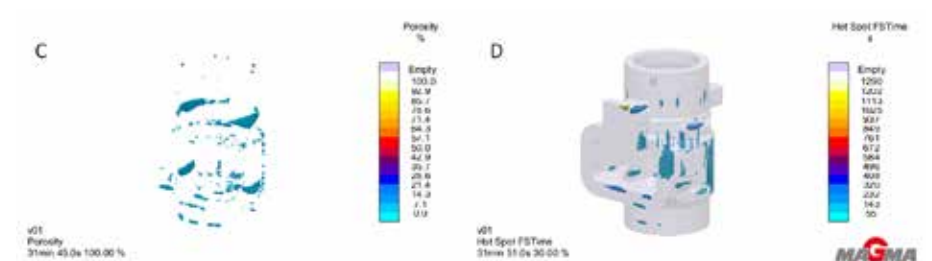


Fig. 12- Soundness (A), Hot Spot (B), Porosity (C), Hot Spot FSTime (D) results of Q701/type C

The stress analysis results of vessels, apparatus and pipelines strongly depend on taking into account the stiffness and flexibility of nozzle-vessel assemblies. Often, when calculating stresses in pipeline systems, an engineer models the connection between the pipeline and the equipment as an anchor piping support, which leads to excessive forces and stresses both in the pipeline itself and in the junction. This also usually produces a typical conflict between piping designers and pressure vessel/equipment manufactures: piping designers try to increase allowable loads to equipment nozzles while equipment manufactures try to keep them very small.

Unfortunately, the scope of analytical methods, available in the stress codes is limited: they help calculate orthogonal junctions only and cover not all the practical methods of strengthening.

At the same time, the finite element method (FEM) is universal. It allows calculating models with arbitrary geometry, as well as loading and fastening conditions. However, the disadvantages of FEM, usually limiting its use, are high requirements to the user's skills and considerable time costs for a finite element model creation.

The results of FEM calculation are the values of displacements and stresses in the nodes. The obtained stresses, usually, sharply decrease with distance from the insertion zone, therefore, the adaptive meshing of the geometry is preferable. In the junction zone, the quality of the final elements is important. As rule, it is defined as a set of constraints on the minimum value of the angle at the vertices of finite elements, also minimizing the maximum angle at the vertices.

The FEM analysis results should be evaluated in the form "the node is operational" (fit stress code demands) or "the node is not operational", which is a non-trivial task. While analyzing results, it is necessary to separate the so-called "peak" stresses obtained in the concentration zones from local stresses. "Peak" stresses are located in a very small area of stress concentrators, they decrease rapidly with distance, and have almost no effect on the evaluation of the strength under static loads of structures made of ductile materials (due to plastic deformations). So it is local membrane and flexural stresses which should be compared with limiting values from codes. "Peak" stresses are used in calculating the cyclic strength and are determined through local stresses taking into account the stress intensification coefficient.

So the usage of general purposes FEM solvers (like ANSYS and others) for practical nozzle stress analysis could be cumbersome and time costly for ordinary engineer. To overcome these limitations, PSRE has developed a NOZZLE-FEM program as a part of PASS software suite, described in two previous articles of this magazine.

NOZZLE-FEM, in contrast to universal FEM solvers (ANSYS, NASTRAN, COSMOS, etc.), does not require special training of the user and significant time costs. Creation of the finite element model and evaluation of the obtained results of stress-strain state (SSS) are performed automatically. User has to select a geometric model, set the parameters (lengths, diameters, angles, thicknesses), select the material, set the loads and press the "Calculate" button. All calculation steps are performed automatically by the program. Program provides a report that shows the initial data, the results of the calculation, including estimates stress-strain state and the conclusion about the operability of the node.

The stress calculation is performed for both radial and oblique nozzles in cylindrical and conical shells, as well as elliptical, spherical and flat bottoms.

NOZZLE-FEM can calculate the joints stiffness, which can be used then in pipeline stress analysis.

NOZZLE-FEM automatically evaluates the strength and stiffness of the radial nozzles, the strength and stability of the supporting element of the frame and the reinforcement of the hole under the action of only pressure. The program also allows to estimate the strength of joints in a corrosive-active hydrogen sulfide - containing medium taking into account.

In addition of stress checking analysis the program can calculate the allowable loads acting on the nozzle.

The program automatically creates the adaptive mesh for specific nozzle/shell geometry. Linear 4-node shell finite elements are used.

The loads are applied at the center of the free end of the nozzle. The values and directions of the forces and moments can be specified in global (associated with the shell) or in the local (associated with the nozzle) coordinate system corresponding to the diagrams in Fig.1

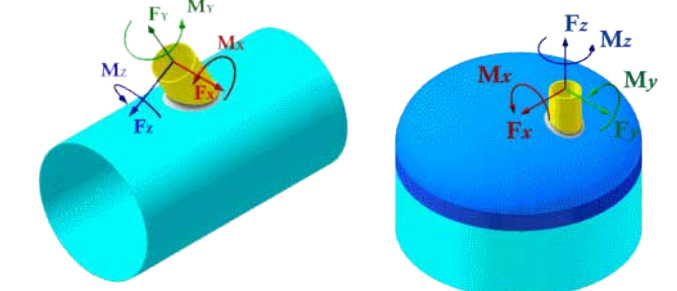


Fig.1. Loads for nozzle on cylindrical shell (a) and dished head (b)

To eliminate the zone of "peak" stresses, NOZZLE-FEM uses the approach similar to that proposed by well-known company Paulin Research Group (author of the NozzlePRO and FEPIPE). The finite elements near the

intersection line of the branch pipe and the shell (the “welding” elements) has a variable thickness. While calculating this thickness, the minimum dimensions of the welded joint, as well as the thickness of the shell and branch pipe (Fig. 2) are taken into account.

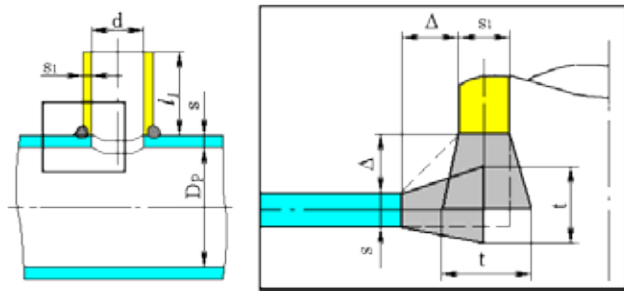


Fig.2. Finite element sizes in “peak” stress zone

When determining the thickness of the “welding” elements, the program ensures the equality of the stiffnesses of the welded seam, the shell and the nozzle in the weld zone.

The thickness of the elements adjacent to the nozzle (shell) on one side is equal to the thickness of the nozzle  $s_1$  (shell  $s$ ), on the opposite side it is determined by formulas:

$$\text{if } s \geq s_1 \quad t = \max \left\{ \begin{array}{l} s + 0,7\Delta \\ s + 0,5s_1 \end{array} \right. ;$$

$$\text{if } s < s_1 \quad t = \max \left\{ \begin{array}{l} s_1 + 0,5\Delta \\ s_1 + 0,5s \end{array} \right.$$

The maximum values of local stresses are determined for elements directly adjacent to the “welding” elements. The stresses for the welding elements themselves are not determined and are not output.

The accuracy of the results depends on the size of finite elements. NOZZLE-FEM calculates using one of five levels of the geometric model meshing. The first level corresponds to the mesh with the least number of elements, which makes it possible to perform calculations with a

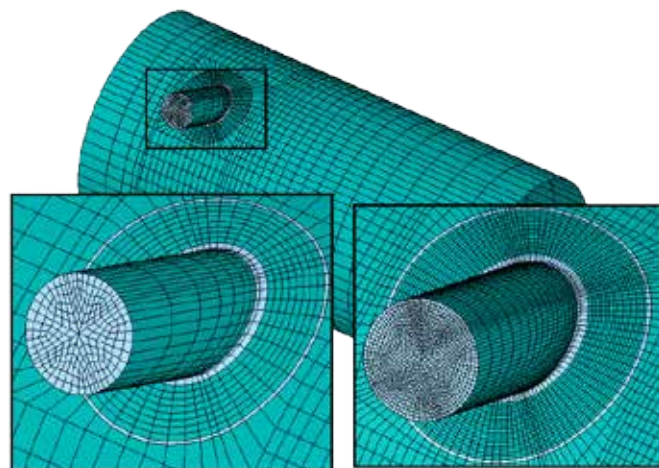


Fig.3 Finite element models, corresponding to 1st (a) and 5th (b) levels of meshing

minimum of computer RAM and time. Figure 3 shows an example of a meshes for radial tapping into a cylindrical shell with an overlap ring, corresponding to the first and fifth levels.

The accuracy of calculated stresses also depends on the nozzle features (the presence of an overlap ring, the angle of inclination etc.), the difference in thickness of the shell and nozzle, the thickness of the welded seam, the edge effects etc. To estimate the influence of these factors, we made a number of comparative calculations.

Evaluation of the results was carried out by the relative error value for various loading types. The relative error of the 5<sup>th</sup> level of meshing is assumed to be up to 5%.

Figure 4 shows the effect of the meshing levels of nozzle depicted in Fig. 3 on the relative error of the maximum stresses for various loads.

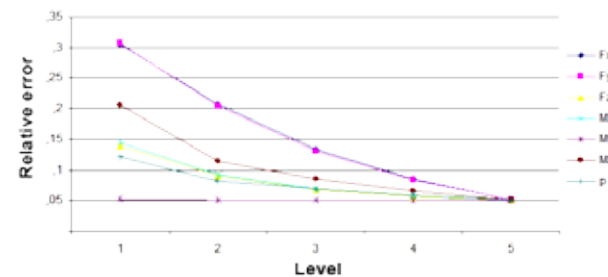


Fig.4 Relative error of maximum stress values for various loads vs meshing level

Figure 5 shows the effect of mesh level on the results of a radial nozzle without a pad.

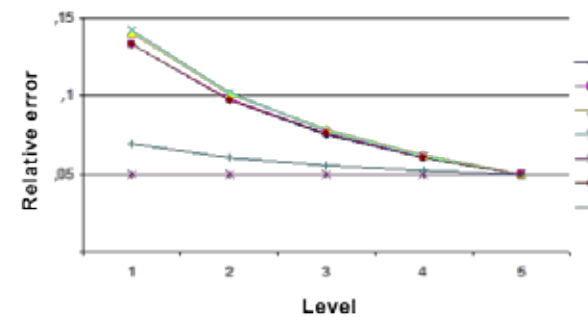


Fig.5. Relative error of maximum stress values of radial nozzle (without a pad)

An example of the stress distribution from the action of the moment for the 1<sup>st</sup> and 5<sup>th</sup> levels for a nozzle with a trim ring is shown in Fig. 6

Similar analysis was made to estimate the effect of the ratio of the thickness of the shell and nozzle on the accuracy of the solution at different levels for radial and oblique nozzles both on cylindrical and conical shells, as well as on the head (Fig. 7,8).

The results of the comparison shows that when the meshing level is increased, the obtained values of the maximum stresses also increased. The level affects the stresses from the action of forces and moments much stronger than the stresses from a pressure. The effect of the level is increased when the trim ring is applicate or the thickness of the shell relative to the thickness of the nozzle is increased.

For taking into account the quality of the mesh, the so-called «Mesh factors» are introduced into the results obtained, related to relative error  $\delta$  as  $1+\delta$ . Their values are obtained based on comparative calculations performed for various nozzles. For each level, the maximum values of relative error are selected.

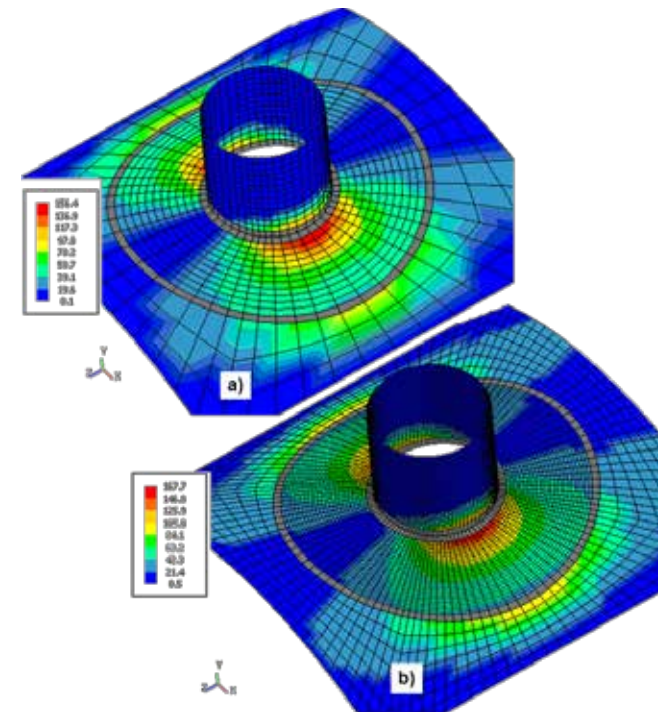


Fig.6 Stresses on the external surface (PL + Pb + Q), MPa of the 1st and 5th levels from the action of the moment  $M_z = 10000 \text{ N m}$

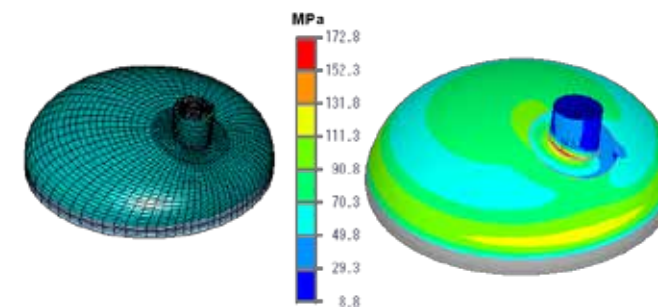


Fig.7 Membrane stresses (PL + Pb) for the nozzle on the dished head with a trim ring

Mesh factors provides an additional safety factor in calculation the allowable stresses for the corresponding mesh level.

Table 1 shows the accepted mesh factors, depending on meshing level.

Mesh Level	1	2	3	4	5
Mesh factor	1,3	1,2	1,14	1,09	1,05

Table 1

In addition software can calculate the table of allowable loads.

To determine the allowable loads on the nozzle, calculations are made to determine the maximum stresses from the action of different forces, moments and pressure separately (in the absence of the action of the others). For each type of stress (membrane and bending), a minimum safety factor is determined with allowance for the mesh factor.

As a result the program forms a table of individual allowable loads (Table 2).

$F_x, \text{ N}$	$F_y, \text{ N}$	$F_z, \text{ N}$	$M_x, \text{ Nm}$	$M_y, \text{ Nm}$	$M_z, \text{ Nm}$	$p, \text{ N MPa}$

Table 2

Further, the allowable loads on the nozzle are determined in the absence of pressure. In this case, the loads are determined from the condition that,

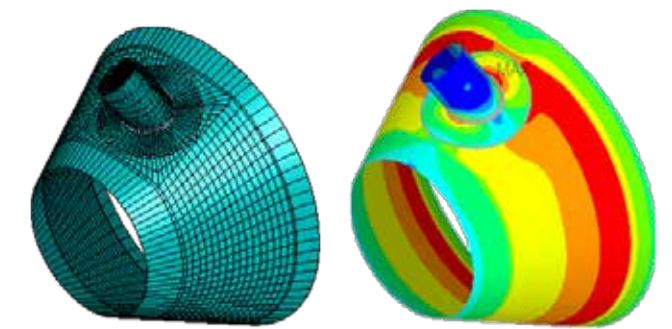


Fig.8 Stresses on the outer surface of the conical shell

when they act simultaneously on the nozzle in the absence of pressure, the maximum stresses do not exceed the allowable ones. The practice of calculations shows that this condition is satisfied when the load is equal to 1/3 of the allowable individual loads.

If the design pressure is not equal 0, the allowable loads are reduced by a value  $1-p/[p]$ , where  $p$  is the design pressure;  $[p]$  – allowable pressure value, which is determined from Table 2.

The calculated loads form the table of allowable loads on the nozzle at the design pressure, which can be used for piping stress analysis.

It should be noted that the allowable loads at the design pressure are conservative. As a rule, when they are applied simultaneously, the maximum stresses are 50-80% of the allowable values. Therefore, in a footnote to the table, it is pointed out that if the loads exceed the allowable values, an additional calculation is necessary to perform with specified combination of the loaded.

### Joint stiffness

The stiffness (flexibility) of the joint is determined for the point of application of forces in each direction in the global coordinate system. When determining the stiffness of the nozzle, the possible reduction in thickness due to corrosion and manufacturing errors is not taken into account.

The stiffness of the joint is defined as the ratio of the applied forces (moments) to the corresponding displacements (angles) (Table 3).

Linear, N/mm			Angular, Nm/deg		
$C_x$	$C_y$	$C_z$	$MC_x$	$MC_y$	$MC_z$

Table 3

### Conclusion

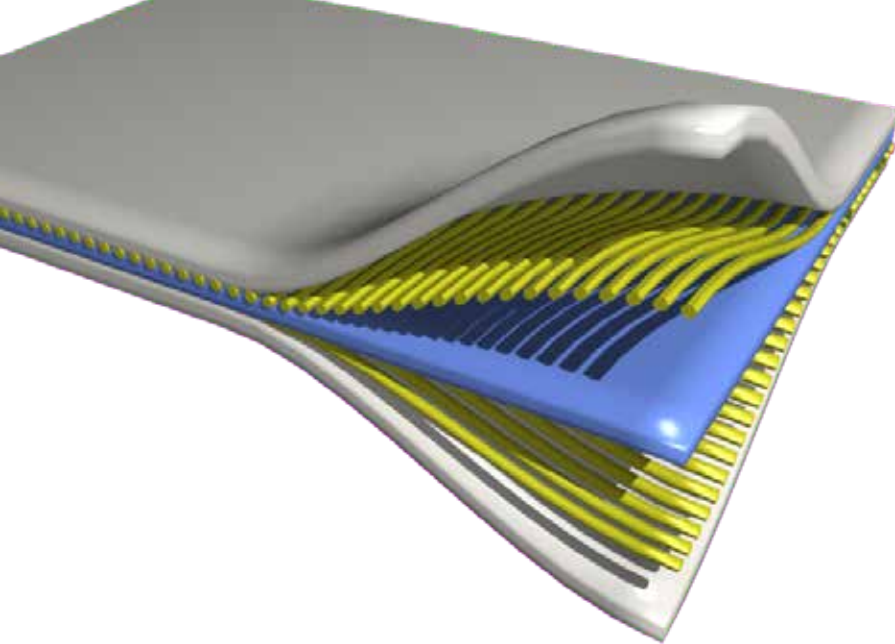
Currently NOZZLE-FEM is used by about 350 companies in many countries.

Simple and user-friendly interface, low requirements to the user's skills, high accuracy of solving problems provide program's efficiency in stress analysis of nozzles and pipelines.

The program has a direct interface with the pressure vessel stress analysis program PASSAT (which is also part of PASS).

Using “mesh factors” unlike other programs (including NozzlePRO) allows engineer to take into account the effect of finite element sizes on the accuracy of the results.

Andrey Krasnokutsky, Alexey Timoshkin – PSRE Co



# Multiscale FEM analysis system embedded in ANSYS Workbench using ACT technique

FEM analysis for composite material is very tough due to exist anisotropic material behavior. It seems that a lot of CAE engineers are having difficulties in order to get material constants. Multiscale analysis technique is very useful to resolve this problem. All material constants can be evaluated by using this technique without real material tastings. We have developed Multiscale analysis CAE tool named "CMAS" from 2006, and released 1st version in Japan at 2007. This time, we have released the same tool in global market via ANSYS App Store. The main objective of this paper is to present the functions of our Multiscale CAE tool and some analysis examples which are compared with experimental results in order to validate analysis accuracy. CMAS is embedded to ANSYS Workbench GUI using ACT (ANSYS Customization Toolkit) techniques. So, we are expected that the usage is very simple and leading high performance and productivity for ANSYS users.

## Introduction

Composite materials have been applied in many varieties of fields. FRP (Fiber Reinforced Plastics) is useful to save the weight of transport tools such as car, train, ship, airplane owing to very high specific stiffness and strength in particular. This purpose and measures will not be changed for future in that environmental loading reduction is required as eternal theme. However, composite materials are cumbersome from a standpoint of CAE engineer. The cause of this problem is that composite has three unique problems as below

- Issue 1. Material modeling  
There are innumerable combinations of materials configuring composite materials. While this has a great advantage in the sense that the scope of material design will widen, a problem is

that it is very difficult to build a material database as in the case of metal. Performing a material test each time the combination of material changes, and preparing a material physical property value that is necessary for analysis are difficult and demanding tasks. The real usefulness of analysis which is performing the trials and errors of product design at a low costs, will fade. A major problem in acquisition of physical property values is the fact that material behavior is anisotropic. For example, in the case of fiber reinforced plastic, since the rigidity of the fibers is high as compared to resins, the rigidity of the fibers in the oriented direction becomes extremely high as compared to the orthogonal direction. In order to realize these material behaviors analytically, it is necessary to evaluate the rigidity in various tensile directions and pure shear directions through material tests, which will cost a dramatically large amount as compared to isotropic materials.

- Issue 2. Dependence on molding process  
Composite material properties are also strongly depended on molding process especially injection process. In the case of injection molding process, the distribution of fiber orientation is changed by various conditions such as position of gate or type of resin and so on. So, we cannot get good results without considering molding process by means of resin flow analysis. We don't explain the detail because this paper does not focused on this issue.
- Issue 3. Multiple failure modes  
The fracture and damage behavior cannot also be simulated easily. This problem stems from the fact that the mechanism of fractures is diverse. For example, the possible causes of the

origin or progress of fractures and damage in laminates of fiber reinforced plastics are mixture of

- Interfacial Delamination between fibers and the resin
- Ruptures of fibers
- Occurrence and progress of cracks within the resin
- Delamination between layers

and various other factors. Even when only crack extension is taken into consideration, if hard materials such as fibers, etc. are intervened within the matrix phase, the extension of cracks is inhibited, and therefore, the path of progress strongly depends on the material microstructure. That is, unless analysis is implemented by taking into consideration the material microstructure, the fracture and damage behavior of composite materials cannot be accurately predicted, and it is not possible to acquire knowledge that can be used in material design from the simulation results.

Our Multiscale CAE tool mentioned in this article will be able to help to resolve the issue of no.1 and no.3 in the above list.

## Multiscale CAE System

Multiscale CAE system named CMAS is add-in tool of ANSYS that has been developed jointly by three companies, namely, Nitto Boseki Co.,Ltd., Quint Corporation, and Cybernet Systems Co., Ltd. under the guidance of Prof. Kenjiro Terada of Tohoku university, with the purpose of resolving the issues concerning mainly material modeling. By using the two functions of homogenization analysis and localization analysis that this analysis tool possesses, it is possible to implement Multiscale analysis in view of the inhomogeneous material microstructure of composite material which is fiber reinforced plastic or metal, honeycomb, filler dispersion, lattice structure and so on.

## Homogenization: CAE as a material test device

Homogenization analysis can be used to acquire information about prediction of physical property values of inhomogeneous materials. The flow of homogenization analysis is shown in Figure 1. Here, an inhomogeneous microstructure of a composite material is prepared as an analysis model (hereinafter, called in micro model). We provide some modeling templates to create micro scale model for typical structure of composite in easy way using Design Modeler. A typical example of a micro scale model is shown in Figure 2. Micro scale model can be created by only setting geometrical information such as volume fraction and radius of fiber and so on. In the case of composite having randomness such as multiple filler or short fiber, the micro model is made by Monte Carlo method that the position of particle is defined based on pseudorandom number. Therefore the different model is created every time even if the

same value is setting to modeling template. But, it is fine for us because several studies have proved that the position of filler or fiber does not affect homogenization analysis results. One the other hand, the size or angle of fiber is important to identify the material constants. Figure 3 is showing the GUI to create micro scale model for example of multiple filler structure. We can create micro model having any size distribution of filler by specifying cumulative existence probability as a functions of filler size.

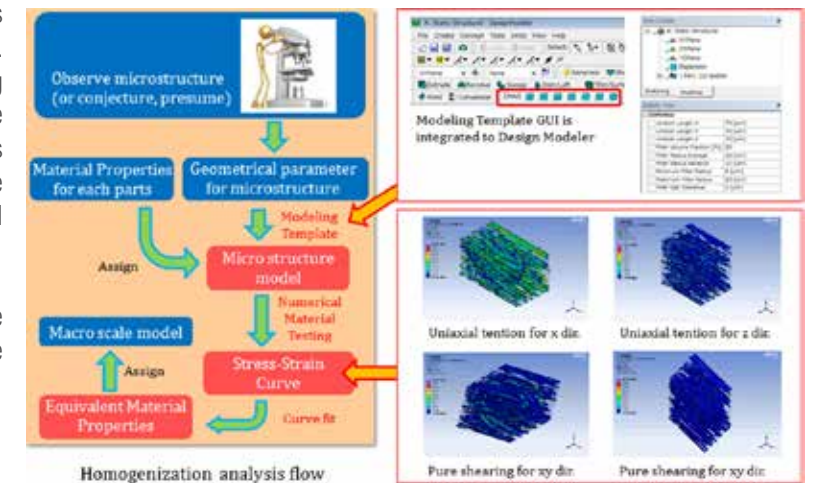


Figure 1 - Homogenization analysis flow

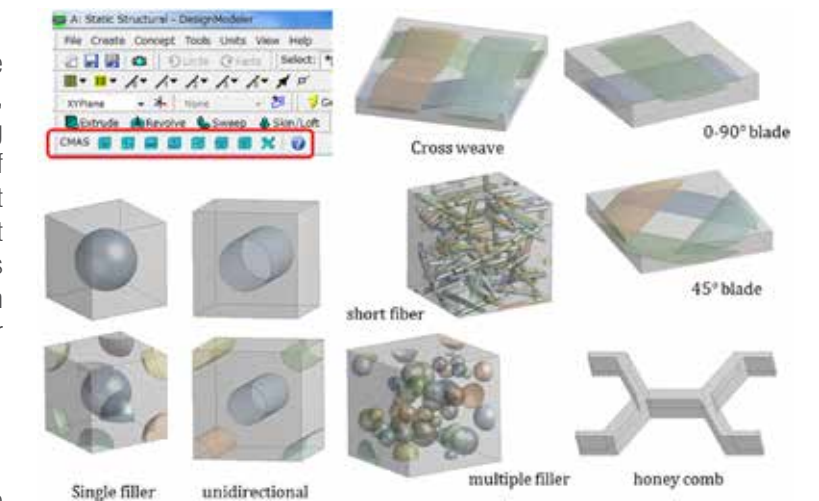


Figure 2 - Template to create micro scale model

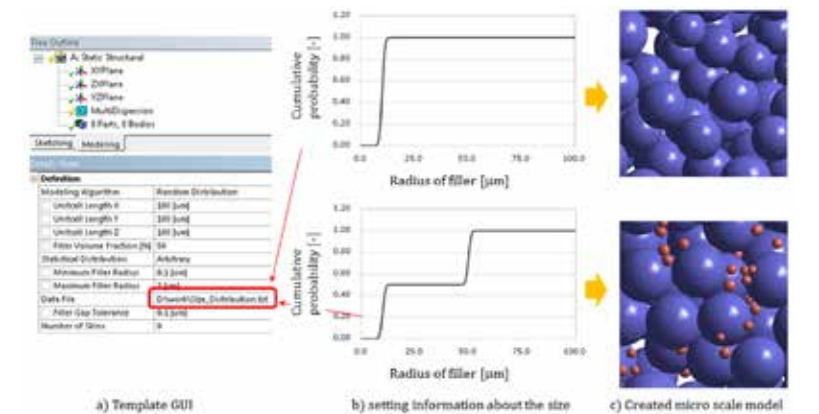


Figure 3 - Template for micro scale model creation in the case of multiple filler structure

Analysis Field	Analysis Type	Material Models	Material anisotropy
Structural	Linear	Elastic Coefficient	Anisotropic & Orthotropic
		Density	-
		Thermal Expansion	Orthotropic
	Non-Linear	Elasto-Plastic	Orthotropic (Hill)*2
		Visco-Elastic	Anisotropic (Anisotropic generalized Maxwell)*1,2
		Hyper-Elastic	Orthotropic (Kariske)*2
Creep	Orthotropic (Hill)*2		
Thermal	Linear	Thermal Conduction	Anisotropic & Orthotropic
		Specific Heat	-
Fluid	Linear	Seepage coefficient	Anisotropic & Orthotropic
Electromagnetic	Linear	Permittivity	Anisotropic & Orthotropic
		Permeability	Anisotropic & Orthotropic
		Electrical Resistivity	Anisotropic & Orthotropic

Table 1 - Supported material constants which can be evaluated by homogenization analysis

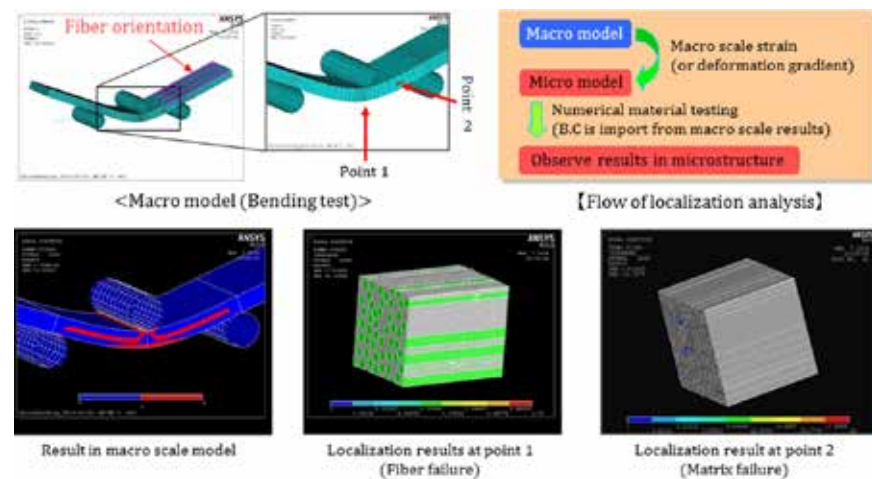


Figure 4 - Localization Analysis Flow and analysis example

As a next step, it is possible to acquire the apparent macroscopic material response for any deformation mode (such as the stress-strain curve) by implementing a virtual material test. At this time, it is assumed that the micro scale model is cyclically arranged in an infinite direction, and an ideal single stress field can be easily applied to a single unit cell model. A huge advantage is the fact that the difficult tests for example pure shearing mode can also be easily applied for simulation during the actual material test.

By fitting the apparent material response thus obtained in the anisotropic material model of ANSYS, the material physical property value can be acquired. CMAS can identify the physical parameter for many varieties of field as shown Table 1. CMAS support not only the properties for linear properties but also non linear properties such as elasto-plastic, creep, visco-elastic and hyper elastic. All of these material models are supported an-isotropic phenomena. While the fitting function of the anisotropic material model is not provided as a standard function in

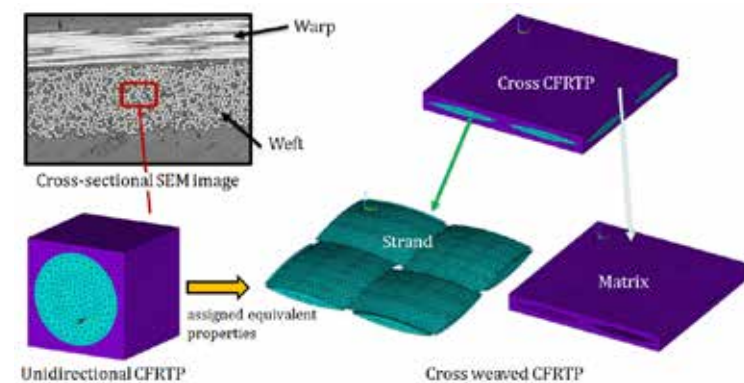


Figure 5 - Analysis approach for cross weaved composite microstructure

ANSYS, it is implemented as a function of CMAS using user programmable features. Material constitutive law of generalized Maxwell model extended to an-isotropic characteristics is also provided. Material constants for all constitutive law can be easily identified using material response data for 6th deformation modes which mean uniaxial tension for xx,yy,zz and pure shearing for xy,yz,xz.

#### Localization: CAE as a microscope

If the material constants for fractures of the composite material can be acquired by using the homogenization technique, etc. described above, it is possible to estimate the existence of occurrence of fractures in the actual structure, and also the fractured region by various general-purpose CAE tools typified by ANSYS. However, it is not possible to estimate the specific factors of the fracture in the analysis of the model in which an originally inhomogeneous material is substituted by a homogeneous material. This problem can be resolved by using the localization analysis function of CMAS.

We will introduce the localization analysis function by using a simple analysis example. Figure 4 shows example of implementation of a three-point bending test of a composite material. The specimen is a unidirectional reinforced material in which fibers are oriented in the longitudinal direction, and the fracture strength is acquired by homogenization

analysis. It can be confirmed that the fractured region indicated in red exists in the bottom and top surfaces, as well as the mid surface of the specimen. With the help of the localization analysis, a part of the region of the homogenized analysis model can be zoomed, and the results in microstructure can be evaluated. The localization point 1 in Figure 4 shows the result of localization of

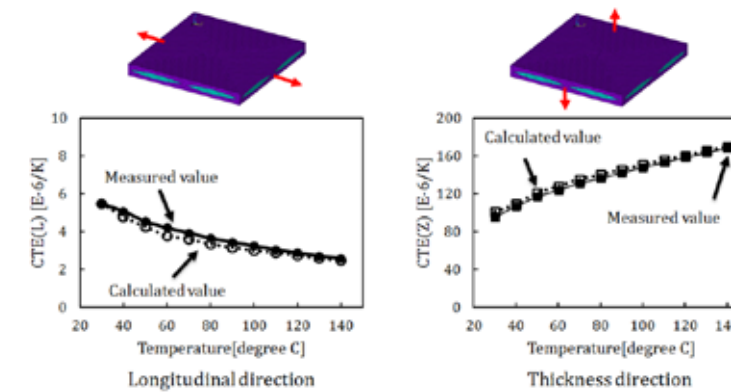


Figure 6 - Thermal expansion coefficients for each direction as results of homogenization analysis

the bottom surface of the specimen and point 2 shows the result of localization of the mid surface. Since the bottom surface of the specimen exhibits a deformation mode in which pulling occurs in the direction of the fibers, the fibers that have a lesser rupture strain than the resin break first, which results in fracture of the composite material. On the other hand, since the shear deformation mode is prevalent in the mid surface, the fibers are almost unaffected by the stress, and it can be confirmed that the fracture occurs as a result of debonding of the material interface between the fibers and the resin and also by the crack progress inside the resin.

#### Analysis Examples

##### Thermal expansion coefficient for Cross weaved carbon fiber reinforced plastic.

Thermal expansion coefficient of cross weaved carbon fiber reinforced thermoplastic (CFRTTP) is identified by homogenization analysis. Figure 5 shows analysis model for homogenization analysis, which parameters for geometry are identified based on the observation of cross-sectional SEM image. Two types of micro scale model are prepared. Unidirectional CFRTTP model is used to homogenize fiber bundle region, and resultant equivalent material constants are assigned the fiber bundle parts in cross weaved meso scale model. Figure 6 shows the results obtained by homogenization and experiment using laser interferometer system thermal dilatometer. Thermal expansion coefficients for the longitudinal direction are very low comparing to thickness direction because the carbon fiber oriented to longitudinal direction has minus coefficient whereas resin has big plus coefficients. It can also be confirmed that the analysis results are very good agreement with experimental results.

#### Model reduction

Homogenization analysis can also be used to simply the complex fem model. Figure 7 is the example conducted for this purpose. There are many circular holes arranged periodically. We cannot help to avoid making large amount of elements in order to model

the holes. It is not recommended to fill the hole by the material constants same as around parts, that is the cause of overestimation the rigidity. The right hand side of figure 7 shows the homogenization model which has equivalent materials constants evaluated by homogenization analysis. The analysis object can be simplified and the elapsed time to finish analysis is reduced about 96% comparing the case of the model having many holes. Validity of homogenized analysis results are also confirmed by checking the results of maximum displacement and stress. The results of directed model are assumed as true value. The maximum stress in homogenized model is evaluated by sub-modeling technique because the maximum stress is located at the neighborhood of the hole. We can say that the homogenization technique can be simplified the model maintaining the analysis accuracy.

#### Conclusions

In this paper, it is presented the functions and analysis example of Multiscale analysis tool named CMAS which is embedded to ANSYS Workbench. CMAS has two types of functions which is homogenization and localization analysis. Homogenization analysis can evaluate macroscopic material behavior for any deformation mode and material constants for inhomogeneous materials such as composite, lattice structure and so on. Localization analysis can observe any results item distribution in microstructure in inhomogeneous materials. We are expected that it can help CAE engineers who have trouble preparing an-isotropic materials constants or post processing about in microstructure in materials.

Koji Yamamoto - Cybernet Systems Co.,Ltd. Tokyo, Kenjiro Terada - Tohoku Univ., Intern. Research Inst. of Disaster Science  
Norio Hirayama - Nihon University, College of Industrial Technology

For more information: Marco Perillo, EnginSoft  
m.perillo@enginsoft.com

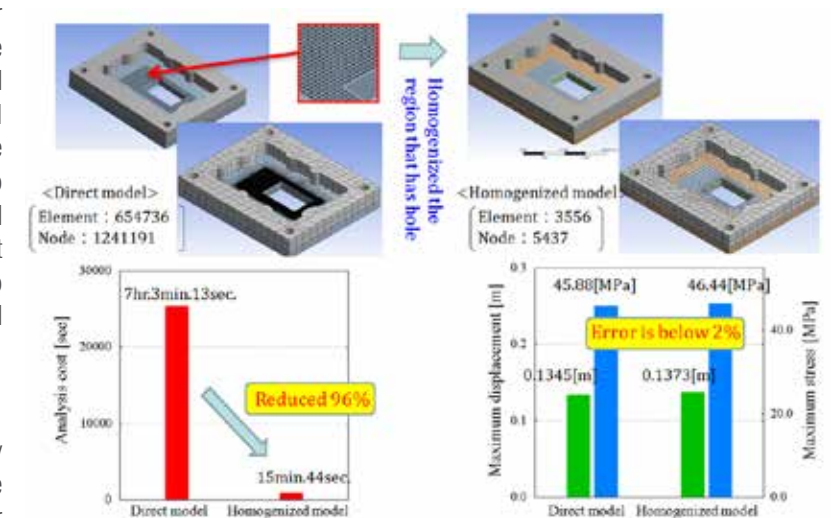


Figure 7 - Analysis example to simplify the model shape

# Short preview of ANSYS Mechanical R19 new functionalities



The new 19 release of ANSYS will be presented in the first months of the next year, as recently announced at the International CAE Conference 2017 in Vicenza. The trend metrics of the development of ANSYS Mechanical environment aim at strengthening the capabilities in engineering problem solving in new specific application areas, as well as helping its numerous users at quickly answering to demanding technical specifications with precise and reliable results.

The novelties are here summarized in key-words:

- ANSYS Mechanical interface: improvement of the performances and of the usability of the different pre and post processing tools
- Development and introduction of new advanced tools and functionalities
- Development of new simulation suites of the product (i. e. Additive Manufacturing)
- Turbomachines
- Multiphysics interaction
- System simulation



Fabricated Structures – Complex system management in ANSYS SpaceClaim

## ADDITIVE MANUFACTURING

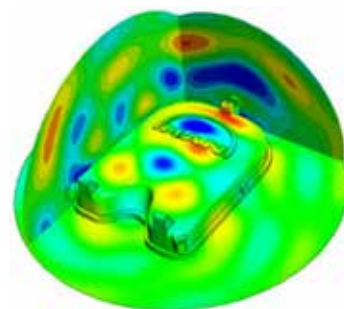
One of the main fields of development of ANSYS Mechanical software will be that devoted to Additive Manufacturing. The 18 release already included tools for topological optimization and geometries regeneration starting from STL files which provided a real support in the design of component for Additive Manufacturing. The 19 release will introduce new functionalities inside the dedicated suite, that will allow to lighten the internal structure of a component, taking advantage of lattice structures patterns and simulating the whole productive process, verifying the thermo-structural performances in the elements transient state during their generation.



Structural lightening through a cellular microstructure in ANSYS SpaceClaim

## NVH

The development of the ANSYS Mechanical tool within the NVH environment, already started in the 18 version, will proceed also in the 19 release through the introduction of modula for acoustic analysis (modal and harmonic analyses), of Structure Borne Sound formulation and improvement of the product performance in the logic setting of the workflow and post processing tools.

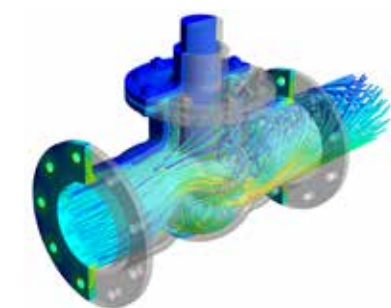


Acoustic pressure

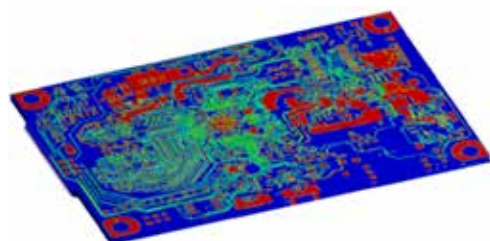
## FABRICATED STRUCTURE

A considerable evolution in the tool will be introduced in terms of big model management in SpaceClaim. The possibility of dealing with geometric topologies will be further enhanced thanks to the introduction of the internal mesher in SpaceClaim, able to reduce the iterations between CAD/CAE environments during the preparation phase at its minimum level.

For more information: Fabio Rossetti, EnginSoft  
f.rossetti@enginsoft.com



Fluid-structural interaction in ANSYS AIM



Trace Mapping in ANSYS Mechanical on electronic components

# Multi-Body-Simulation Unlimited



RECURDYN  
EUROPE

FunctionBay GmbH, the German distributor of RecurDyn software and related simulation-based services and EnginSoft SpA, the Italian leading provider of Computer Aided Engineering tools and simulation services, are today launching together RecurDyn Europe GmbH.

This new company will empower the promotion of RecurDyn, as well as other linkable CAE technologies, within the European area. RecurDyn Europe will lead a capillary network of local distributors, providing coordination, rationalization of resources, marketing means, technical support, and man power.

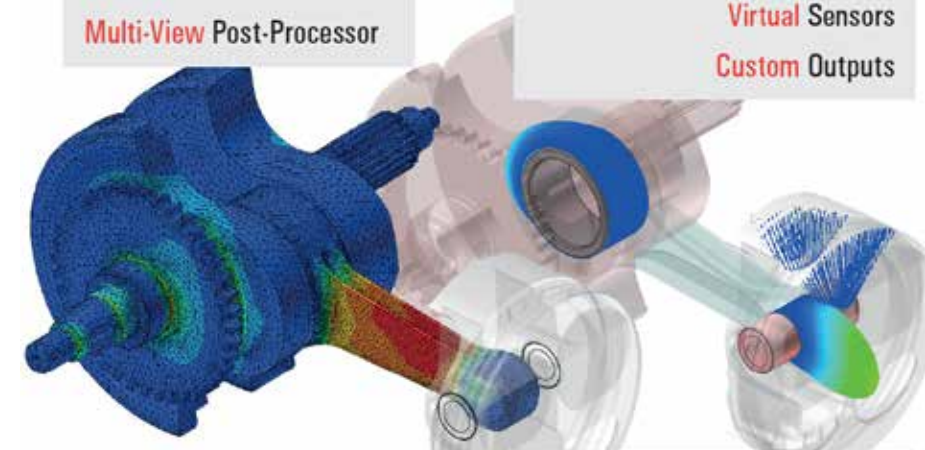
Since both founding companies are already successful players in the software market, RecurDyn Europe is born with the right means to become a reference. First, the product RecurDyn has outclassed its historical competitors in terms of power, ease of use, and productivity. Second, European users of RecurDyn will have access to an unprecedented technical support, delivered by engineers who have a long term on-field experience. The idea behind RecurDyn Europe is to maximize the benefits of a network approach: bringing the best possible answer at each node in the shortest time.

Thanks to this privileged channel, the needs and the highlights of the European customers will constantly address the development and the growth of RecurDyn.

RecurDyn is a premium multi-body simulation software, with an intuitive interface for fast modeling and high productivity. The technology hosts powerful algorithms and an optimized solver that deliver unique capabilities for both contact simulation and flexible body simulation.

Interactive Mouse Modeling  
Optimized Multi-Core Solver  
Customizable Interface  
Multi-View Post-Processor

Premium Contact Technology  
Enhanced Hydrodynamic Bearing  
Virtual Sensors  
Custom Outputs



Linear Flex Bodies  
Non-Linear Flex Bodies  
Internal Mesher  
Internal CMS Solver

INTERFACE TO:  
MATLAB™ & FMI (Mechatronics)  
Particleworks™ (CFD)  
modeFRONTIER™ (Optimization)  
KissSoft (NVH)

The package includes a programming environment for task automation and customization. A wide library of vertical modules (toolkits) completes the suite for fast modeling and simulation of selected dynamical systems.

A project powered by  
FunctionBay Germany GmbH and EnginSoft SpA

[www.recurdyn-europe.com](http://www.recurdyn-europe.com)

# Sigmatix Launches EZtol – A New 1D analysis tool

Sigmatix expands its precise, easy-to-use mechanical variation and tolerance analysis software product portfolio with its new 1D analysis tool



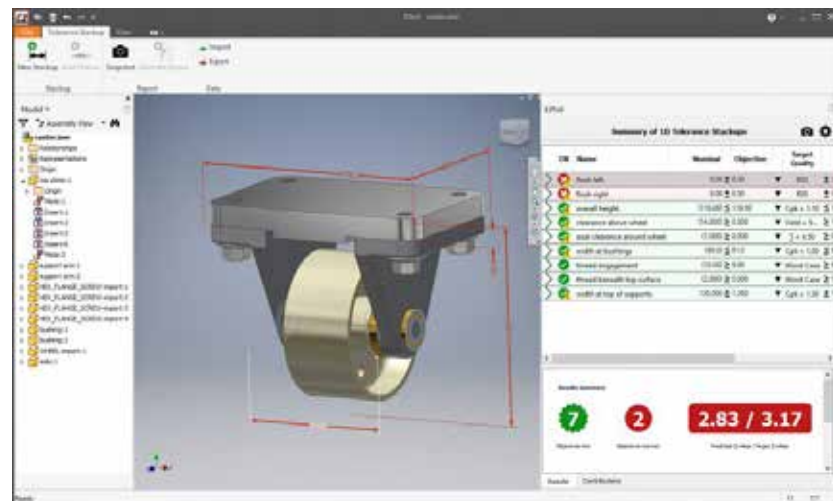
MCKINNEY, Texas – April 5, 2017 – Sigmatix, global experts in GD&T and mechanical variation, announced the latest solution in their product portfolio – EZtol. This 1D analysis tool is designed to enable designers and engineers to quickly understand the impact of part and assembly variation on the fit and performance of their products.

Why a 1D analysis tool when Sigmatix already offers a more robust analysis tool, CETOL 6 $\sigma$ , capable of predicting the impact of more complex 3D interactions that occur in production? Engineers often use hand calculations or spreadsheets to conduct tolerance stackup analyses, but unless they are specifically considering more complex interactions like the rotation of surfaces their calculations may not fully account for all the variation that can occur in the critical functional requirements. EZtol not only performs these 1D stackup analyses far more efficiently than manual methods with the numerous additional benefits mentioned below, but it can also detect many scenarios where 1D treatment may be insufficient. When such scenarios are identified a caution symbol is added to the results row as well as a note to indicate that the calculated 1D results may be underestimating the actual variation the design will have during production. Users can then decide whether or not to use more advanced tools like CETOL 6 $\sigma$  to get a better understanding of how the design will actually behave. No other solution available on the market today combines the ease of use of EZtol with a visual indication of the limitations of 1D treatment of the tolerance stackup.

- Builds the analysis on top of the 3D design model:
- Uses the actual nominal distances between surfaces/features from the design.
- Helps to ensure all components in the loop are included.
- Shows the optimum dimensioning scheme for the single analysis.
- Automatically calculates the worst-case, RSS, and statistical results of the analysis. Metrics for statistical results can be reported as: Cpk, Sigma, DPMO, or % Yield.
- Lists of contributors sorted from largest to smallest.
- Define multiple tolerance stackup analyses on the same model.
- Provides a summary table showing the objectives and results of each stackup analysis along with a visual indication of whether the requirement has been met.
- Stores the dimensions, with tolerances, defined for each part so that the user doesn't have to re-enter them for each loop. This also allows the automatic updating of all analyses when the user makes a modification to a tolerance used in multiple analyses.
- Generates detailed report with graphical view of the dimension loop over the models involved and a graphical presentation of results and the top contributors.
- Provides an indication that the tolerance stackup may not be 1D in nature including a note that the results provided may underestimate the actual variation that will occur during production.

"We are delighted to be able to expand our software offerings to include EZtol. We are recognized globally for providing tolerance analysis and GD&T software solutions, as well as industry-leading training and consulting services, and this really rounds out our product portfolio," stated Chris Wilkes, President and CEO of Sigmatix. "EZtol really bridges the gap between manual tolerance stackups and an advanced tool like CETOL 6 $\sigma$  quite nicely."

Sigmatix Launches EZtol – A New 1D analysis toolEZtol has been designed to make it easier to create, manage and report upon multiple 1D tolerance analyses in an assembly. It will work with files from most major CAD systems, without having to utilize a CAD license to work with models. Some of the other highlights of EZtol are:



For more information:  
Enrico Boesso, EnginSoft - e.boesso@enginsoft.com

# MapleSim Explorer advances MBSE democratization through organization-wide sharing of MapleSim models



MapleSim Explorer, part of Maplesoft's recently released MapleSim 2017 system-level modeling software, is a new "cost-effective deployment solution" that enables product development organizations to "make the knowledge embedded in their MapleSim models available to more people," the company says. MapleSim Explorer "powers informed decision making throughout the organization" by helping systems modeling leads within engineering organizations "make the knowledge embedded in their MapleSim models available to other engineers to support informed decision making."

This new advance in the democratization of model-based systems engineering (MBSE) follows on the company's release this past summer of MapleMBSE, which helps engineers create, maintain and validate product requirements efficiently and with fewer errors—a technological breakthrough that, in our view, for the first time lets engineering organizations adopt an MBSE approach to requirements management without forcing every engineer on the project to be an expert in complex MBSE tools. See how MapleMBSE from Maplesoft radically expands accessibility of model-based systems engineering. <http://www.3dcadworld.com/maplembse-maplesoft-radically-expands-accessibility-model-based-systems-engineering/>

## MapleSim: Advanced system-level physical modeling and simulation platform

MapleSim is an advanced system-level modeling tool suite that enables innovation and reduces development risk, allowing

engineering organizations to create better products, faster. With MapleSim, engineers can easily create virtual models, now more and more referred to as Digital Twins, before the product design is finalized, allowing them to explore conceptual designs, discover and correct unexpected interactions between subsystems early in the design process, validate product performance, and more. Now, with the easy way to share and explore models offered by MapleSim Explorer, engineering organizations can avoid overloading their systems modeling experts with requests that do not require modeling expertise, while still getting the answers they need, Maplesoft says.

## MapleSim Explorer lets more people run simulations of any MapleSim model

The MapleSim Explorer runs simulations of any MapleSim model, and allows users to change model parameters, investigate and plot any model variables, view 2D simulation results and 3D simulation animations, and analyze the model using built-in MapleSim Apps such as Parameter Sweep, Optimization, and Monte Carlo.

"A lot of engineering knowledge gets embedded in Digital Twins and other virtual models, but it's difficult to get that valuable information out to everyone who needs it, when only modeling experts can access the model," says Dr. Chad Schmitke, MapleSim Senior Director at Maplesoft. "With the MapleSim Explorer, organizations can make their MapleSim models available to more people, so they can leverage the engineering knowledge contained in the model and get the answers that will help them make better decisions, quickly and efficiently."

The MapleSim Explorer is a complementary deployment solution to the MapleSim Server. The MapleSim Explorer is a standalone product that provides individuals with direct access to MapleSim models and simulation results. By comparison, the MapleSim Server allows engineers to explore MapleSim models through interactive web applications, using only a standard web browser.

For more information:  
Giovanni Borzi, EnginSoft - g.borzi@enginsoft.com

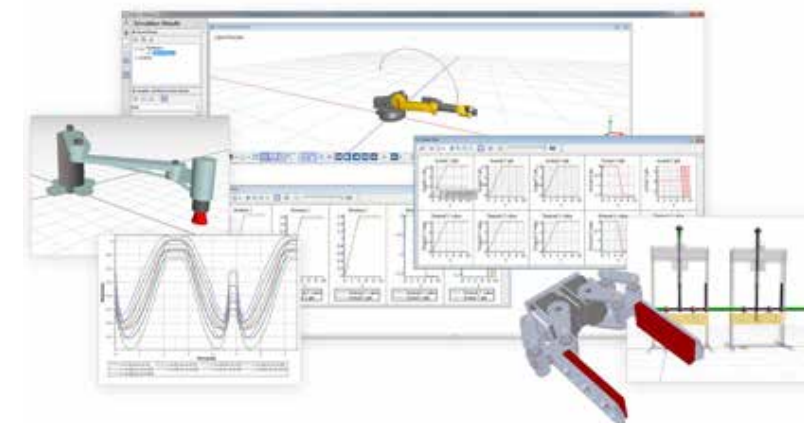


Fig. 1 - MapleSim Explorer supports informed decision making through organization-wide sharing of MapleSim models

# International CAE Conference and Exhibition 2017

## SIMULATION: THE SOUL OF INDUSTRY 4.0

Vicenza, 6<sup>th</sup>-7<sup>th</sup> November 2017



1200 worldwide participants affirm that simulation is the soul of industry 4.0 as the International CAE Conference reached its 33<sup>rd</sup> edition, on the 6<sup>th</sup>-7<sup>th</sup> November in Vicenza, this year's hub for technology and virtual simulation.

Industry 4.0, the forth industrial revolution, is inevitable and will transform the innovation, design and production processes in every field. This pressing topic has characterized the International CAE Conference and Exhibition, the major event in the field of Simulation Based Engineering and Sciences. The 2 day event held at the Vicenza Convention Centre, hosted renowned experts, stakeholders of academia, industry and the research world from Europe, the United States, in addition to Japan, Korea, Russia, Turkey, South Africa and Brazil.

Stefano Odorizzi, Scientific Director of the International Conference, Researcher & Professor of Padova University and CEO & co-founder of EnginSoft, opened the conference to a captured audience for the both the plenary session and the Smart Manufacturing round table.

The outstanding plenary session was delivered by Professor Jinhwan Choi, accredited in the area of mechanical engineering and systems dynamics; Emilio Juarez, 3D Printing Director EMEA at HP; Tom Kindermands, ANSYS Vice-President; Eric Landel, Head of Simulation techniques

at Renault; Christopher Lasseur, Head of the MELISSA Project at the European Space Agency and many more.

Each Speaker highlighted the vital role of simulation in relation to Industry 4.0; Technology, which will support and simplify the production systems of the future; System Digitalization, which allows for real-time models to simulate the system behavior from an elementary component in a plant to a complete production time; and Techniques and Simulation for Big Data Analysis and Artificial Intelligence that will enable the extraction of useful information from the analysis of complex phenomena to increase reliability.

Such pervasive simulations use data in real time to replicate the physical world in a virtual model (digital twin), including machines, products and people: each physical object has its virtual twin and the data collected from the physical object can be compared with the virtual twin, in order to identify the performance problems and to predict the solution and the optimizations of the real model.

The round table, chaired by Giovanni De Luca, director of Rai Veneto, was introduced by Tullio A. M. Tollo, director of Itia CNR Institute and president of CTS Cluster Fabbrica Intelligente. Several representatives of Italian politics, academia and industry, including: Stefano Miotto, director



of Confindustria Veneto, Antonio Bonaldo, Director of Research Districts and Networks of Veneto Region, Franco Deregibus, responsible for the Digital Innovation Hub Piemonte Region and Fulvio d'Alvia, Director of RetImpresa.

Their discussions focused on the role of SMEs, which constitutes 95% of the Italian industry, whom will soon be (if not already) involved with the improvement and evolution of the production processes on the road towards smart manufacturing. In order to encourage the new enterprise culture, the National Plan for Industry 4.0, apart from subsidies for investments, includes the creation of the new opportunities provided by the Digital Innovation Hubs and by the Competence Centres 4.0. The round table offered a clear overview of the European, national and regional strategies towards digitalization, underlining the importance of creating networks, together with training and innovation, to support organization and Universities developing new competences and evolving to meet complex requests and expectations.

The industry sessions, rich in contributions from over 100 industry experts, widely covered the variety of applications across numerous sectors: Aerospace and Defence, Transportation, Biomechanics, Civil Engineering, Energy, Oil&Gas, and many more. The participants were enlightened with how the Chernobyl New Safe Confinement large span arch roof was

built by Cimolai, they gained insights into how simulation supported the optimization of race engines at Ducati Corse, and how today's technology was used to simulate a high performance running shoe, they also learnt how failure scenarios of oil pipelines can be analyzed and the techniques adopted to analyze electric car innovations.

The exhibition area gathered more than 60 exhibitors at the forefront innovation, presenting projects, products and results concerning virtual simulation. The International CAE Conference and Exhibition showcased the most advanced technologies for 3D printing, as well as sophisticated and brand-new electronic systems for the emerging drones industry and furthermore the Desert Lyon, a robot developed to operate under extreme working conditions such as the clearing of land mines.

Chris Wilkes, President & CEO of Sigmatrix, a returning sponsor of the event said, "The International CAE Conference is an excellent opportunity for many industries tied to simulation based engineering. Many development teams know that simulation based engineering can save time and money. But there are so many more advantages that can be extracted from the International CAE Conference proceedings such as the ability to create "digital twins" of their products, allowing expanded understanding into performances and beneficial insight with respects to maintenance."

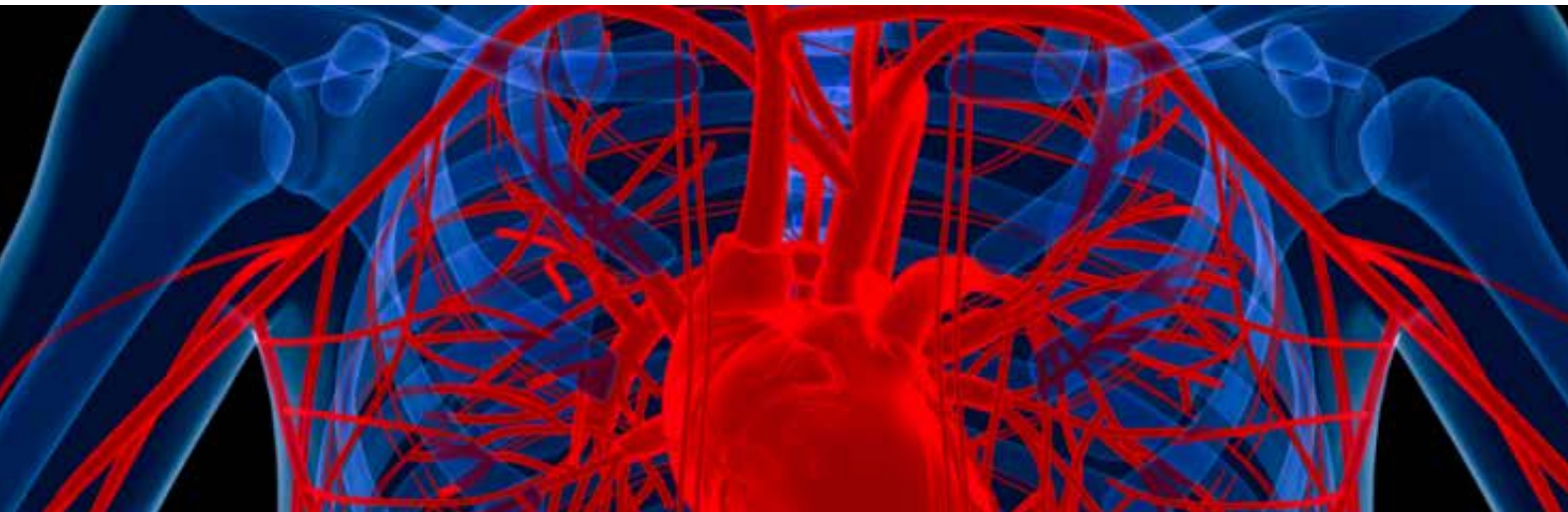
The Poster Award contest returned this year with the support of recognized institutions; CISM, Intellimech, NAFEMS, SIMAI, TCN Consortium, TechNet Alliance, and The Apulian Aerospace District along with EnginSoft, to award the best young researchers, students and academics from national and international Universities and Research Centres. With over 300 submitted projects, almost 50 of them reached the finals and five outstanding posters demonstrating the use simulation in new emerging scenarios were presented with a prize.



This latest edition of the International CAE Conference has certainly been the most successful one to date, both in terms of participation and the exceptional drive to transfer knowledge from all sectors. Nevertheless the focus is already on next year's event, guided by the fast evolving world we strive to reflect this landscape in our annual event, building upon this engineering community in Simulation Based Engineering and Sciences to deliver valuable insights from industry.



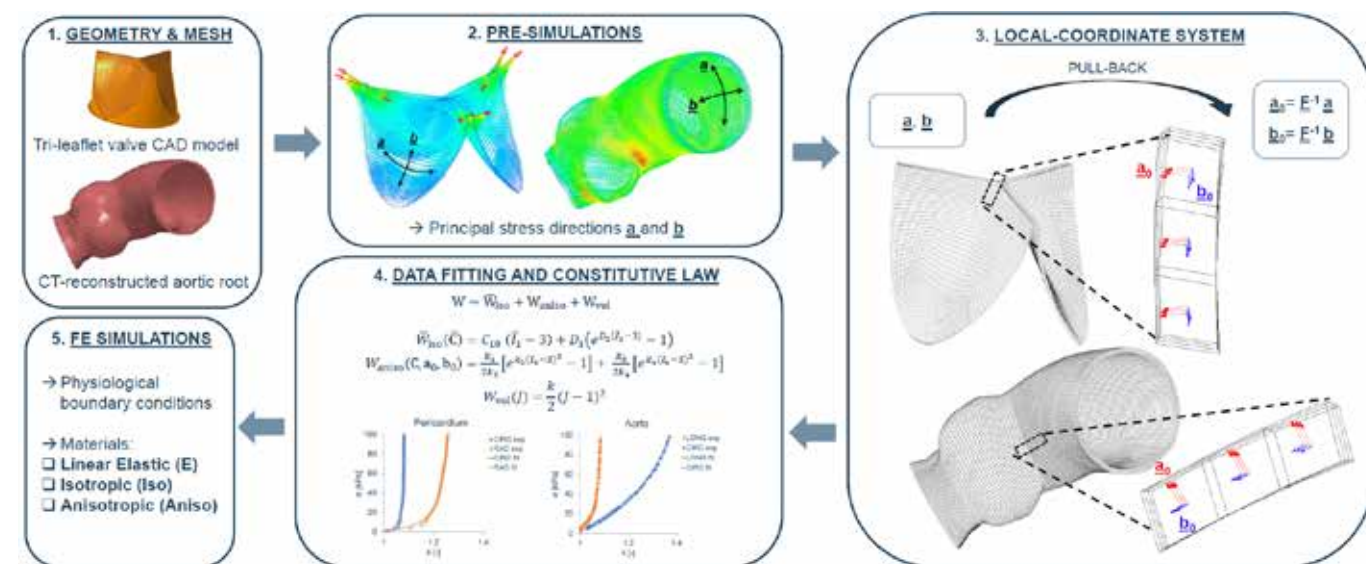
# On the importance of Anisotropy in Biological Materials: Application to Aortic Tissues



Accurate modelling the constitutive mechanical behaviour of the materials in FE simulations is crucial to capture the mechanical response of cardiovascular tissues. We have updated the ANSYS LS-DYNA list of materials with a user-defined material to model a hyperelastic matrix with up to two families of embedded fibres, whose directions can be set locally. The aim of this study is to compare different material laws with structural analyses on a tri-leaflet valve and an aortic root.

## Materials and Methods

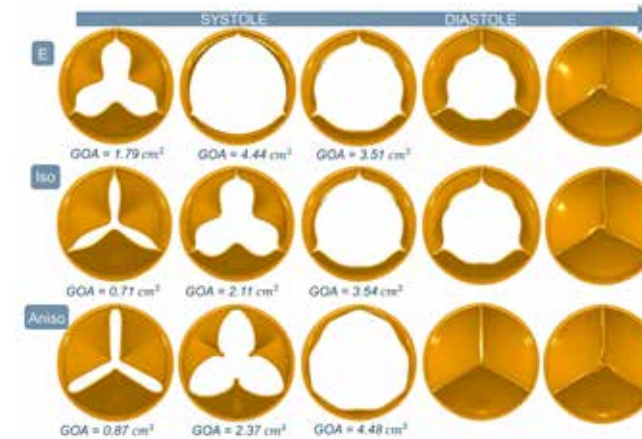
A multi-step algorithm was implemented: (1) the geometry and mapped mesh with eight-node hexahedral solid elements were generated; (2) pre-simulations to obtain the principal stress directions with realistic boundary conditions; (3) implementation of local coordinate systems for each element of the mesh, according to the principal stress directions by means of a Matlab code; (4) user-defined strain-energy function characterized with data from



the literature; (5) FE simulations with linear elastic (E), isotropic (Iso) and anisotropic (Aniso) materials imposing physiological loads.

## Results

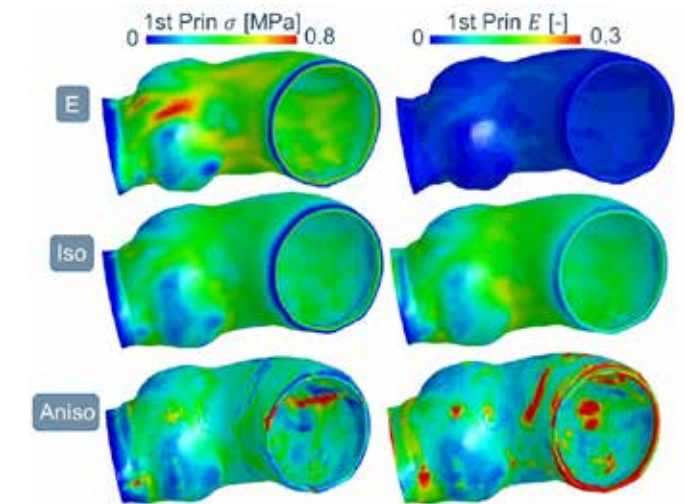
Valve kinematics in five steps during the physiological cardiac cycle for the three material models, linear elastic (E), isotropic (Iso) and anisotropic (Aniso). The Geometric Orifice Area (GOA) is also calculated.



Material parameters and calculation time for one cycle for all the performed simulations with eight CPUs.

	Valve	Aorta	Valve	Aorta
<b>E</b>	$E = 8 \text{ MPa}; \nu = 0.49$	$E = 2 \text{ MPa}; \nu = 0.49$	3 h 46 m	0 h 20 m
<b>Iso</b>	$D_1 = 0.16 \text{ kPa}; D_2 = 14.88$ $\nu = 0.49$	$D_1 = 12.39 \text{ kPa}; D_2 = 2.57$ $\nu = 0.49$	30 h 9 m	5 h 7 m
<b>Aniso</b>	$C_{10} = 5 \text{ kPa}; \nu = 0.49$ $k_1 = 0.576 \text{ kPa}; k_2 = 230.67$ $k_3 = 9.487 \text{ kPa}; k_4 = 7.59$	$C_{10} = 5 \text{ kPa}; \nu = 0.49$ $k_1 = 50.31 \text{ kPa}; k_2 = 0.56$ $k_3 = 82.51 \text{ kPa}; k_4 = 57.53$	31 h 5 m	6 h 46 m

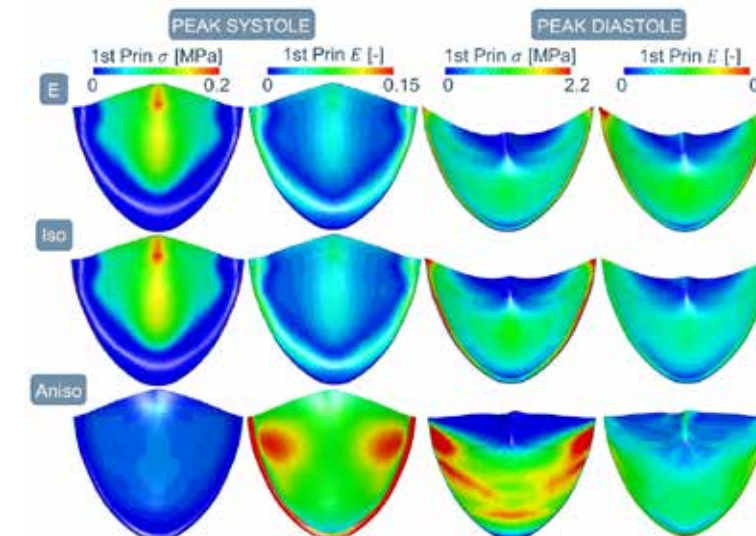
First principal stress and strain in the systolic peak for all the aorta models.



## Conclusions

The main relevance of this work is the implementation of a user-defined material, which allows to model in ANSYS LS-DYNA a hyperelastic matrix with two different families of embedded fibres, whose directions are locally defined. The comparison of the three different material models confirmed the importance of the choice of the constitutive law in modelling soft materials. The models showed different opening and closing timing – for the valve, different strain and stress distribution and different calculation time. More investigation is required to analyse the influence of the anisotropy with fluid-structure interaction simulations and how the orientation of the fibres influences the material behaviour, as well as to compare our simulations against experiments.

First principal stress and strain in the systolic and diastolic peaks for all the valve models.



Nicole Casalini, Giulia Luraghi, Francesco Migliavacca, José Félix Rodriguez - Politecnico di Milano



# Mechanical Analysis of the Toroidal and Poloidal Field Coils for DEMO<sub>nstrating</sub> Nuclear Fusion Reactor



Magnet system: 1. Poloidal Field Coils - 2. Toroidal Field Coils - 3. Central Solenoid

The DEMO magnet system consists of 18 toroidal magnets (TFC), 6 poloidal magnets (PFC) and a central solenoid (CS). Operating currents and intense magnetic fields generate high stresses in these structures. In the pre-design phase in-depth mechanical analyses are needed so as to obtain a structurally and competitively solid power reactor for the future world energy demands. Separate ANSYS static structural analyses for the TF and PF are here presented. A topology optimized design for the intercoil supports is also given.

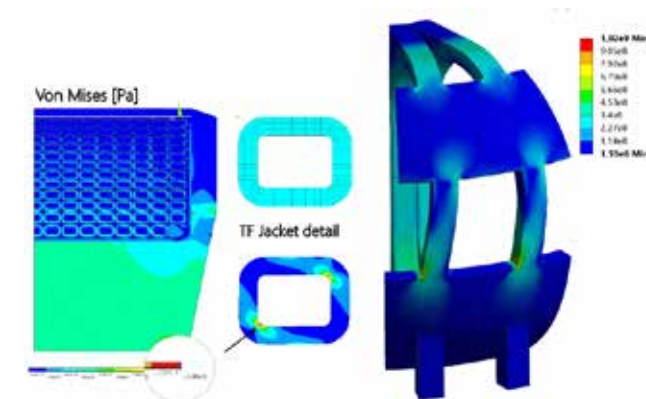
### TFC

The D-shaped toroidal coils generate the toroidal magnetic field  $B_\phi$ , which is the primary confinement solution for the plasma. Each magnet is comprised of a winding pack (WP) and a steel casing. The ENEA WP2

design configuration consists of 202 superconducting cables, capable of carrying high currents ( $i = 70.8$  kA/cable) when cooled below the critical temperature of 4.5 K. At full operation (EOF scenario). The maximum toroidal field on the magnet is  $B_\phi \approx 12$ T.

### Mechanical analysis (EOF scenario)

$B_x, B_y, B_z$  data obtained from a magnetostatic analysis have been used to derive the Lorentz forces  $\{F = iL \times B\}$  in a MATLAB routine. Two analyses have been carried out: a fully-detailed, 2D GEN plane strain APDL model, and a 3D Static Structural Workbench model:

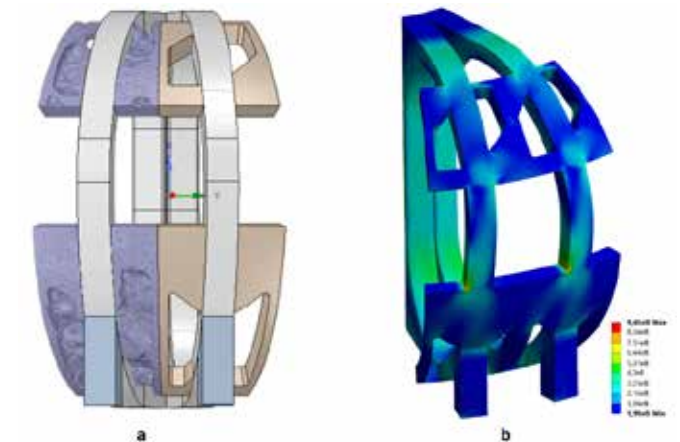


Von Mises eqv. Stress: (LHS): Inner-leg cross section at the equatorial plane. ANSYS APDL model; (RHS): 3D ANSYS Workbench model.

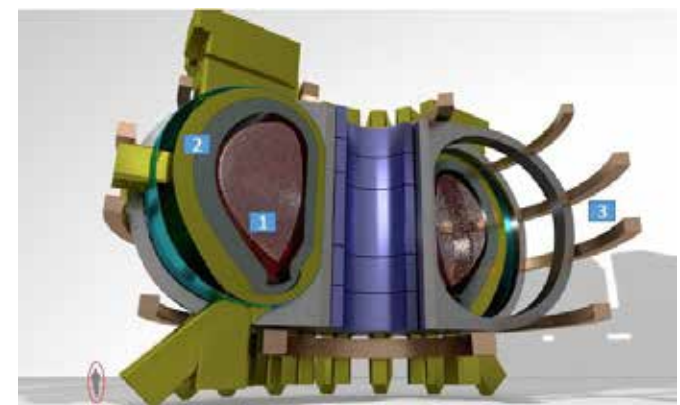
- The 2D model focuses on the equatorial TF inner leg; the loads have been applied in the WP at each S/C cable centroid, and magnet cool down effects have been included.
- The 3D model of the magnet features a homogenized WP, the load has been defined as body force density, and the presence of the Outer Intercoil Structures, which support the Out-of-Plane displacements.

### Optimization

The out-of-plane component of the electromagnetic load exerts flexio-torsional strains and stresses in the TFC, causing the magnet to bend and twist. The Outer Intercoil Structures (OIS) act as supports for this load, inducing rigidity in the toroidal direction. Their optimum design problem has been tackled via a Topology Optimization analysis, choosing a minimum compliance (maximum global stiffness) objective, and a 40% mass reduction as constraint. The engineered new shape of the OIS shows very good response to the magnet load in terms of stresses, indicating that it is possible to decrease their mass without undermining their structural requirement.



TOPOLOGY OPTIMISATION: a. Topology density and engineered design; b. Mechanical validation analysis



DEMO reactor: 1. Plasma - 2. Vessel - 3- Magnet system

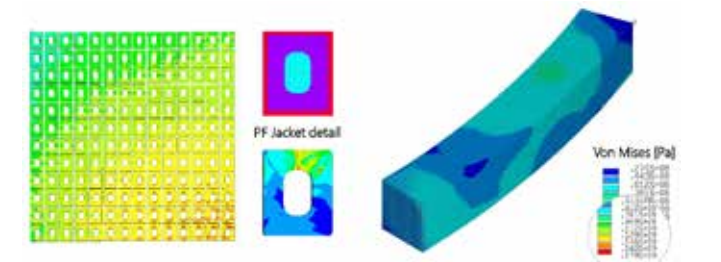
### PFC

the circular poloidal coils surrounding the TFC system produce a vertical field  $B_z$  that ensures plasma equilibrium. These magnets are mechanically connected to the TFCs through flexible plates and sliding supports that allow radial shifting. This work focuses on the PF#4, the largest of the poloidal magnets, with a radius of 17 m and a section

composed of 168 S/C wires. The magnetic field and the current are lower than the TF, and reach maximum values of respectively  $B_\phi \approx 5$  T,  $i = 55$  KA/cable.

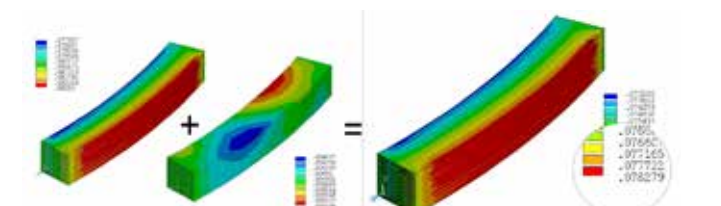
### Mechanical APDL analysis (EOF scenario)

Along the toroidal direction in correspondence of each TFC the magnetic field has a peak of intensity. There are 18 TF so the system can be easily studied in cyclic symmetry with a period of 20 degrees. Field values in each section, transformed into Lorentz forces, have been applied to superconducting cables. 168 application points and 40 interpolation sections are used in the considered repetition period of the load, with a maximum value 246 MN/m<sup>3</sup>.



(LHS): full detailed cross section PFC analysis - (RHS): 20 degree 3D sector PF#4 model

The PF coils operate below the critical temperature for the Ni3Sn superconductor, hence the effect of cool down on the structure is to be considered. Different thermal expansion coefficients between the jacket steel and epoxy filler induce potentially critical tensional states. Since the analysis remains within linear elasticity, nodal displacement solution can be summed by superposition of effects.



Cool Down (compression) + Lorentz Forces (traction) = Total max Displacement 7,8 cm

### Conclusions

- The TF innerleg 2D section analysis shows critical stress peaks (1.13 GPa) in the jacket corners. Parametric optimization for the jacket thicknesses and curvature radii may alleviate this issue;
- The TF global 3D analysis is used as basis for a topology optimization of the OIS between the magnets; an engineered optimum design is proposed;
- The PF coil tensional state is compliant with stress limits. However, the interaction between jacket and insulation must be thoroughly characterized, as a failure on the insulation may lead to magnet collapse.

Lorenzo Giannini, Alessandro Anemona  
University of Rome "La Sapienza", ICAS scrl

Lorenzo Zobili, Giordano Tomassetti  
University of Rome "Tor Vergata", ENEA



# A Multiscale Simulation Framework of the Accumulative Roll Bonding Process Accounting for Texture Evolution



## Motivation

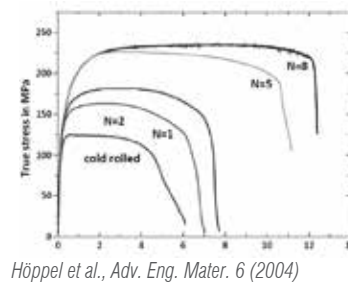
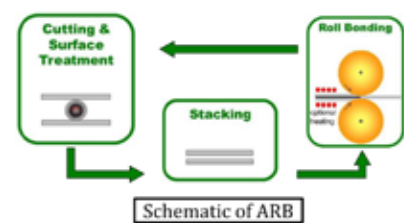
Accumulative Roll Bonding (ARB) is a promising severe plastic deformation process for achieving materials with enhanced properties. Due to repeated stacking and roll bonding, a large amount of plastic deformation is accumulated, resulting in an ultra-fine-grained (UFG) microstructure, and consequently, high strength.

- Currently, no comprehensive simulation framework available for ARB
- Adoption of new materials, however, hinges on the possibility to reliably model the deformation behavior and failure of the material during processing and in-use conditions

- Doubling of number of elements in each ARB pass due to stacking of sheets
- Multiscale approach needed to incorporate a microstructural model
- Memory of solution state -> multiple pass simulations require the carry-over of material state from one pass to another
- Computationally intensive -> development and implementation of efficient numerical algorithms required for simulations in realistic time frames

## Methods and simulations details

- Elements of the multiscale framework:
- Structural response – explicit FEM
  - Material response – visco-plastic selfconsistent (VPSC) model
  - Multi-level parallelization: MPI based domain decomposition of the structural response + openMP based thread parallelization of the material response
  - Selective probing: linear stress update performed when VPSC is not called

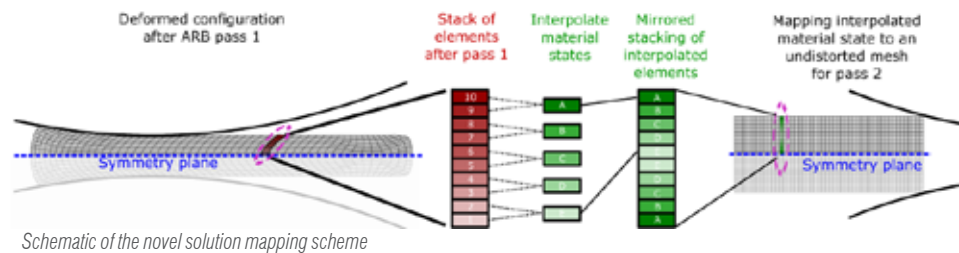


Hausöl et al., Adv. Eng. Mater. 12 (2010)

Höppel et al., Adv. Eng. Mater. 6 (2004)

## Challenges

- Conventional rolling simulations are insufficient - anisotropy in yield surface depends on the number of ARB passes
- Mesh distortion due to large amount of thickness reduction (50%)



Schematic of the novel solution mapping scheme

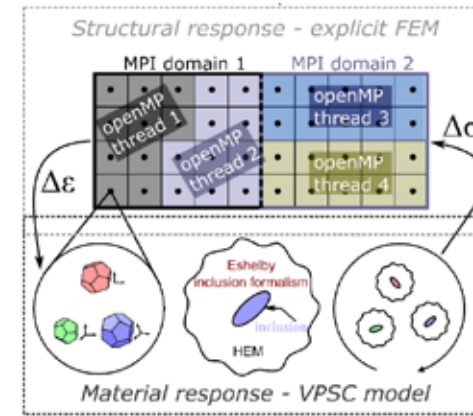
## Novel solution mapping scheme

- Transfers complete material state from one pass to another
- Material state mapped onto a completely new mesh -> No mesh distortion problems
- Only microscopic variables used for mapping -> CRSS  $g^{(a)}$ , cumulative shear  $\Gamma$ , grain shape  $F_g$ , grain orientation  $g_c$

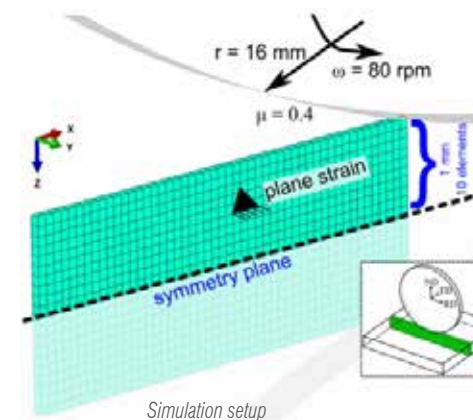
## Simulation details:

- Plane strain rolling, roller  $\phi = 32$  mm
- Feedstock – two AA5754 Al alloy sheets
- Mesh – 500 brick elements (C3D8R)
- Random texture with 250 grains per integration point

Challenges in the modeling of ARB: Due to large thickness reduction and the role of friction, the yield properties of the rolled sheet differ from conventionally rolled sheets and are difficult to predict

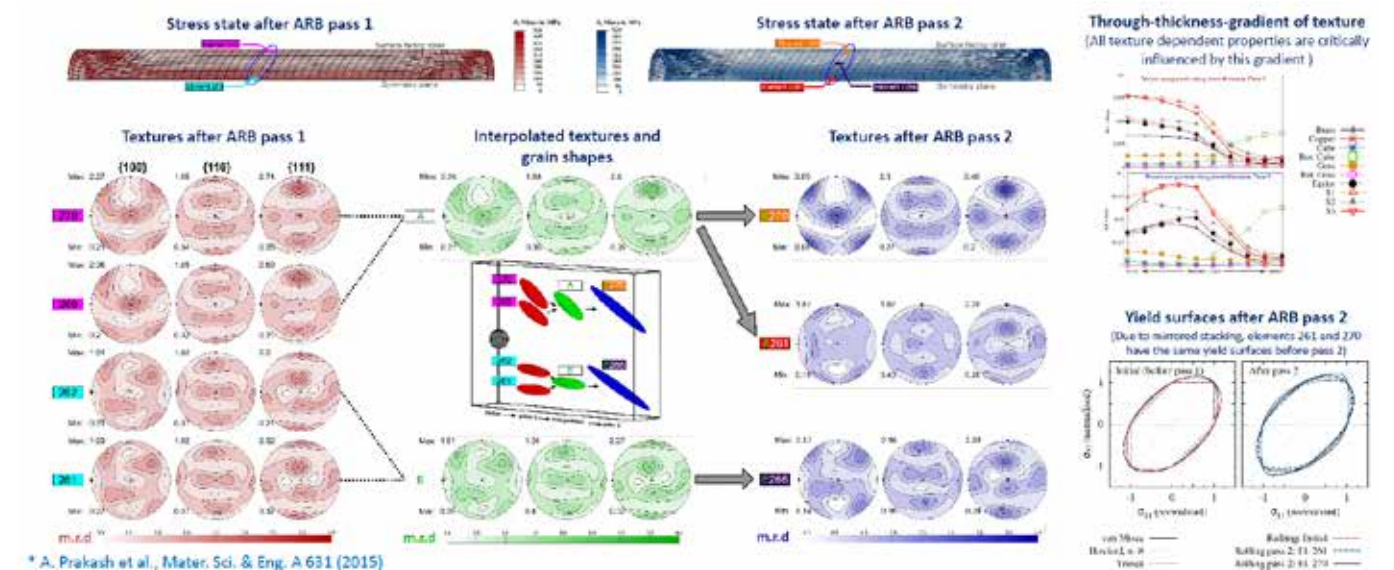


Schematic of the multiscale framework with multi-level parallelization



Simulation setup

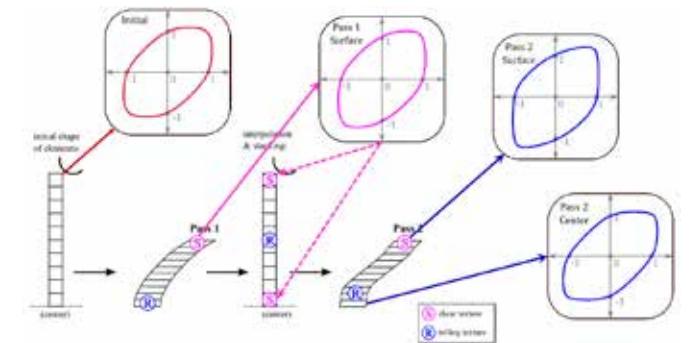
## Results



\* A. Prakash et al., Mater. Sci. & Eng. A 631 (2015)

## Conclusions

- Proposed multiscale framework able to capture evolution of texture and resulting anisotropy during ARB
- Novel solution mapping scheme enables simulation of multiple ARB passes and facilitates usage of constant number of elements in each pass
- Material state mapped onto a completely new mesh -> mesh distortion problems circumvented



Yield surface evolution in the rolled sheet as seen in simulations of two-pass ARB

- Multilevel parallelization (MPI+openMP) helps reduce simulation times by up to 70%
- Through-thickness-gradient of material properties -> yield behavior of surface elements differs from those in the center -> must be accounted for in subsequent simulations like e.g. deep drawing
- Effect of stacking of sheets: gradient of texture depends on number of ARB passes; shear experienced by elements in lower surface is reduced in subsequent pass; yield behavior significantly different when compared to conventional rolling
- Proposed framework not restricted to ARB alone; can be used for other forming processes like conventional rolling, deep drawing etc.

A. Prakash, H.W. Höppel, E. Bitzek  
Friedrich-Alexander-Universität Erlangen-Nürnberg, Erlangen, Germany

W. G. Nöhring  
École Polytechnique Fédérale de Lausanne, Switzerland

R.A. Lebensohn  
Los Alamos National Lab, Los Alamos, USA



# Structural optimization and geometric modeling of lattice structures for Additive Manufacturing

Additive manufacturing technologies enable the fabrication of innovative components not achievable by other technologies, such as cellular structures, characterized by lightness and good mechanical properties. In this work a new structural optimization and geometric modelling approach is proposed to design regular cellular structures as a function of material, loads and constraint conditions. Several cell types were studied and a classification as a function of relative density and compliance was proposed. The method aids the design process of cellular structures for additive manufacturing and the results drive the choice of the best cell type as a function of the boundary conditions. In this way many advantages are achieved such as lightness and less expensive components.



### Method

The proposed design method is based on the substitution of a solid model with cellular structures, obtaining a wire model computed repeating a unit cell inside a part. Based on diameters of the beams, material, loads and constraints, a finite element (FE) model is built. Then the FE analysis is performed, obtaining for each beam a value of utilization. This index identifies the level of usage of the material for each element and is similar to the ratio between the actual Von Mises stress and the maximum admissible stress.

When the utilization of each beam is inside an established range, the optimal solution is found. In other cases, based on the actual radius and utilization of each beam, new radii are computed and the FE model is re-built and re-analyzed (Fig. 1).

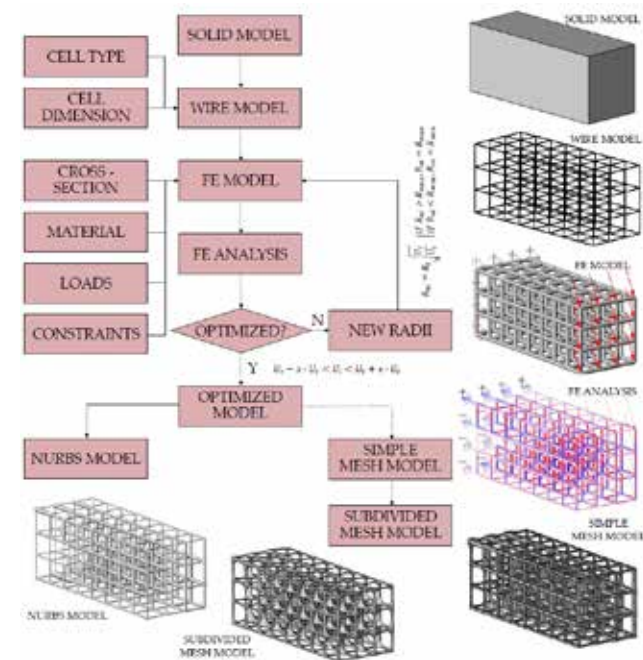


Fig. 1 Framework of the proposed design method.

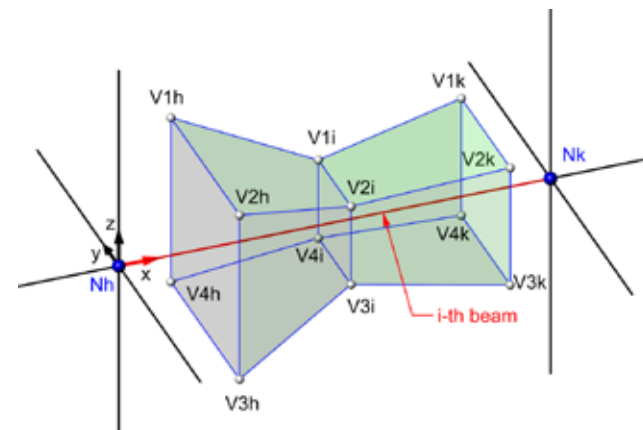


Fig. 2 Modeling a mesh around a beam.

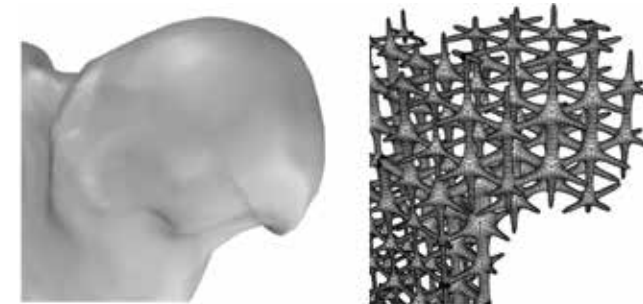


Fig. 3 Example of the proposed method.

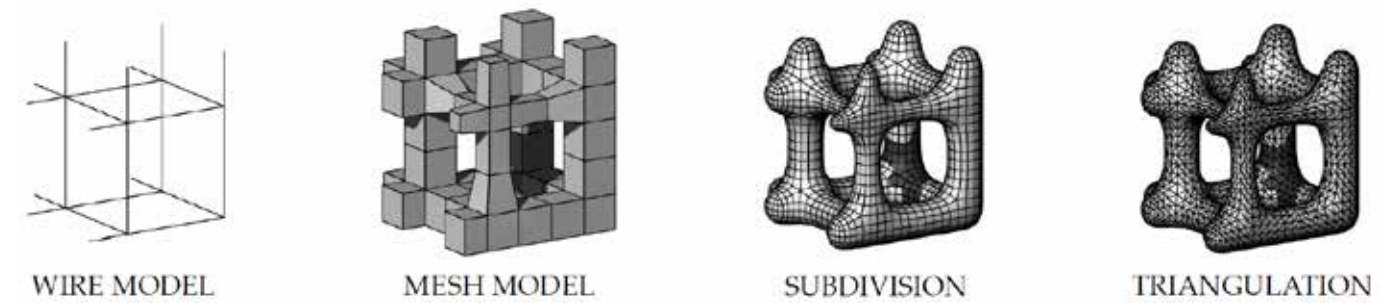


Fig. 4 Framework of the proposed approach: from a wire model and optimized diameters, a mesh was built. Then a subdivision scheme is applied. Halving each face, a triangular mesh is computed

As a result of the optimization process a radius for each beam is found. Then around of each wire of the model a cylinder with spherical caps is drawn and finally a boolean union was carried out among all the elements obtaining a NURBS model. This approach highlights some limits related to boolean operations (which often fails and demands high computational resources), sharp edges (inducing stress concentration), NURBS high complexity (inducing difficulties in model visualization and determining extremely large file dimension). To overcome these limits a specific modelling procedure was developed for cubic cell (Fig. 2,4), consisting in:

- the definition of a simple and consistent mesh model, approximating each beam element (cylinder) by 8 planar mesh faces (the cylinder assumes a double truncated pyramidal shape as in Figure 2);
- the application of subdivision surface schemes (Catmull-Clark) to create fillets and round off the beam sections, obtaining a mesh suitable for data exchange in Additive Manufacturing.

The whole approach was integrated in the same CAD environment (Rhinoceros® 5 by Robert McNeel & Associates) adopting IronPython as programming language, Karamba as FE solver, Grasshopper as graphical algorithm editor and Weaverbird for subdivision surface.

### Test cases and results

A cantilever beam with dimension 30x30x80 mm was adopted as solid model to optimize. The cantilever beam was filled with 6 type of cells having dimension equal to 10 mm (Fig. 5a). Two cantilever beam load conditions were applied: 50 N vertical force and 50 N axial compressive force. The load force was distributed in the nodes lying in the free end of the cantilever. The nodes of the beams lying in the opposite face of the cantilever were adopted as fixed supports. The material used in the design and optimization process is polyamide 12. Figure 5b,c,d,e show the compliance index D (max displacement/force) and relative density  $\rho$  (volume fraction) behaviour for the two load cases. Other test cases were carried out adopting different shapes, materials and boundary conditions. Figure 6 shows a visual comparison between the proposed method and topology optimization.

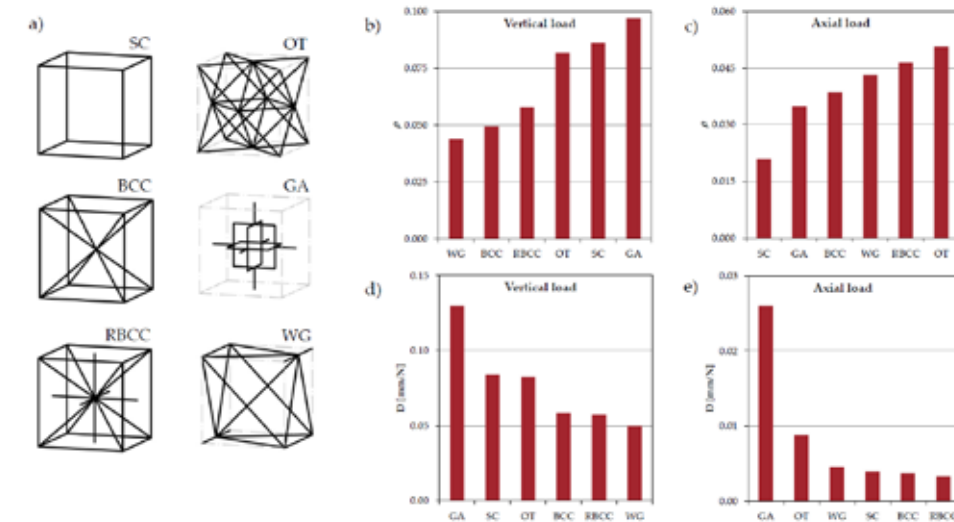


Fig. 5 Results: a) Cell types investigated; relative density  $\rho$  b) under vertical load and c) under compression; compliance index D of the structures d) under vertical load and e) under compression.

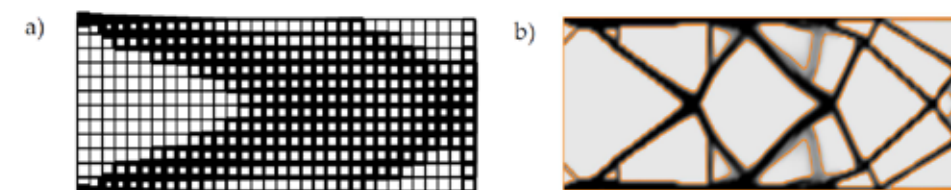


Fig. 6 Proposed method on a cubic cell (a), vs topology optimization (b).

**Acknowledgment**  
This work was partially supported by the grants "FSE 2105-116-2216-2016: Development of fatigue test machine for the investigation of cellular structures fabricated by additive manufacturing technologies" and "BIRD175287/17: Development of design and geometric modeling methodologies aimed at enhancing the peculiarities of additive manufacturing technologies".

Gianpaolo Savio, Andrea Curtarello, Stefano Rosso, Roberto Meneghello, Gianmaria Concheri  
University of Padova



# Electro-thermal Finite Element Analysis for biomedical application. Reconstruction of a phantom: from EM safety up to treatment planning

Thanks to the rapid growth of the computer hardware resources, nowadays it is possible to create numerical phantoms of human bodies which are sophisticated enough to guarantee an high level of computational accuracy. In case of bio-electromagnetic compatibility, the implemented models can be used to assess realistic conditions of exposure for common situations in real life (e.g. exposure due to a telecommunication device, microwave oven leakage, etc.), or for analyzing the conditions under electromagnetic therapy (e.g. hyperthermia, electrostimulation, etc). In this poster, we show the

main steps of numerical implementation that are necessary to obtain reliable results from a large-complex 3D multiphysical coupled model of a human body.



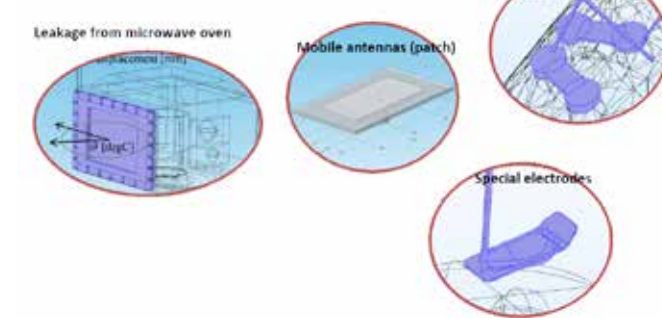
### Verification of the mathematical formulation

$$\lambda_{0j} = \frac{c}{f_j} = \frac{1}{f_j \sqrt{\epsilon_0 \mu_0}} \gg d, \quad j = 1, \dots, m$$

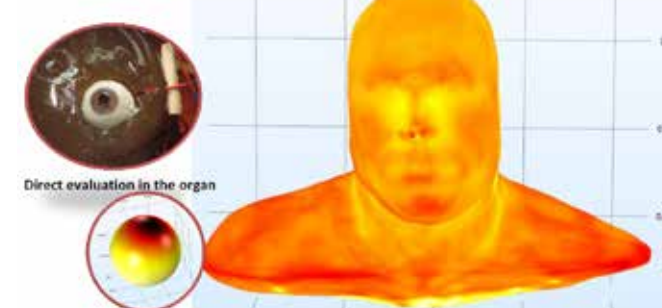
$$\delta_{ij} = \frac{c}{2\pi f_j \sqrt{\frac{\epsilon_i}{2} \left[ \sqrt{1 + \left( \frac{\sigma_i}{2\pi f_j \epsilon_i} \right)^2} - 1 \right]}} > d_{et}, \quad i = 1, \dots, n, \quad j = 1, \dots, m$$

$$\gamma_{ij} = \frac{\sigma_i}{2\pi f_j \epsilon_i} \gg 1, \quad i = 1, \dots, n, \quad j = 1, \dots, m$$

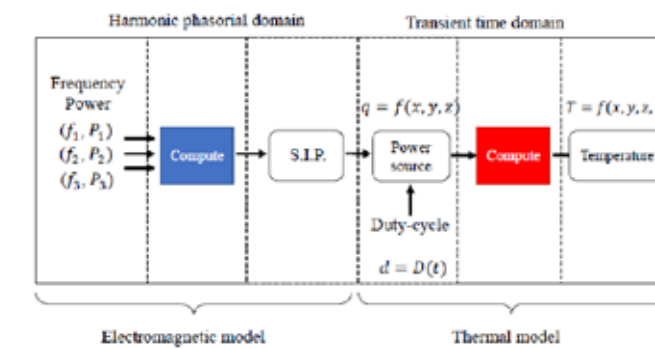
### Possible emitting devices



### Example of experimental trial for model-validation



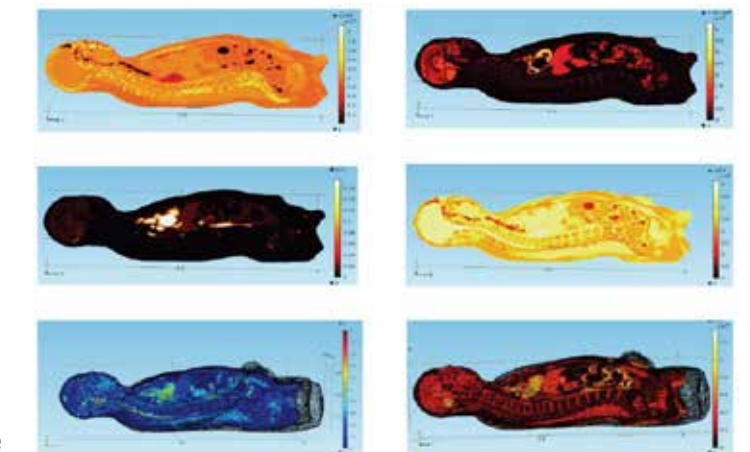
### Multiphysics domain analysis



### Comments

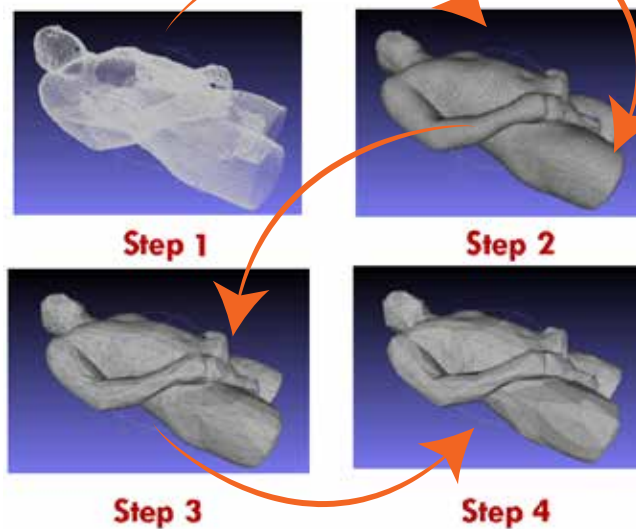
Based upon the numerical predictions that can be made with the reconstructed numerical model, it has been possible to obtain practical information under certain exposure conditions (the detailed results have been already submitted to Scientific Journals). As any CAE user knows, validation is a fundamental issue before analyzing the numerical results. Indeed, simplified experimental trials must be constructed and used to calibrate, and then to validate the implemented model.

### Reconstruction of the material properties



Christian BIANCHI, Michele FORZAN, Fabrizio DUGHIERO  
University of Padova

Reparation of topological errors:  
non-manifold edges, volume intersections,...



Step1 - Step2 : from cloud points to triangular connectivity  
Step2 - Step3 : from connected surface to reduced number of vertices  
Step3 - Step4 : from reduced number of vertices to an optimized set of vertices



Poster Award Prize Ceremony in Vicenza

# A summary from the metal forming & steelmaking session @ 33<sup>rd</sup> CAE Conference



Unmissable date since many editions, the session focused on Metal Forming processes took place also during the latest International CAE Conference. Mainly oriented to the hot and cold deformation processes of metals, the event has been renovated this year with the extension to Steelmaking processes, naturally and strongly linked to the hot forging processes. Aim of this edition was to point out the added value arising from the integration between different technologies during design of both part and related manufacturing processes. The agenda aimed to investigate different topics, where forged products are key points on the supply chain from raw material to final product, such as:

- Steelmaking and Energy applications
- Hot forging for Automotive components
- Hot forging for Heavy equipment components
- Calibration and process optimization
- Advanced application of forging processes

Starting from steelmaking area, two interesting works have been presented. Dr. Marco Turchetti (ESTECO) presented the activities performed during the iCAST project in collaboration with ERGOLINES, on the development of a new technology for 'assisted solidification' of steel in order to improve the quality of the final cast slab, by modeling, simulation and numerical optimization of key parameters of the process and plants. Dr. Luca Marioni (MINES ParisTech) presented the results achieved during his PhD in collaboration with TRANSVALOR S.A., demonstrating the latest studies about the numerical evaluation on the effects of electro-magnetic stirring during continuous casting.



Source: BERCO SpA

Dr. Jochen Heinzmann (HIRSCHVOGEL Umformtechnik GmbH) demonstrated the benefits achievable by considering the effects of the production process into the numerical analysis of the component's in-service life in automotive sector. The approach has been applied on a common rail for Diesel IC engine. This integration can be performed by involving the supplier in the product development process and in engineering partnerships early on, leading to favorable conditions for finding economical solutions that benefit both parties. The complete case is reported on dedicated article at pag. 30 of this in this issue. Moving to the heavy equipment, particularly referring to undercarriage components of earth moving machines overhauling, Dr. Raffaele De Scisciolo (BERCO S.p.A.) presented how, thanks to the FEA approach and the continuous support of EnginSoft, the Company was able to reduce time-to-market from 6 to less than 2 weeks, build dies only after virtual validation, save 15-30% of steel and increase robustness of some processes. Beside the production point of view, also product benefits have been shown, obtainable by the integration of residual stresses derived from the manufacturing processes with multibody simulation of the full vehicle interaction with the terrain.

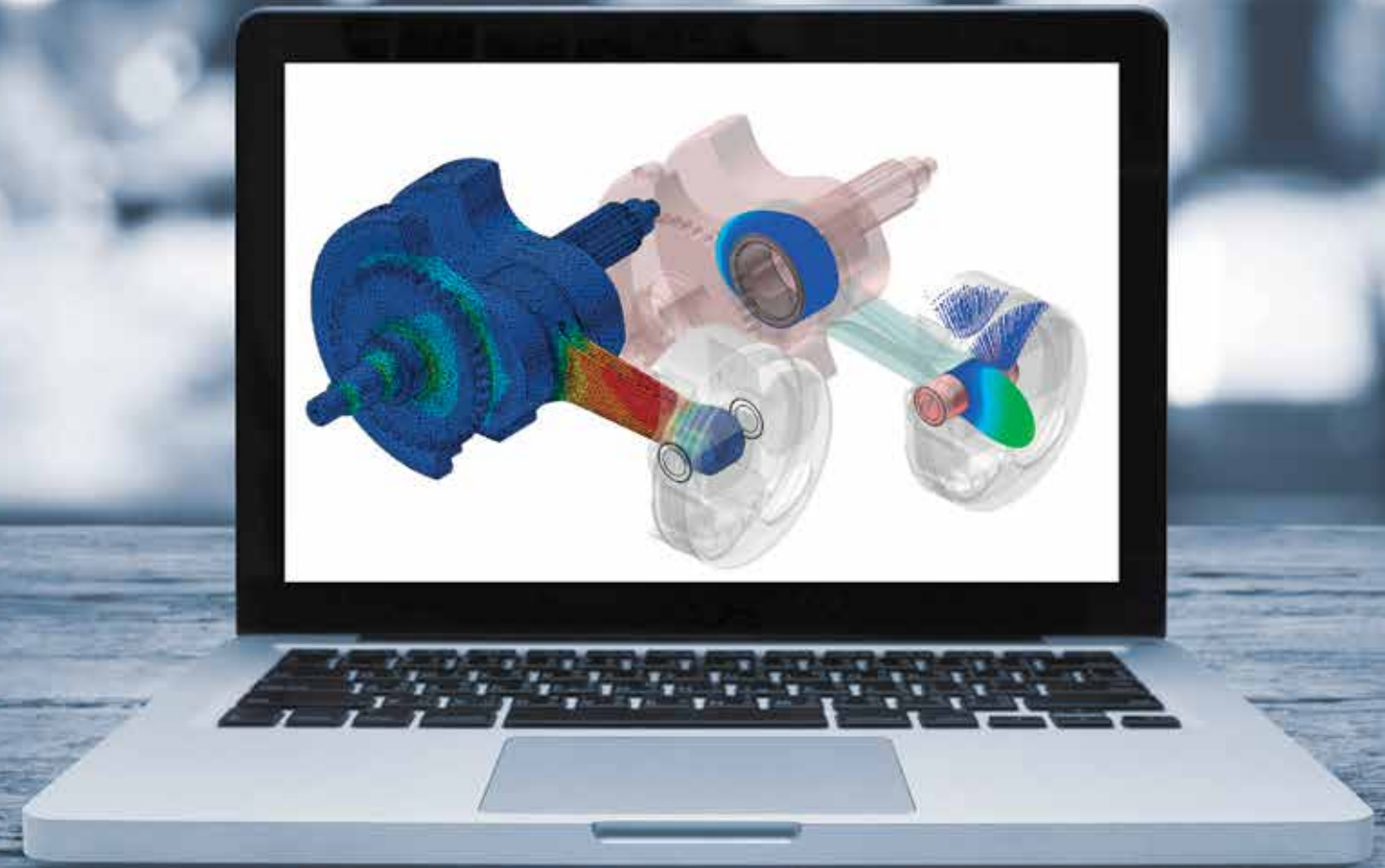
Dr. Iñaki Pérez (Fundación TECNALIA Research & Innovation) showed several interesting examples concerning how the numerical optimization provides an impressive help during the design of the manufacturing process (reducing material waste and equipment requirements), as well as sensible increases on simulation reliability by inverse analysis from experimental data. Dr. Laëtitia Pegie (Customer Service Department Director at TRANSVALOR S.A.) presented several applications focused on the benefits of numerical simulation to improve the quality of products and processes. Concerning the integration with the Steelmaking industry,. Finally, in order to highlight the manufacturing processes as a whole, Dr. Antoine Navarro (Product Manager at TRANSVALOR S.A.) anticipated the next developments concerning microstructural evolution, welding processes and additive manufacturing.

The session, and the whole CAE Conference, highlighted the path for the future. Nowadays, the advantages arising by the adoption of CAE technologies are well-known about the manufacturing processes. Now the challenges refer to the integration between components and processes design, having different objectives, strategies and tools. This is the one of the key-point of the Industry 4.0 strategy. Metal forming is not more only a suppliers' matter. OEMs are more and more interested on how their components will be produced, creating strong collaborations with Tiers and Suppliers. Hence, deeper understanding about advanced material modelling, production optimization and quality monitoring is becoming mandatory since the preliminary design phase of components and assemblies. Thanks you to all the speakers and the participants for sharing their experiences during the session and the entire 2-days Conference, which has proved once again as an international key-event for the CAE technologies.

For more information:  
Federico Fracasso, EnginSoft - f.fracasso@enginsoft.com



## EnginSoft Training Center



# DRIVE YOUR CAREER!

Dive into our 2018 full training offer!



[www.enginsoft.it/formazione](http://www.enginsoft.it/formazione)

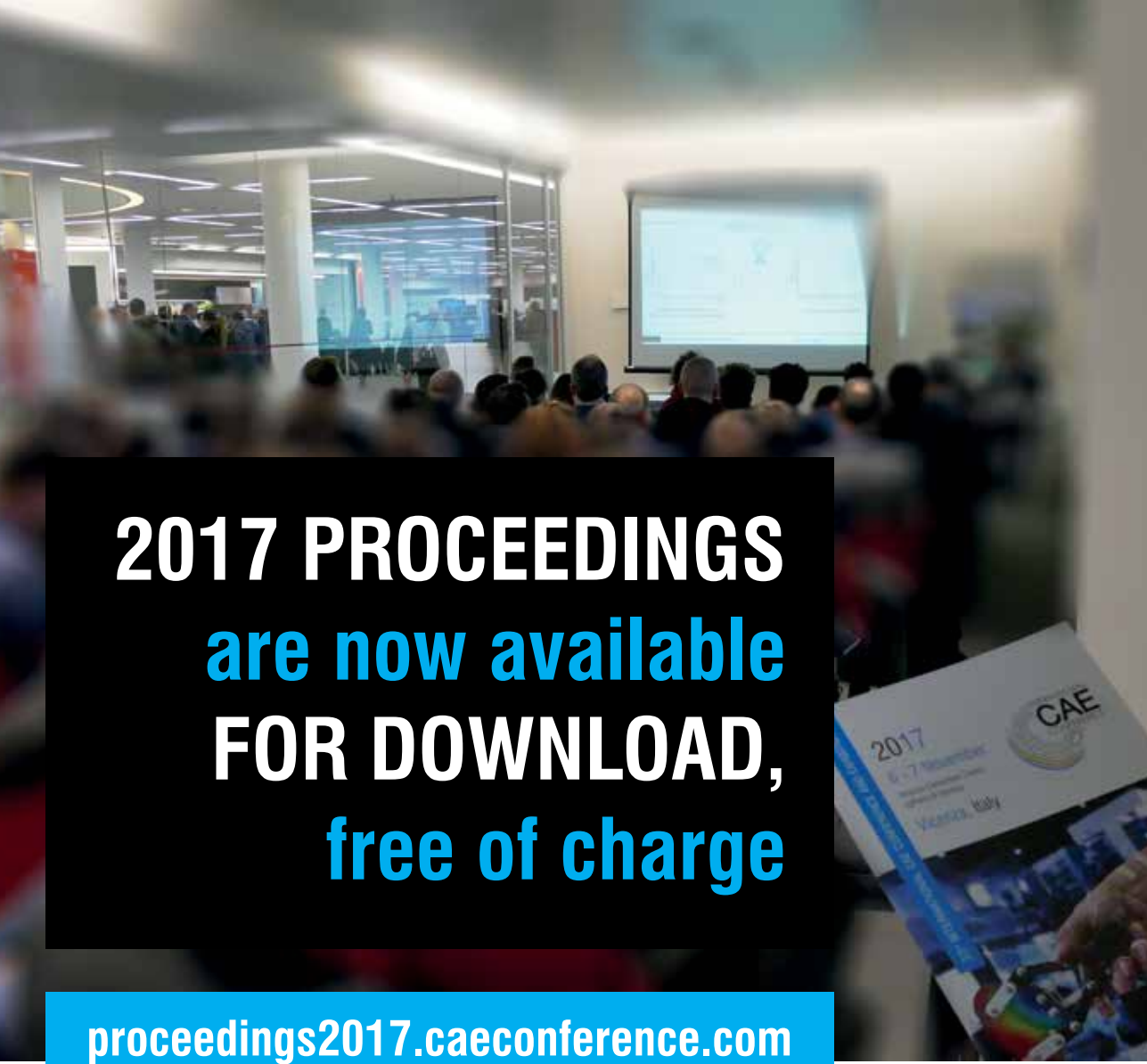
33<sup>rd</sup> INTERNATIONAL CAE CONFERENCE AND EXHIBITION

2017

6 - 7 November

Vicenza Convention Centre  
@Fiera di Vicenza

Vicenza, Italy



**2017 PROCEEDINGS**  
**are now available**  
**FOR DOWNLOAD,**  
**free of charge**

[proceedings2017.caeconference.com](http://proceedings2017.caeconference.com)



[WWW.CAECONFERENCE.COM](http://WWW.CAECONFERENCE.COM)